Design and Synthesis of Caged Thiols for Development of Photo-Activatable Peptides, Inhibitors and Biomaterials

A Dissertation

SUBMITTED TO THE FACULTY OF THE GRADUATE SCHOOL OF THE UNIVERSITY OF MINNESOTA BY

Mohammad Mohsen Mahmoodi

IN PARTIAL FULLFILLMENT OF THE REQUIREMENTS FOR THE GRADUATE DEGREE OF DOCTORAL PHYLOSOPHY

Mark D. Distefano, Advisor

June, 2017

Acknowledgement

I was 22 years old when I moved to US, a new environment and culture far away from my family, in order to pursue my graduate studies. Thus far, this has been the most challenging journey in my life full of numerous learning and growing experiences. I would have never imagined that I would grow this much academically and as a person. This could not have been done without the support and help of many people.

First, I would like to extend my sincere thanks to my advisor Mark Distefano for giving me this great opportunity to be a part of his fantastic research group. He was a great mentor full of encouragement, patience, and support helping me overcome the obstacles and challenges I faced during my research.

A big thank you goes to MDD group members past and present. Thank you for your help and support you have provided me all these years. As in particular, my old friend and teacher Dr. Mohammad Rashidian, for his help, support and guidance both in academic a personal life. Dr. John Dozier for his humorous and supportive personality and his help for reviewing my proposals. Dr. Dan Mullen for teaching me peptide synthesis. Dr. Charuta Palsuledesai for teaching me mammalian cell culture. I would also like to thank all of my collaborators: Professor David Bank and his group members for their help on two-photon laser. Professor Molly Shoichet and her lab members Stephanie Fisher and Dr. Roger Tam for their contribution. Dr. Guillermo Marques for his help on confocal microscopy experiments.

My PhD experience was a full of challenges and disappointments. I was not able to overcome these difficulties without the support of my family back home and also my great friends in Minneapolis: Davood Taherinia, Fazel Zare Bidoky, Mohammad Danesh Yazdi, Hamidreza Badri, Shahrzad Zaferanloo, Mahdi Ahmadi, Mammad Nasiri, Sara Parhizgari, Reza Halvagar and Mohammad Amin Tadayon. I am very blessed and thankful to have you as my friends.

Lastly, I must thank my mom and dad, and my sisters for their endless love, help and support. You have always been a great source of inspiration, motivation and encouragement for me. I love you and this thesis is all dedicated to you.

To my parents,

Mahdi and Aghdas Mahmoodi

and my sisters, Narges and Najmeh

My endless gratitude
for I would never made it this far without you

Table of Contents

Preface vi

Introduction vii

Table of Figures x

Table of Schemes xiv

List of Tables xv

1 Photo-cleavable protecting groups for thiols: Synthesis, biological and biomaterial applications 1

1.1 Introduction 1

1.2 *Ortho*-nitrobenzyl based caging groups 3

1.3 Coumarin-based caging groups 14

1.4 Nitrodibenzofuran Cages for Thiols 23

1.5 p-Hydroxyphenacyl Cages for Thiols 26

1.6 Benzoin and Benzoyl Cages for Thiols 30

1.7 Conclusion 31

2 Nitrodibenzofuran: A One- and Two-Photon Sensitive Protecting Group That Is Superior to Brominated Hydroxycoumarin for Thiol Caging in Peptides 35

2.1 Introduction 35

2.2 Results and Discussion 39

2.2.1 Synthesis and Studies of the Photolysis of Bhc- Protected Cysteine-Containing Peptides. 39

2.2.2 Use of Nitrodibenzofuran for Development of Caged Cysteine-Containing Peptides. 49

2.2.3 Light Activation of a Caged Peptide inside Live Cells. 57

2.3 CONCLUSION 63

2.4 Experimental Section 64

3 6-Bromo-7-hydroxy-3-methyl coumarin (mBhc) is an efficient multi-photon labile protecting group for thiol caging and three-dimensional chemical patterning 74

3.1 Introduction 74

3.2 Results and Discussion 77

3.2.1 Design and synthesis of a coumarin-based caging group for efficient thiol protection 77

3.2.2 Photo-physical properties of an mBhc protected thiol 85

3.2.3 One- and two-photon activation of protein prenylation 88

3.2.4 Two-photon patterning using a mBhc-caged thiol 91
3.3 Conclusion 94
3.4 Experimental Section 95
4 Development of caged farnesyltransferase inhibitor for photo-chemical modulation of Ras-localization 105
4.1 Introduction 105
4.2 Result and Discussion 107
4.2.1 Synthesis and Photo-chemical Properties of Caged FTI 107
4.2.2 Photo-triggered Release of FTI Inside Cells and Modulation of Ras Localization 110
4.3 Conclusion 113
4.4 Experimental Section 113
5 Synthesis of a nitrodibenzofuran-based caging group with red-shifted absorption 117
5.1 Results and discussion 118
5.1.1 Synthesis of 7-amino nitrodibenzofuran (AminoNDBF) 118
5.2 Conclusion and future directions 120
5.3 Experimental secion 120
6 References 124

Preface

Please note the following:

Chapter 2: **Mahmoodi, M. M.**; Abate-Pella, D.; Pundsack; T.J., Palsuledesai C. C.; Goff, P. C., Blank D. A.; Distefano, M. D. “Nitrodibenzofuran: A One- and Two-Photon Sensitive Protecting Group That Is Superior to Brominated Hydroxycoumarin for Thiol Caging in Peptides***” J. Am. Chem. Soc***., 2016, 138 (18), pp 5848–5859.

Chapter 3: **Mahmoodi, M. M.**; Fisher, S. A.; Tam, R. Y.; Goff, P. C.; Anderson, R.; Wissinger, J. E.; Blank, D. A.; Shoichet, M. S.; Distefano M. D. “6-bromo-7-hydroxy-3-methyl coumarin (mbhc): an efficient photo-cleavable protecting group useful for thiol caging in peptides and creation of three-dimensional chemical patterns in hydrogels” ***Org. Biomol. Chem.***, 2016, 14, 8289–8300.

Introduction

The ability of light to traverse various chemical and biological barriers and be modulated by time and amplitude makes light- regulated molecules unique tools for a plethora of applications in the areas of chemistry and biology and biomaterials. Photo-removable protecting groups, also known as caging groups, are one of the most important light-regulated tools, which can be utilized to mask specific functional groups in molecules such that they can be cleaved on demand upon irradiation. In biological applications, this typically involves masking a biomolecule with a caging group to produce a compound whose biological activity is either increased or decreased upon uncaging. The recent development of two-photon-sensitive protecting groups, which allow uncaging using near-infrared (near-IR) irradiation, has resulted in significant improvements in the spatiotemporal resolution of uncaging as well as increased penetration with lower photo-toxicity; the latter attribute is of particular importance for the use of caged molecules in tissue samples or intact organisms that are essentially opaque to UV light. Additionally, two-photon un- caging approaches have proved to be extremely useful for creating novel biomaterials; in that strategy, laser irradiation is used to unmask a specific caged functionality pre-incorporated into a hydrogel or matrix, such that it can be used to immobilize peptides, proteins or cells in a three dimensionally controlled fashion.

Differences in the chemical reactivity of various functional groups means that there is no single protecting group that can be universally employed for caging applications. Sulfydryl-containing compounds play critical roles in various aspects of cellular function. Hence, significant effort has gone into development of photo-activatable thiol-containing peptides or small molecule substrates as tools to elucidate or dissect cellular pathways; under many conditions, thiols are the most reactive nucleophiles present in biological systems. Importantly, they are prone to oxidation and are also relatively poor leaving groups compared with phosphates and carboxylates. Those features render the design of photoremovable thiol protecting groups challenging.

Ortho-Nitrobenzyl (ONB) compounds are the most commonly used caging groups for sulfhydryl-protection. ONB groups provide free thiols in high yield upon photolysis, however, they are poor chromophores and they generally lack two-photon sensitivity. To address these limitations, several research groups have used coumarin-based protecting groups (e.g., brominated hydroxycoumarin, Bhc) for caging applications, due to their high one- and two-photon sensitivity.

In this work, we analyzed the photolysis of several Bhc-protected thiol-containing peptides and small molecules. Those experiments revealed that Bhc-caged thiols exhibit variable uncaging yields and that their photolysis frequently leads to the formation of an unwanted rearrangement product.

To circumvent this problem, we explored and designed two alternative highly efficient thiol caging groups that can be uncaged upon one- and two-photon irradiation. we initially explored using nitrodibenzofuran (NDBF) as a thiol caging group. Cysteine-containing peptides were prepared where the thiol was protected with an NDBF group. To probe the utility of this protecting group for biological experiments, thiol group uncaging was carried out using a K-Ras-derived peptide containing an NDBF-protected cysteine. Irradiation of that molecule in the presence of protein farnesyltransferase (PFTase) and farnesyl diphosphate (FPP) resulted in the formation of the free thiol form and subsequent enzymatic conversion to a prenylated species. In order to illustrate the utility of this strategy for the development of caged peptides that can be activated via irradiation inside live cells, the thiol of a cell-penetrating peptide known to be a substrate for palmitoyl acyltransferase was protected as a NDBF thioether. Irradiation of human ovarian carcinoma (SKOV3) cells, preincubated with the probe, resulted in migration of the peptide from the cytosol/Golgi to the plasma membrane (visualized via confocal microscopy) due to enzymatic palmitoylation. These data suggest that the NDBF group should be useful for caging thiols in peptides and potentially larger proteins assembled via native chemical ligation for biological applications.

As another approach, guided by mechanistic studies of the photo-triggered isomerization of Bhc-thiols, we developed 6-bromo-7- hydroxy-3-methylcoumarin-

4-ylmethyl (mBhc) as an alternative coumarin-based caging group that can afford efficient thiol release upon one- and two-photon irradiation. To test the efficiency of mBhc for thiol-protection in peptides, we have synthesized a K-Ras-derived peptide where the thiol was protected by mBhc. One- and two-photon photolysis of the caged peptide resulted in clean conversion to the free compound with no photo-isomerization. Irradiation of the caged peptide using a near-IR laser in the presence of an enzyme (protein farnesyltransferase, PFTase) resulted in the generation of a free thiol-containing peptide which was then enzymatically farnesylated.

To further evaluate the utility of this novel caging group for biomaterial applications, an mBhc-protected thiol was covalently incorporated into a hydrogel. Using a 740 nm two- photon laser from a confocal microscope, patterns of free thiols were generated inside the matrix and visualized by reaction with maleimide functionalized fluorophores. Such 3D patterns could be useful for a variety of applications in tissue engineering. Such highly tuned matrices allow artificial extracellular environments to be created that can be used to study cell migration, differentiation and cell–cell interactions.

Lastly, we strived to develop a novel NDBF-based caging group with red-shifted absorption maxima and improved two-photon uncaging efficiency. Inspired by previous studies, we elected to modify the structure of NDBF by adding an amine as a donor group, to generate a donor-acceptor system. Hence, 2-bromo-2-(7-(dimethylamino)-3-nitrodibenzofuran-2-yl)acetate was synthesized in 9-steps. Initial analysis of spectral properties of the designed molecule showed the absorption maxima (λmax) to be 440 nm. This is110 nm red-shifted relative to λmax of NDBF. The uncaging efficiency of this novel protecting group remains to be tested.

Table of Figures

Figure 1-1 An overview of various photo-removable protecting groups that have been used for sulfhydryl protection. (1) ortho-nitrobenzyl (ONB) derivatives, (2) coumarin derivatives, (3) nitrodibenzofuran (NDBF), (4) para-hydroxyphenacyl (pHP), (5) 2-Benzoylbenzoic acid. 2
Figure 1-2 An overview of various ONB-based photo-removable protecting groups that have been used for sulfhydryl protection. 3
Figure 1-3 Structures of model caged peptides utilized by Hagen and coworkers to study the photo-chemical properties of CNB and CDMNB when utilized for cysteine protection. Figure was adapted and reproduced from Kotzuer et. al. [23]. 5
Figure 1-4 Synthetic scheme for ubiquitylation of U2B. The first step includes ligation of ONB-caged polypeptide to peptide thioester generating **14**. Subsequent irradiation of **14** with UV light released the latent cysteine readily utilized for the next round of ligation. Second ligation followed by desulfurization resulted in formation of ubiquitylated U2B. The figure was adapted and reproduced from McGinty et. al. [24]. 6
Figure 1-5 The mechanism of phosphate-triggered SEAlide activation which is readily reactive toward chemical ligation. The figure was adapted and reproduced from Aihara et. al. [20]. 7
Figure 1-6 Strategy developed by Otaka and coworkers for peptide/protein synthesis using photocaged SEAlide moiety. The figure was adapted and reproduced from Aihara et. al. [20]. 8
Figure 1-7 A) Reaction mechanism for disulfide bond formation via photocleavage of the DMNB group followed by subsequent thiolysis through S-pyridinesulfenyl activation. B) This strategy was employed for the synthesis of α- conotoxin. The figure was adapted and reproduced from Karas et. al. [25]. 9
Figure 1-8 A) Schematic representation of the peptide photo-release and concomitant farnesylation of the caged peptide. B) Farnesylation of caged peptide before and after irradiation quantified via ^{3}H-FPP assays. The figure was adapted from Degraw et. al. [26] and reproduced. 10
Figure 1-9 (A) Synthesis of caged cofilin mutant, B) Rhodamine-labeled F-actin filaments are not cleaved by caged cofilin, (C) 15 min UV photolysis released the mutant enzyme resulted in actin depolymerization. Cleavage sites are shown by arrows. The figure was adapted from Ghosh et. al. [27] and reproduced. 11
Figure 1-10 (A) Primary sequence of the leucyl suppressor tRNA, $Leu5_{CUA}$. (B) The active site of leucyl tRNA-synthetase is shown with a bound leucyl sulfamoyl adenylate inhibitor (green). The residues randomized in generating the synthetase library are in yellow. The catalytic domains of synthetase are in pink. (C) Structure of o-nitrobenzyl cysteine being incorporated using this tRNA/Synthetase pair. The figure was adapted from Wu et. al. [30] and reproduced. 13
Figure 1-11 An overview of various coumarin-based photo-removable protecting groups that have been used for sulfhydryl protection. 14
Figure 1-12 A) Structures of Fmoc-cysteine protected with coumarin-based hydrophilic coumarin-based photo-removable protecting group, B) Wavelength selective uncaging of caged cysteines. The figure was adapted from Kotzuer et. al. [32] and reproduced. 15

Figure 1-13 Two-step wavelength selective photolysis of caged resact. The figure was adapted from Kotzuer et. al. [32] and reproduced. 16
Figure 1-14 Synthesis of caged farnesyl transferase inhibitor **53**..... 17
Figure 1-15 Morphology of fibroblast ciras-3 cells treated with Bhc-FTI. A) Untreated cells, B) treated with 2.5 μM FTI, C) treated with 2.5 μM Bhc-FTI with no irradiation, D) treated with 2.5 μM Bhc-FTI followed by 1h two-photon irradiation at 800 nm. The figure was adapted from Abate et. al. [34] and reproduced..... 18
Figure 1-16 A) Schematic illustration of multi-photon chemical patterning in hydrogel incorporating caged thiol moieties, B, C) Representative figures for the simultaneous 3D patterning of biotin–CNTF–633 (green) and barstar–SHH–488 (red). The figures were adapted from [36] and [35]..... 19
Figure 1-17 Photo-rearrangement mechanism of Bhc protected cysteine..... 20
Figure 1-18 A, B) Illustration of potential effects of C-3 substitution on photo-isomerization process. C) Uncaging reaction of mBhc-protected peptide. The figure was adapted from Mahmoodi et. al. [33] and reproduced..... 21
Figure 1-19 Comparison of two-photon patterning using Bhc- and mBhc-caged thiol. Uncaging of Bhc or mBhc-conjugated HA hydrogels, and subsequent immobilization of Alexa Fluor 546. The figure was adapted from Mahmoodi et. al. [33] and reproduced.. 22
Figure 1-20 Photo-uncaging of KKKSKTKC(NDBF)VIM and subsequent farnesylation by PFTase enzyme. The figure was adapted from Mahmoodi et. al. [16] and reproduced.. 24
Figure 1-21 Schematic Representation of NBD-HexC(NDBF)LC-OMe uncaging and subsequent palmitoylation. The figure was adapted from Mahmoodi et. al. [16] and reproduced. 25
Figure 1-22 Live-cell experiments showing temporal control of enzymatic palmitoylation via NDBF-thiol caging. (A) Images obtained by fluorescence confocal microscopy illustrating intracellular localization of fluorescently labeled peptide 20 in SKOV3 cells, before (top) and after (bottom) UV exposure. (B) Quantification of colocalization of peptide and membrane dye via Pearson's coefficient analysis, indicating a significant increase in plasma membrane localization of peptide upon irradiation. The figure was adapted from Mahmoodi et. al. [16] and reproduced..... 26
Figure 1-23 A) Mechanism of tyrosine phosphatase catalysis, and inactivation via pHP protection, B) In vivo enzymatic assays, showing restoration of tyrosine phosphatase activity upon UV irradiation which leads to pHP uncaging. The figure was adapted from Mahmoodi et. al. [38] and reproduced..... 28
Figure 1-24 A) Thiol derivatives caged by pHP group. B) Product yields generated by 312 nm irradiation of pHP caged thiols. The figure was adapted from Mahmoodi et. al. [39] and reproduced. 30
Figure 1-25 Structures of 3,5-dimethoxybenzoin (DMB) caged phenylmethylthiol and 2-benzoylbenzoic acid caged aliphatic thiol. The figures were adapted from [40] and [41]..... 31
Figure 2-1 (A) Uncaging reaction of Bhc-protected cysteine-containing peptide **5** upon UV irradiation. LC-MS analysis of photolysis of peptide **5**: (B) EIC chromatogram (m/z = 635.20−635.30) of a sample of **5** in photolysis buffer, (C) EIC chromatogram (m/z = 635.20−635.30) of sample of **5** after 120 s photolysis showing the formation of a photoisomer, and (D) EIC chromatogram (m/z = 551.20−551.30) of a standard sample of free peptide **6b** showing that no uncaged product was detected upon photolysis of **5**.... 42

Figure 2-2 (A) Photolysis of Bhc-protected Boc-cysteamine and the resulting photolytic products. (B) 1H NMR spectrum of Bhc-protected Boc-cysteamine (top) and the corresponding photoisomer (bottom). 49
Figure 2-3 (A) HPLC quantification of disappearance of the starting peptide (**17b**) and formation of the uncaged peptide (**6b**) as a function of irradiation time at 365 nm. (B) HPLC quantification of uncaging of **17a** as a function of two-photon irradiation time (800 nm, pulsed Ti:Saphire laser, 210 mw, 80 fs pulse width). Photolysis reactions were performed in 200 and 300 µMsolutions of **17b** and **17a** respectively, containing 1 mM DTT in 50 mM PB, pH 7.5. 54
Figure 2-4 (A) Photo-uncaging of **17** and its subsequent farnesylation by enzyme. (B) EIC chromatogram (m/z = 511.62) of a 7.5 µM solution of **17a** in prenylation buffer containing PFTase without irradiation. (C) EIC chromatogram (m/z = 431.95) of a solution of **17a** after 2.5 min irradiation at 800 nm (Ti:sapphire laser, 170 mW, 90 fs) in prenylation buffer without PFTase. (D) EIC chromatogram (m/ z = 499.99) of **17a** after 2.5 min irradiation at 800 nm (Ti:sapphire laser, 210 mW, 90 fs) in the presence of PFTase, showing the formation of farnesylated peptide **19a**. 59
Figure 2-5 Live-cell experiments showing temporal control of enzymatic palmitoylation via NDBF-thiol caging. (A) Images obtained by fluorescence confocal microscopy illustrating intracellular localization of fluorescently labeled peptide 20 in SKOV3 cells, before (top) and after (bottom) UV exposure. (B) Quantification of colocalization of peptide and membrane dye via Pearson's coefficient analysis, indicating a significant increase in plasma membrane localization of peptide upon irradiation. 60
Figure 3-1 Photolysis reaction of Hc-protected Boc-cysteamine. (A) Structures used in this study. (B) EIC chromatogram (m/z = 334.09, calcd for $[M(\mathbf{7})\text{-tBu+K}]^+$ = 334.01) of a 50 µM solution of **7** in photolysis buffer (50 mM phosphate buffer, pH 7.4 containing 1 mM DTT) before irradiation, (C) EIC chromatogram (m/z = 334.09, calcd for $[M(\mathbf{7})\text{-tBu+K}]^+$ = 334.01) of a 50 µM solution of **7** in photolysis buffer after 6 min irradiation at 365 nm, this data clearly indicates generation of the photo-isomer, (D) EIC chromatogram (m/z = 231.01, calcd for $[M(\mathbf{9})+K]^+$ of **7** after 6 min irradiation showing no evidence of generation of **9**, this indicates photolysis leads predominantly to photo-isomerization rather than uncaging. 79
Figure 3-2 Uncaging studies using a peptide with a mBhc-protected thiol. (A) Photo-triggered uncaging of mBhc-protected K-Ras peptide (**18**). (B) EIC chromatogram (m/z = 520.57, calcd for $[M + 3H]^{3+}$= 520.58) of a 100 µM solution of **18** before irradiation, (C) EIC chromatogram (m/z = 520.57, calcd for $[M + 3H]^{3+}$= 520.58) of a 100 µM solution of **18** after 60 s irradiation at 365 nm suggesting that no photo-isomer is generated and only the remaining starting peptide peak is present, (D) EIC chromatogram (m/z = 647.37, calcd for $[M + 2H]^{2+}$= 647.37) of a 100 µM of **18** after 60 s irradiation at 365 nm which clearly indicates formation of free peptide **19**. 84
Figure 3-3 Photophysical properties of mBhc. (A) Absorption and emission spectra of mBhc (**3**) in 50 mM PB, pH 7.4. (B) Time course of photolysis of **18** and Bhc-OAc as a reference at 365 nm and (C) Time course of photolysis of **18** and Bhc-OAc as a reference at 800 nm (pulsed Ti:Saphire laser, 210 mw, 80 fs pulse width) quantified by RP-HPLC. Photolysis reactions were performed in 100 µM (for UV), and 300 µM (for TP) solutions of **18** containing 1 mM DTT in 50 mM PB, pH 7.4. 87
Figure 3-4 Photo-triggered farnesylation of an mBhc-protected K-Ras peptide. (A) Structures of peptides and products relevant to this study. (B) EIC chromatogram (m/z =

520.65, calcd for $[M + 3H]^{3+}$= 520.58) of a 7.5 µM solution of **18** in a prenylation buffer containing PFTase with no irradiation. (C) EIC chromatogram (m/z = 647.45, calcd for $[M + 2H]^{2+}$= 647.39) of a 7.5 µM solution of **18** after 60 s irradiation at 365 nm in prenylation buffer without PFTase showing the formation of free peptide **19**. (D) EIC chromatogram (m/z = 500.06, calcd for $[M + 3H]^{3+}$= 499.99) of a 7.5 µM of **18** after 60 s irradiation at 365 nm in presence of PFTase showing the formation of farnesylated peptide **21**. 89
Figure 3-5 Comparison of two-photon patterning using Bhc- and mBhc-caged thiol. (A) Bhc or mBhc to is conjugated to HA-carboxylic acids using DMT-MM prior to crosslinking HA-furan with PEG-bismaleimide. (B) Schematic representation of two-photon patterning in Bhc or mBhc-conjugated HA hydrogels. A 3D hydrogel scaffold (i) is formed when Bhc/mBhc-modified HA-furan is chemically crosslinked with PEG-bismaleimide (ii).. The resulting photo-labile hydrogel undergoes photolysis of the Bhc/mBhc groups using two-photon irradiation to liberate free thiols in discrete regions of the hydrogel, which then react with maleimide-bearing Alexa Fluor 546 (mal-546) (iii) (C) Visualization of mal-546 patterns in the x-y plane and z-dimension in mBhc and Bhc conjugated HA hydrogels. Regions of interest were scanned 5 to 20 times at a fixed z-dimension. The concentrations of mBhc and Bhc were matched based on UV absorbance. Patterns in mBhc and Bhc conjugated HA hydrogels were imaged at different confocal settings due to Bhc patterns being so faint in comparison to mBhc patterns. (D) The z-axis profile of immobilized mal-546 in mBhc and Bhc conjugated HA hydrogels was quantified with the maximum intensity was centered at 0 µm. 93
Figure 4-1 LC-MS analysis of uncaging of NDBF-FTI to form free FTI by irradiation at 365 nm. Crude LC-MS trace of a 20 µM solution of **2** in 50 mM pH 7.2, A) before irradiation and B) after 90s irradiation. These results clearly show disappearance of NDBF-FTI (m/z calcd for ($[M + H]^+$ 799.3405, found 735.3411) and appearance of free FTI ($[M + H]^+$ 560.2823, found 560.2826). C) MS/MS of pure **2**, D) MS/MS of **1** produced from UV photolysis..... 109
Figure 4-2 HPLC quantification of disappearance of **2** and formation of the uncaged peptide (**1**) as a function of irradiation time at 365 nm. 109
Figure 4-3 GFP-H-ras localization in MDCK cells treated with NDBF-FTI (**2**) after 700 nm two-photon irradiation. Treatments were as follows: A) Vehicle (0.2% DMSO (v/v)). B) 10 µM FTI (1). C) 5 µM NDBF-FTI (**2**), no irradiation. D) 5 µM NDBF-FTI (**2**) plus two-photon irradiation (300 µs/pixel). E) 5 µM NDBF-FTI (**2**) plus two-photon irradiation (300 µs/pixel), this image demonstrates the boundary between irradiated area and non-irradiated area. As expected two-photon laser NDBF-FTI can be locally uncaged in a group of cells, which results in creation of patterns of inhibited versus inhibited cells. 112

Table of Schemes

Scheme 2.1 Synthesis of Bhc-Protected Fmoc-Cys and Incorporation into a Peptide via SPPS. 40
Scheme 2.2 Hypothesized Mechanism of Photoisomerization of Bhc-Caged Cysteine. 45
Scheme 2.3 Synthesis of NDBF-Protected Fmoc-Cys-OH and Incorporation into Peptide Sequence via SPPS. 52
Scheme 2.4 Light-Triggered Uncaging of NDBF-Protected K- Ras Peptide (**17b**). 52
Scheme 3.1 Coumarin-based caging groups discussed in this work. 76
Scheme 3.2 Photo-rearrangement mechanism of Bhc protected cysteine. 78
Scheme 3.3 Illustration of potential effects of C-3 substitution on photoisomerization process. 82
Scheme 3.4 Synthesis of Fmoc-Cys(mBhc)-OH and its incorporation into a K-Ras-derived peptide via SPPS. 82
Scheme 3.5 Schematic representation of (A) synthesis of mBhc and Bhc protected cysteamine, followd by (B) conjugation to HA-carboxylic acids using DMT-MM prior to crosslinking HA-furan with PEG-bismaleimide. 92
Scheme 4.1 Farnesyltransferase inhibitor (FTI, **1**) and caged FTI (NDBF-FTI, **2**). 107
Scheme 4.2 Synthesis of NDBF-FTI. 108
Scheme 5.1 Nitrodibenzofuran and 7-amino nitrodibenzofuran. 118
Scheme 5.2 Synthesis of 7-amino nitrodibenzofuran. 119

List of Tables

Table 1.1 Overview of spectral and photo-chemical properties of thiol caging groups reviewed in this article. 34
Table 3.1 Photophysical properties of mBhc-thiol versus Bhc-OAc. 87

1 Photo-cleavable protecting groups for thiols: Synthesis, biological and biomaterial applications

1.1 Introduction

Photo-cleavable protecting groups, or caging groups, have been increasingly utilized in organic synthesis[1], cell biology[2–5] and biomaterials as a mean for spatio-temporal release of chemicals as well as biomolecules inside living systems.[6,7,8] Covalent attachment of the caging group to a key functionality in the bioactive agent renders the molecule inactive. Subsequent irradiation leads to cleavage of the protecting group, thus resulting in on-demand and localized release of the active moiety. Although providing enough energy for uncaging generally requires high energy ultra-violet (UV) irradiation, recent advances in two-photon cleavable protecting groups have improved the biocompatibility of this technique by using near infra-red light for uncaging.[9–11] This significantly extends the applicability of caging technique by improving spatial resolution, tissue penetration as well as eliminating photo-toxicity.

A variety of photo-cleavable protecting groups have been developed for caging of various functionalities. Alcohols and carboxyl groups are among the most studied functionalities for caging.[4] However, due to differential chemical reactivity and variations in local chemical environments, there is no single protecting group that can be universally employed for caging applications. [1,4,9]

Efficient caging of thiols is particularly desirable because of their abundance as cysteine residues and cofactors in biological systems. Furthermore, thiols share a

significant role in various aspects of biology including signal transduction, apoptosis, enzymology, controlling cellular redox state and cellular defense system.[12–14] Therefore, significant efforts have gone into developingcaging groups for thiol sulfhydryls[14] in order to create photo-activatable probes,[15–17] biomaterials for dissecting cellular pathways,[18] and orthogonal protecting group for the synthesis of complex thiol-containing biomolecules.[19,20] Several properties of thiol reactivity render the design of photo-removable thiol protecting groups challenging and must be considered. Thiols are among the most reactive functionalities present in biological systems. They are prone to oxidation, undergo nucleophilic reactions and also react with free radicals. Importantly, thiols are relatively poor leaving groups compared to alcohols and carboxylates.

The present review summarizes current developments in thiol caging groups and their applications in peptide and protein synthesis, cell biology and biomaterial development (Figure 1-1).

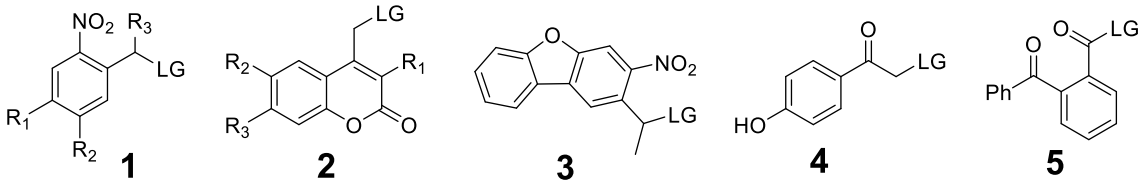

Figure 1-1 An overview of various photo-removable protecting groups that have been used for sulfhydryl protection. (1) ortho-nitrobenzyl (ONB) derivatives, (2) coumarin derivatives, (3) nitrodibenzofuran (NDBF), (4) para-hydroxyphenacyl (pHP), (5) 2-Benzoylbenzoic acid.

1.2 *Ortho*-nitrobenzyl based caging groups

Ortho-nitrobenzyl (ONB) derivatives were initially developed and used as orthogonal protecting groups in organic synthesis. The first application in biochemistry was reported by Kaplan et. al. in 1978, with the synthesis of “caged ATP”.[21] Since then, they have found numerous applications in a variety of biological studies ranking them the most commonly used photo-labile protecting groups.[22] ONB-derivatives have been utilized in a variety of caged biomolecules, many of which are commercially available. The general advantages of ONBs are their ease of synthesis, high yield of conversion to the uncaged product and modest one-photon quantum efficiency. However, ONBs have comparatively low absorptivity and two-photon efficiency, which limits their applicability for studies where deeper tissue or matrix penetration is needed.

ONBs are also the most widely employed approach for thiol protection (Figure 1-2). Multiple research groups have employed ONBs for masking critical cysteine residues during the synthesis of peptides as well as protein ligations.

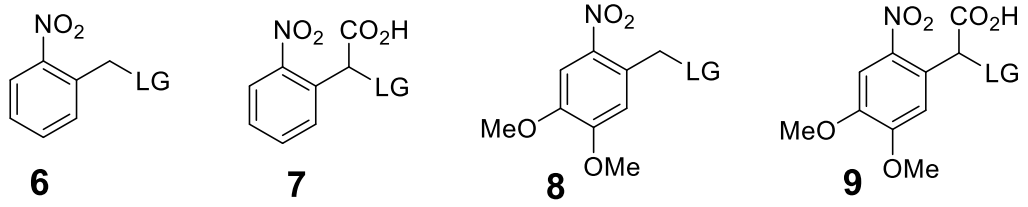

Figure 1-2 An overview of various ONB-based photo-removable protecting groups that have been used for sulfhydryl protection.

Since, protein ligations are performed in aqueous solutions, water soluble ONB-derived α-carboxy-2-nitrobenzyl (CNB, **7**) and α-carboxy-4,5-dimethoxy-2-nitrobenzyl (CDMNB, **9**) have been developed for cysteine protection. Hagen and coworkers studied photolysis properties of CNB- and CDMNB-protected cysteines in peptides (Figure 1-3).[23] It had been previously reported that presence of amines enhances photo-decarboxylation instead of photo-release, therefore, photolysis experiments were carried out in both amine-free PBS or amine-enriched HEPES buffers, and also photolysis of both N-terminal acylated and free N-terminal peptides were studied. Photolysis of caged peptides followed by HPLC analysis revealed that peptide **11b** produced most free peptide (74%) with either zero or very low decarboxylation in the PBS and HEPES buffers, respectively. However, free N-terminal peptide **10a** and **10b** produced the most decarboxylated products. Although decarboxylation was suppressed in amine-containing buffers, the influence of N-terminal amines on elevating decarboxylation was much more significant. Further photolysis studies with different caged peptides revealed that the extent of decarboxylation is case-sensitive and highly dependent on peptide sequence. Generally, these results suggest that CDMNB is superior to CNB for thiol protection due to faster photolysis and longer absorption maxima; however, appropriate measures should be taken to avoid decarboxylation. The quantum yields for peptide **10** and **11** were measured to be 0.04 and 0.07, respectively.

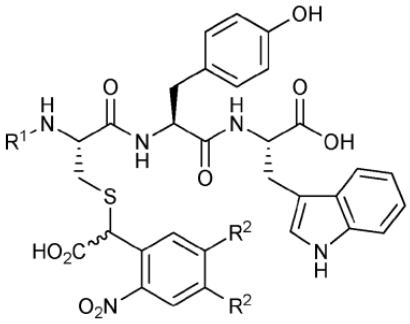

Peptide	R1	R2
10a	H	H
10b	H	OMe
11a	Ac	H
11b	Ac	OMe

Figure 1-3 Structures of model caged peptides utilized by Hagen and coworkers to study the photo-chemical properties of CNB and CDMNB when utilized for cysteine protection. Figure was adapted and reproduced from Kotzuer et. al. [23].

Muir and coworkers used ONB for cysteine protection during expressed protein ligation (EPL).[24] In order to study the relationship between ubiquitylation and upregulation of lysine methylation in different histones via methyltransferase hDotl1. EPL was used for site-specific chemical ubiquitylation of histone H2B (Figure 1-4). Two traceless orthogonal ligations were used to synthesize ubiquitylated H2B (uH2B). Initially, a caged cysteine-linked polypeptide (117-125, A117C mutation, **12**) was ligated to recombinant ubiquitin (1-75)-α-thioester **13** yielding protein **14**. The ligated product was irradiated at 365 nm resulted in deprotection of the caged cysteine residue to give **15**. The obtained free cysteine ultimately was employed for ligating **15** to yield fully ligated uH2B(A117C) **16**. Desulfurization of **16** resulted in the formation of the desired uH2B protein **18**. Successful implementation of this strategy revealed ubiquitylation of H2B directly activates intranuclesomal methylation of H3 K79 protein via hDot1L.

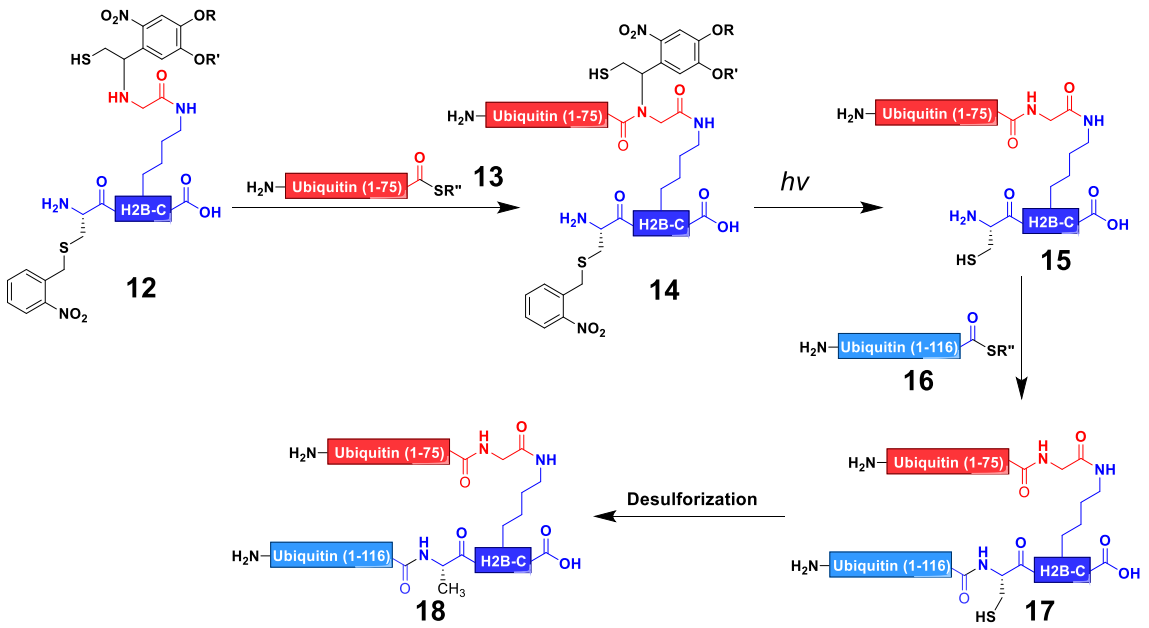

Figure 1-4 Synthetic scheme for ubiquitylation of U2B. The first step includes ligation of ONB-caged polypeptide to peptide thioester generating **14**. Subsequent irradiation of **14** with UV light released the latent cysteine readily utilized for the next round of ligation. Second ligation followed by desulfurization resulted in formation of ubiquitylated U2B. The figure was adapted and reproduced from McGinty et. al. [24].

In an innovative approach, Otaka and coworkers developed a one-pot/sequential native chemical ligation methodology using 4,5-dimethoxy-2-nitrobenzyl (DMNB, **8**, Figure 1-2) photocaged crypto-thioester.[20] They had previously shown that C-terminal N-sulfanylethylanilides (SEAlide) can rearrange to form a thioester upon treatment with phosphate, thus readily ligated to a N-terminal cysteinyl peptide (Figure 1-5).[19] Since, the phosphate could activate any subsequently added SEAlide containing peptide, this methodology could not be applied for multi-step ligation purposes.

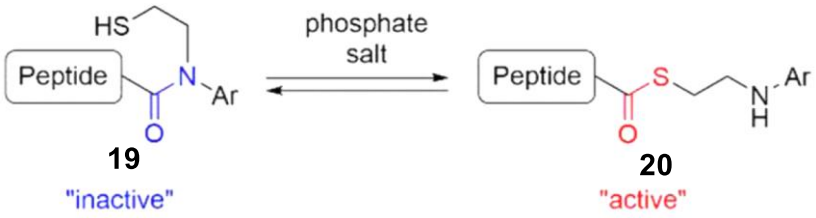

Figure 1-5 The mechanism of phosphate-triggered SEAlide activation which is readily reactive toward chemical ligation. The figure was adapted and reproduced from Aihara et. al. [20].

To address this problem, they developed a photo-activatable SEAlide moiety. This was achieved by caging the sulfhydryl functionality on the SEAlide using DMNB protecting group (Figure 1-6). This enables one-pot sequential native chemical ligation (NCL) using light as an external trigger This strategy was successfully employed in a four-fragment sequential synthesis of 41 amino acid SNX-482 peptide (**29**, Figure 1-6), a potent inhibitor for of R-type Ca^{2+} channels isolated from the tarantula *Hysterocrates gigas*. In the first step, peptides **21** and **22** were ligated under standard NCL conditions to yield peptide **24**. Before each photolysis step, thiophenol was removed via extraction to avoid generation of high energy thiyl radicals which could lead to formation of several byproducts. Photolysis of **24** resulted in deprotection of DMNB group and generated peptide **25**. Addition of thiophenol together with **23** to the solution containing **25** resulted in formation of **26**. Another round of thiophenol extraction followed by photolysis yielded **27**. Finally, NCL between **27** and **28** resulted in formation of fully ligated product **29**. These results demonstrate the utility of combining SEAlide chemistry with thiol photo-caging strategies as a powerful tool for sequential and convergent syntheses of polypeptides and proteins.

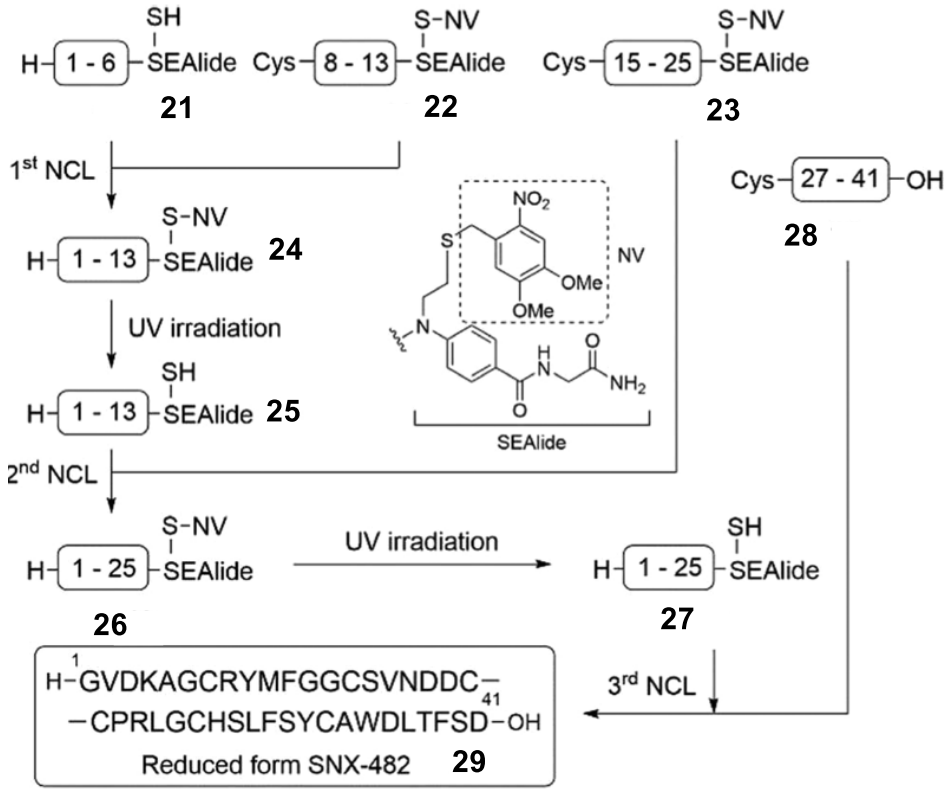

Figure 1-6 Strategy developed by Otaka and coworkers for peptide/protein synthesis using photocaged SEAlide moiety. The figure was adapted and reproduced from Aihara et. al. [20].

In addition to applications in chemical ligations, ONB deriveshave been used for directed disulfide bond formation in peptides. Hossain and coworkers utilized DMNB (also referred to as 2-nitroveratryl group) for photo-cleavable thiol protection in combination with S-pyridinesulfenyl activation to achieve rapid photo-triggered generation of disulfide bonds in peptides (Figure 1-7A).[25] This strategy was successfully employed for the solid phase synthesis of cysteine-rich peptides, including oxytocin, α-conotoxin ImI and human insulin. Synthesis of α-conotoxin ImI **35** is depicted in Figure 1-7. Initially a Fmoc-Cys(DMNB)OMe residue is incorporated into peptide through traditional solid phase peptide synthesis. After

isolation of precursor **32**, disulfide bond formation was achieved upon treatment with dipyridine disulfide (DPDS) to give peptide **33**. S-tbu cleavage of **33** followed by concomitant S-pyr functionalization yielded peptide **34**. Photolysis of **34** at 350 nm resulted in thiol deprotection and rapid in situ disulfide formation to generate desired α-conotoxin ImI. In order to show the utility and versatility of this approach, the same procedure was used for synthesis of more complex human insulin.

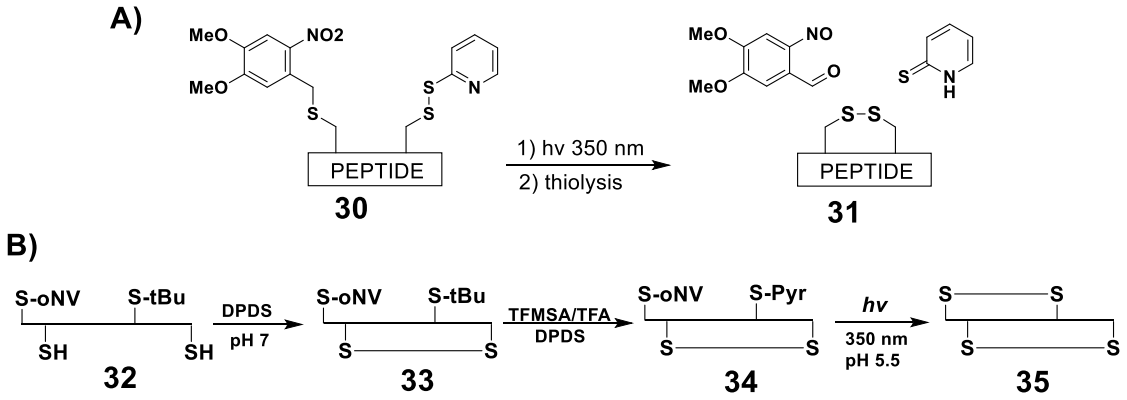

Figure 1-7 A) Reaction mechanism for disulfide bond formation via photocleavage of the DMNB group followed by subsequent thiolysis through S-pyridinesulfenyl activation. B) This strategy was employed for the synthesis of α- conotoxin. The figure was adapted and reproduced from Karas et. al. [25].

Applications of ONB-derived groups for thiol caging is not limited to peptide or protein synthesis. Several reports demonstrated ONBs' utility in development of photo-activatable probes useful for biological investigations. Distefano and coworkers utilized CNB group for cysteine protection of peptides that are substrates for protein farnesyl transferase (Figure 1-8).[26] ^{3}H-FPP (farnesyl diphosphate) assays which were used to quantify the extent of farnesylation, revealed that the caged peptide KKKSKTKC(CNB)VIM was not processed by the

protein farnesyltransferase (PFTase). However, irradiation at 365 nm released the free peptide which was subsequently processed by PFTase and become farnesylated (peptide **37**). The uncaging yield was 60% and the quantum yield was measured to be 0.16 higher the reported value by Hagen and coworkers.

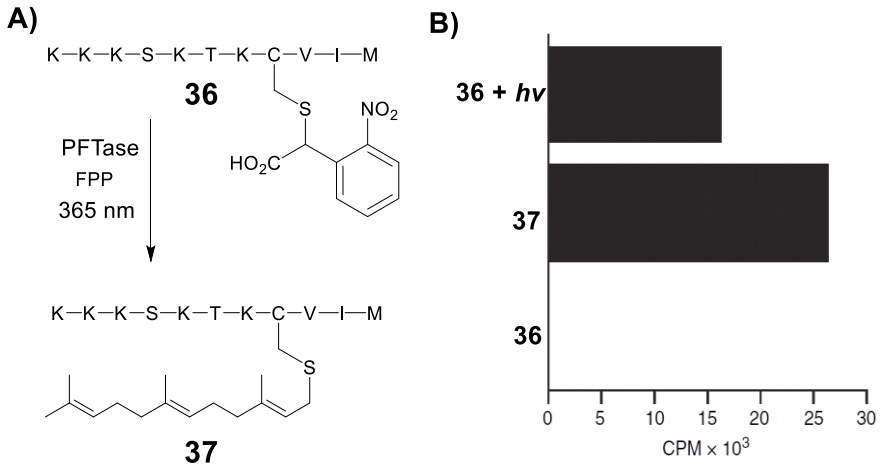

Figure 1-8 A) Schematic representation of the peptide photo-release and concomitant farnesylation of the caged peptide. B) Farnesylation of caged peptide before and after irradiation quantified via ^{3}H-FPP assays. The figure was adapted from Degraw et. al. [26] and reproduced.

Lawrence and coworkers used CNB for development of a caged protein involving in cell signaling pathway.[27] Cofilin plays a pivotal role in cell motility through polymerization and depolymerization of actin filaments. This enzyme is regulated via phosphorylation of Ser-3 residue. However, S3C mutants of cofilin are unable to be phosphorylated and thus remain constitutively active. Using CNB on the Cys-3 thiol, they have created a caged cofilin which, according to in vivo assays shown in Figure 1-9, could not depolymerize actin. However, UV irradiation of the caged enzyme restored the activity of the mutant enzyme and resulted in actin

depolyermization. HPLC assays revealed photolysis of caged cofilin could restore 90% of its activity. Next, in order to further elaborate the role of cofilin in cell motility, the developed photo-activatable protein was injected into cells. Through acute and local activation of the caged enzyme via irradiation, they demonstrated that cofilin polymerizes actin, generates protrusions and determines the direction of cell migration.[28]

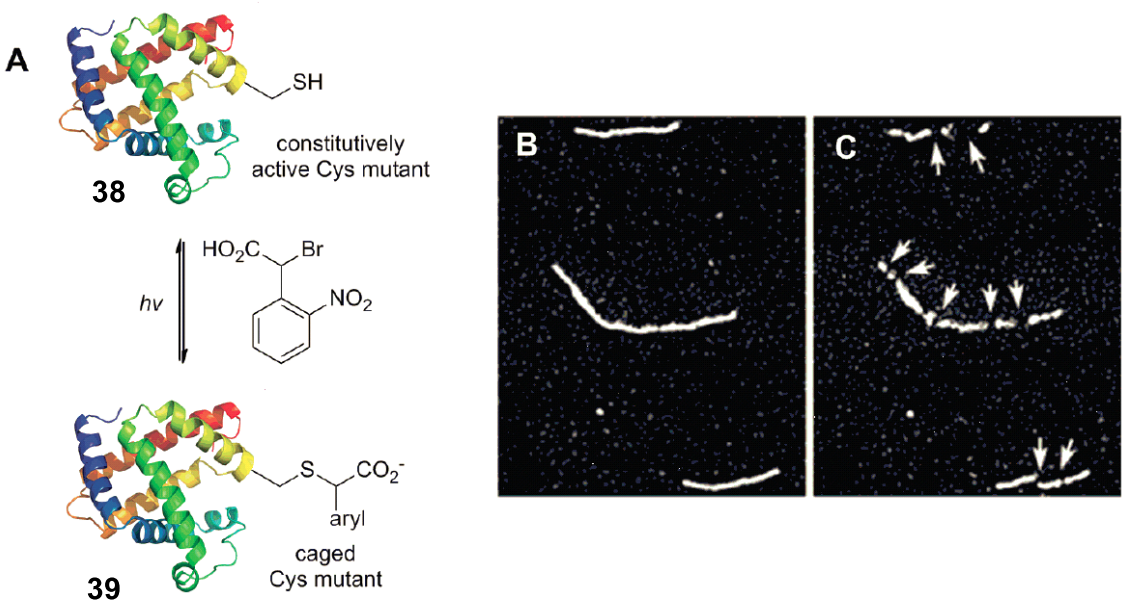

Figure 1-9 (A) Synthesis of caged cofilin mutant, B) Rhodamine-labeled F-actin filaments are not cleaved by caged cofilin, (C) 15 min UV photolysis released the mutant enzyme resulted in actin depolymerization. Cleavage sites are shown by arrows. The figure was adapted from Ghosh et. al. [27] and reproduced.

Bayley and coworkers utilized ONB, CNB, DMNB groups for caging a critical cysteine residue in the catalytic subunit of cAMP-dependent protein kinase (PKA).[29] They compared the efficiency of each caging group toward deactivation of PKA as well as their ability to restore the enzymatic activity upon UV irradiation and photo-cleavage. In this case, ONB was the best caging group, since not only

did the ONB-protected PKA show the least residual activity, but also protein activity was restored to the highest degree upon irradiation. ONB-caged PKA showed 20-30 fold increase in protein activity upon photolysis, making it useful for biological experiments. Photolysis of CNB- and DMNB-caged PKA, however, resulted in only 2-3 fold increase in activity. They also studied the effect of pH on uncaging efficiency of ONB. Analysis of photolysis reactions at different pHs revealed that the uncaging is significantly more efficient under slightly acidic (pH 6) relative to slightly basic conditions (pH 8.5). The quantum yield was measured to be 0.84 in acidic conditions which is significantly larger than that of basic ones which was measured to be 0.14.

As an alternative to chemical methods for protein caging, Schultz and coworkers for the first time used unnatural amino acid incorporation technique to genetically incorporate caged cysteine into different proteins (Figure 1-10).[30] They generated a new orthogonal *Escherichia coli* tRNALeu/leucyl tRNA-synthetase pair that was used to selectively incorporate caged ONB-cysteine **40** into protein in yeast in response to amber nonsense codon TAG. This strategy was used to generate a caged cysteine protease, caspase 3. The activity of the caged enzyme was measured in cell lysates before and after 10 min UV irradiation. In vitro enzymatic assays revealed that 40% of the caged caspase was converted to the active enzyme under aforementioned photolysis conditions.

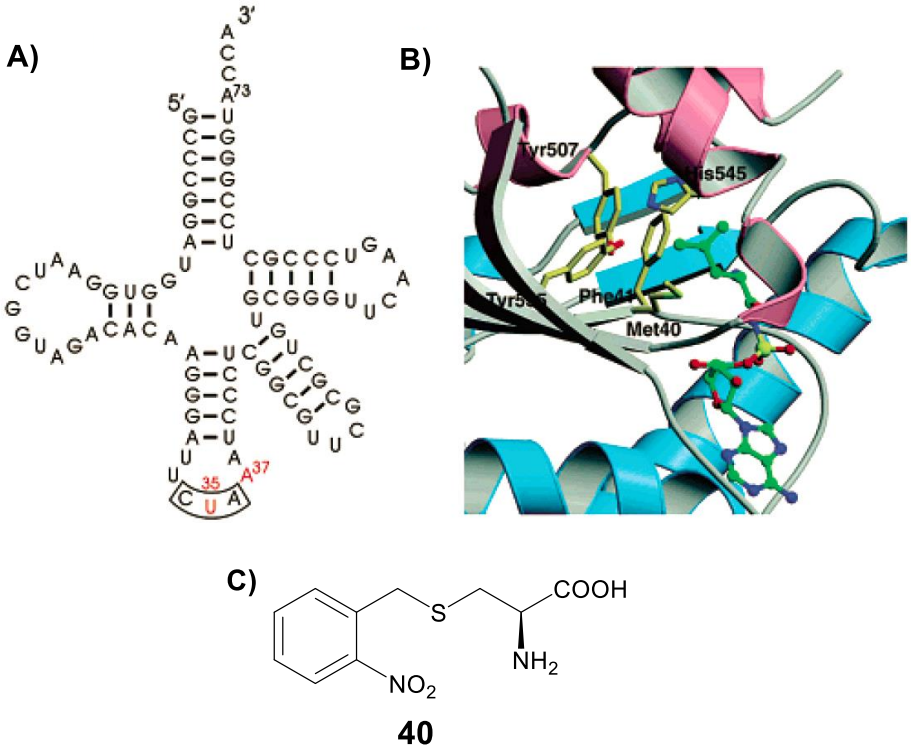

Figure 1-10 (A) Primary sequence of the leucyl suppressor tRNA, Leu5$_{CUA}$. (B) The active site of leucyl tRNA-synthetase is shown with a bound leucyl sulfamoyl adenylate inhibitor (green). The residues randomized in generating the synthetase library are in yellow. The catalytic domains of synthetase are in pink. (C) Structure of o-nitrobenzyl cysteine being incorporated using this tRNA/Synthetase pair. The figure was adapted from Wu et. al. [30] and reproduced.

Using the same technique but a different approach, Deiters and coworkers engineered the molecular structure of caged cysteine and homocysteine and were able to employ an existing M. barkeri pyrrolysine tRNA synthetase (PylRS) mutant to express caged protein in bacteria and mammalian cells.[31]

1.3 Coumarin-based caging groups

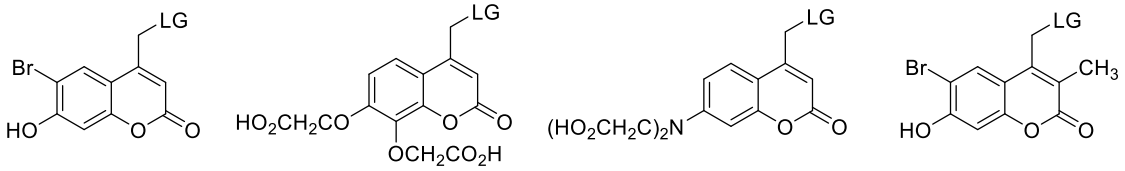

Figure 1-11 An overview of various coumarin-based photo-removable protecting groups that have been used for sulfhydryl protection.

Coumarin-based caging groups (Figure 1-11) have generally been used for protection of carboxyls and alcohols. Attractive features of coumarins relative to their ONB-based counterparts are their high absorptivity at longer wavelengths, faster uncaging rate, fluorescent properties, improved solubility and larger two-photon cross-section However, the application of coumarin-based caging groups for thiol protection has only been studied in recent years mostly by Hagen,[32] Distefano[16,33,34] and Shoichet[35–37] groups.

Hagen and coworkers developed two water soluble coumarin-based derivatives, [7,8-Bis(carboxymethoxy)coumarin-4-yl]methoxycarbonyl] (7,8BCMCMOC, **42**, Figure 1-11) and [7-[bis(carboxymethyl)amino]coumarin-4-yl]methoxycarbonyl] (BCMACMOC, **43**, Figure 1-11). These two compounds were utilized for the development of caged cysteines. In their design, both of the caged cysteines were masked through thio-carbamate linkages(Figure 1-12), and the developed caged moieties were incorporated into peptides using solid-phase peptide synthesis. Because the light absorption characteristics ofcompounds **42** and **43** are highy

differentiable, withλ_{max} of 324 nm and 385 nm, respectively, they were able to be irradiated and removed in a wavelength-selective fashion. As shown in Figure 1-12B, a mixture of **45** and **46** was first photolyzed at 402 nm and subsequently at 325 nm, and the amount of released cysteine was quantified. As predicted, irradiation at 402 nm resulted in deprotection of cysteine **46** while further photolysis at 325 nm resulted in the deprotection of the remaining cysteine. However, uncaging of **46** at 402 nm and **45** at 325 nm produced cysteine with only 60 and 40% yield respectively.

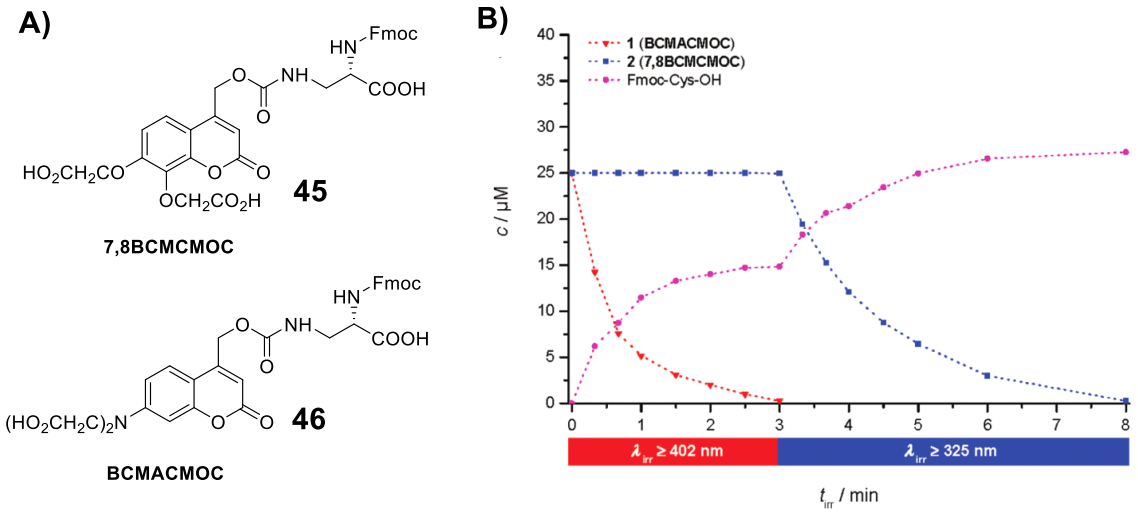

Figure 1-12 A) Structures of Fmoc-cysteine protected with coumarin-based hydrophilic coumarin-based photo-removable protecting group, B) Wavelength selective uncaging of caged cysteines. The figure was adapted from Kotzuer et. al. [32] and reproduced.

This wavelength-selective binary system was then used for the synthesis of a caged model peptide called resact (**50**, Figure 1-13). Resact is a 14-mer peptide containing two cysteines which is well studied as the sperm attractant in the sea urchin *Arbacia punctulata*. In order to avoid any intramolecular S- to N- acyl shift during the solid phase synthesis, Fmoc cleavages were carried out via short

treatment with DBU, and the N-terminal amine was also acetylated. As expected, photolysis of the caged peptide at 402 nm resulted in selective uncaging of Cys^1; however, S-acyl transfer from Cys^8 to Cys^1 resulted in the generation of an equimolar mixture of 7,8BCMCMOC-masked Cys^1 and Cys^8.. Although, subsequent irradiation at 325 nm led to the generation of fully deprotected peptide, these results reveal limitations in applicability of thiocarbonates for selective thiol caging and also cysteine protection in peptides, particularly those with free N-terminus.

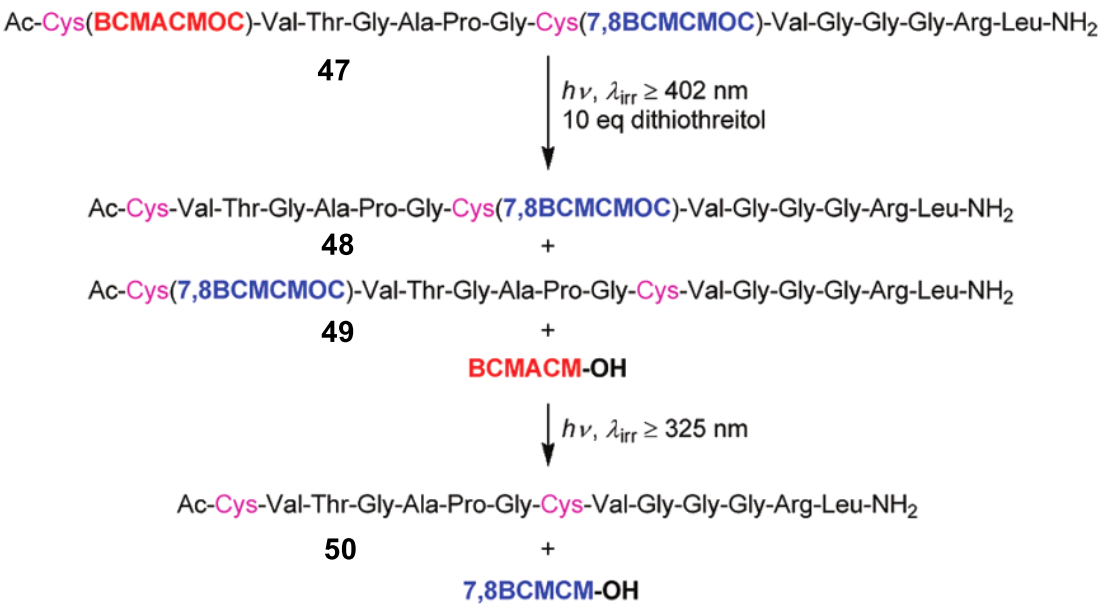

Figure 1-13 Two-step wavelength selective photolysis of caged resact. The figure was adapted from Kotzuer et. al. [32] and reproduced.

As an alternative to Hagen's thiocarmbamate-linked thiol protection, Distefano and coworkers developed a caged farnesyl transferase inhibitor in which the thiol functionality is masked by a bhc (bromohydroxy coumarin) protecting group

through direct thioether linkage(Figure 1-14).[34] HPLC analysis of photolysis experiments revealed that the uncaging yield achieved by one-photon process is > 60% and > 40% via two-photon irradiation. The quantum yield was measured to be 0.074. Interestingly, LC-MS analysis of the photolyzed mixtures revealed generation of a small amount of photo-isomeric byproduct which was attributed to S- to N-alkyl shift. The designed caged inhibitor was then used for photo-controlled modulation of farnesylation inside different types of cell lines. For example, treatment of the caged PFTase inhibitor **53** with fibroblast cells resulted in no change in cell morphology in comparison with vehicle treated cells. However, exposure of the caged inhibitortreated cells to either one- (365 nm) or two-photon (800 nm) irradiation resulted in radical morphological changes similar to cells treated with free inhibitor. This experiment was one of the first two-photon triggered cellular experiments utilizing caged thiols.

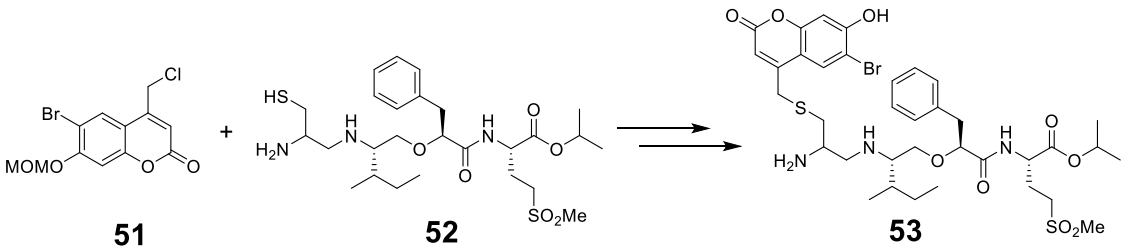

51 **52** **53**

Figure 1-14 Synthesis of caged farnesyl transferase inhibitor **53**.

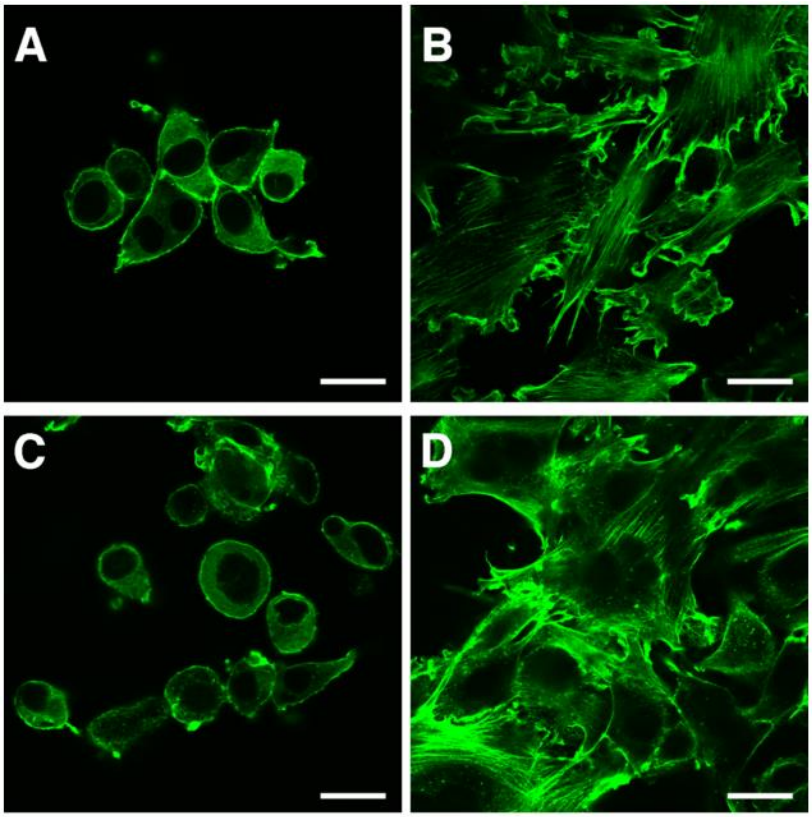

Figure 1-15 Morphology of fibroblast ciras-3 cells treated with Bhc-FTI. A) Untreated cells, B) treated with 2.5 μM FTI, C) treated with 2.5 μM Bhc-FTI with no irradiation, D) treated with 2.5 μM Bhc-FTI followed by 1h two-photon irradiation at 800 nm. The figure was adapted from Abate et. al. [34] and reproduced.

Shoichet and coworkers for the first time harnessed caged thiols for photo-patterning purposes in biomedical applications. In their design, bhc protected cysteamine moieties were incorporated into hydrogel matrix. Upon irradiation via two-photon laser, highly defined volumes of free sulfhydryl groups were generated and ultimately used as anchors to immobilize different types of thiol reactive biomolecules such as maleimide-linked peptides and proteins (Figure 1-16A).[36] As an example, they employed this strategy to create three dimensional patterns of stem-cell differentiation factors sonic hedgehog (SHH) and ciliary neurotrophic

factor (CNTF) inside agarose gel (Figure 1-16 B, C).[35] To achieve this, they initially used two-photon sulfhydryl uncaging to sequentially immobilize maleimide-barnase and maleimide-streptavidin. Orthogonal physical binding pairs, barnase-barstar and streptavidin-biotin, were then employed to immobilize fusion proteins barstar–SHH and biotin–CNTF, resulting in highly defined bioactive 3D patterned hydrogels. This technique sets the stage for the development of highly defined, chemically complex scaffolds, which enables the study of the effect of extracellular matrix on cell fate, migration and differentiation.

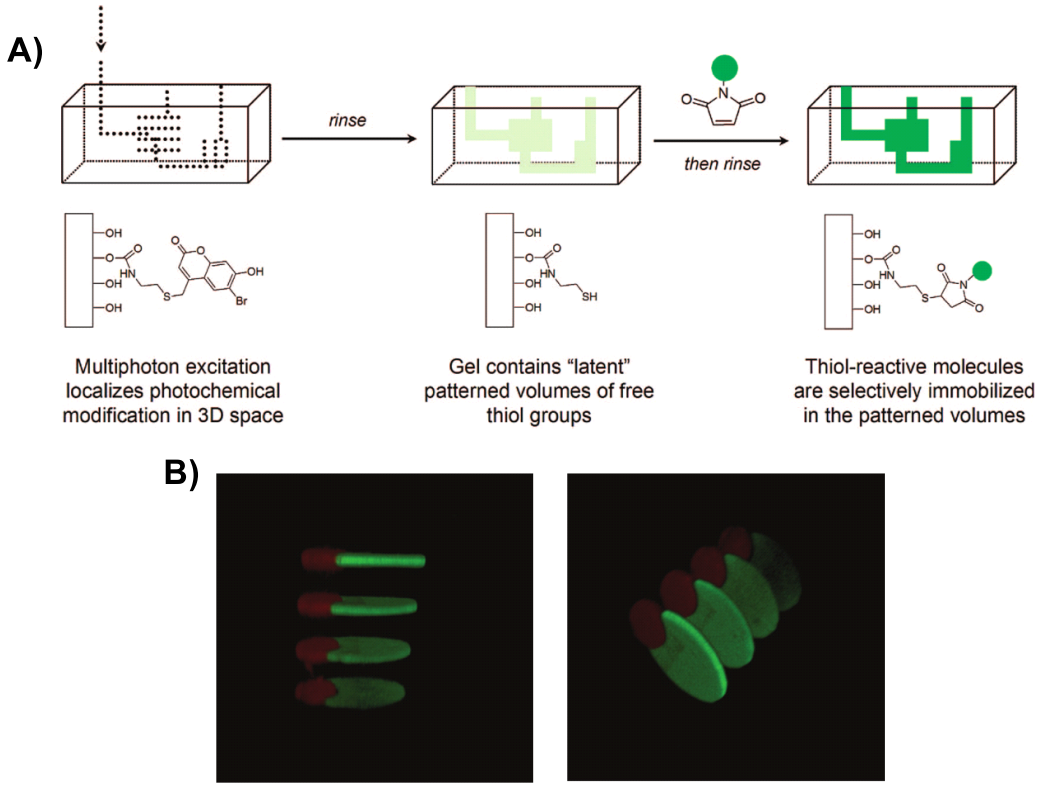

Figure 1-16 A) Schematic illustration of multi-photon chemical patterning in hydrogel incorporating caged thiol moieties, B, C) Representative figures for the simultaneous 3D patterning of biotin–CNTF–633 (green) and barstar–SHH–488 (red). The figures were adapted from [36] and [35].

Despite the reported use of Bhc for successful thiol protection, further studies by Distefano and coworkers on caged peptides revealed that the uncaging efficiency of Bhc, along with other relevant coumarin-based protected thiols, are significantly limited by an unwanted photo-isomeization reaction pathway.[16] Thorough mechanistic analysis of photolysis of caged small molecules as well as peptides, they have demonstrated that the major product of photolysis of Bhc-protected thiols is not the free thiol, but rather an isomeric product formed via the two step process depicted in Figure 1-17. They have proposed that the first step involves a photo-induced 1,3 shift of the thiol from the exocyclic position to the endocyclic 3 position yielding intermediate **55**, which undergoes tautomerization to produce the final photo-rearranged product **56**. These results demonstrate that coumarin-based caging groups, and Bhc in particular, are not efficient caging groups for thiol protection.

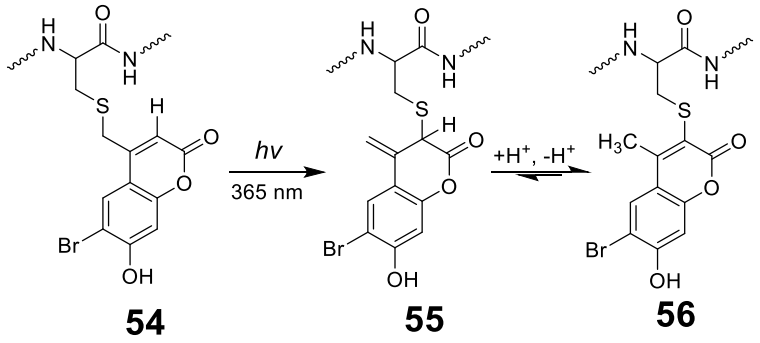

Figure 1-17 Photo-rearrangement mechanism of Bhc protected cysteine.

In an effort to create a more efficient coumarin-based protecting group, Distefano and coworkers developed 6-bromo-7-hydroxy-3-methyl coumarin-4-ylmethyl (mBhc, **44**, Figure 1-11) as a Bhc analogue which yields efficient thiol release upon both one- and two-photon photolysis.[33] Guided by the mechanism of Bhc photo-isomerization, they hypothesized that replacing hydrogen at the endocyclic 3 position with a methyl group would eliminate the photo-isomerization pathway. An

analogous intermediate to **55** would be unable to rearomatize, and furthermore, unfavorable syn-pentane type steric interactions between the sulfhydryl and methyl groups would destabilize the necessary conformation of thiol migration (Figure 1-18 A, B). The designed mBhc group was used for thiol protection in peptides, and HPLC analysis of photolysis reactions revealed that conversion of the mBhc protected peptide to the free peptide proceeded cleanly without any byproduct formation due to undesired photoisomerization. Spectral properties of mBhc showed minimal alteration relative to those of Bhc. The uncaging quantum yield (at 365 nm) and two-photon action cross-section (at 800 nm) of mBhc caged thiol was measure to be 0.013 and 0.16 GM, respectively.

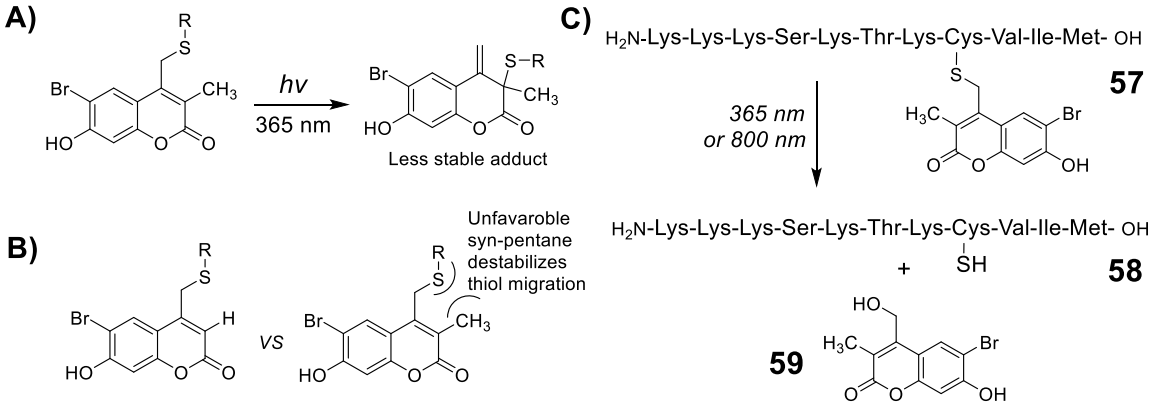

Figure 1-18 A, B) Illustration of potential effects of C-3 substitution on photo-isomerization process. C) Uncaging reaction of mBhc-protected peptide. The figure was adapted from Mahmoodi et. al. [33] and reproduced.

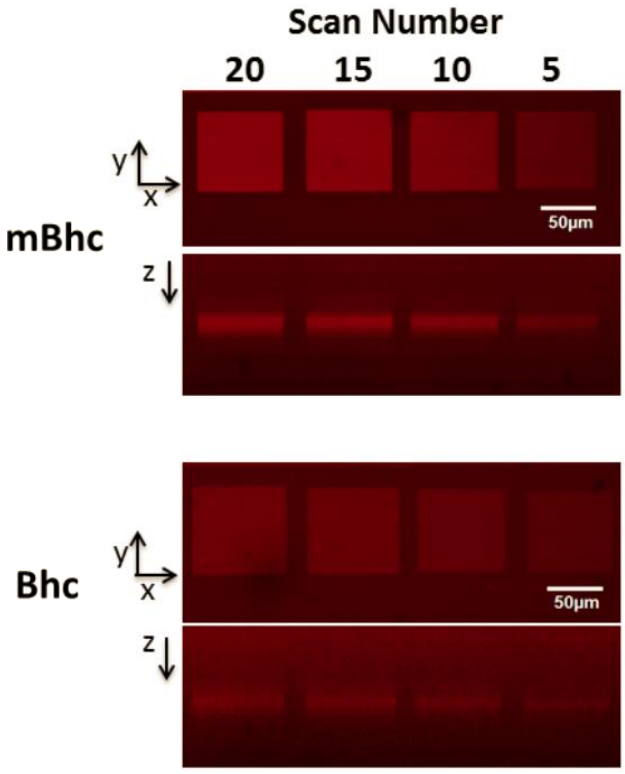

Figure 1-19 Comparison of two-photon patterning using Bhc- and mBhc-caged thiol. Uncaging of Bhc or mBhc-conjugated HA hydrogels, and subsequent immobilization of Alexa Fluor 546. The figure was adapted from Mahmoodi et. al. [33] and reproduced.

To demonstrate the utility of this new caging group for biomedical application, in collaboration with Shoichet's group, they incorporated mBhc caged cysteamine into cross-linked hyaluronic acid hydrogels.[33] Using multiphoton irradiation at 800 nm, they generated highly localized free thiols inside hydrogels which then reacted with maleimide-Alexa Fluor creating 3D fluorophore patterns. The photo-patterning efficiency of hydrogels incorporating mBhc versus Bhc protected thiols were measured by comparing the intensity of immobilized fluorophore upon similar laser exposure. As shown in Figure 1-19, the intensity of thiol labeling was 4-fold higher in hydrogels prepared using mBhc compared with Bhc due to the greater uncaging efficiency of the former. These results demonstrate mBhc as a coumarin-based

caging group able to mediate efficient thiol release upon both one- and two-photon irradiation and represents a marked improvement over Bhc.

1.4 Nitrodibenzofuran Cages for Thiols

The Nitrodibenzofuran (NDBF) caging group, developed by Davies and coworkers, has also been used for alcohol and carboxyl protection. The NDBF scaffold contains an *o*-nitro moiety, which can be likened to the previously described ONB-based caging groups. NDBF possesses the attractive features of ONBs, fast uncaging rate, large molar absorptivity, high quantum yields and high two-photon sensitivity. These improved properties demonstrated with alcohol and carboxyl protection highlight NDBF as an attractive candidate for variety of additional caging applications including thiol protection.

In an effort to develop one- and two-photon activatable cysteine containing peptides, Distefan d coworkers for the first time applied NDBF for thiol protection.[16] They have synthesized Fmoc-Cys(NDBF)OH and incorporated it into various peptides of interest through traditional Fmoc-based solid-phase peptide synthesis (SPPS). Since thiol protection was through stable thioether bonds, there was no evidence of protecting group migration or removal during SPPS, which is often observed when using thiocarbamate-protected cysteines. Using this strategy, they have developed a cysteine-protected version of the K-Ras derived peptide substrate for PFTase (**60**, Figure 1-20). Incubation of the caged peptide with PFTase resulted in no peptide recognition by the enzyme. However, irradiation at either 365 nm (one-photon) or 800 nm (two-photon) resulted in free peptide release, which was subsequently recognized by PFTase and became

farnesylated. HPLC analysis of the photolyzed samples over the course of irradiation time revealed one-photon uncaging quantum yield to be 0.2 at 365 nm and two-photon action-cross section to be 0.13 GM at 800 nm. Clean and quantitative conversion of the caged to the free peptide without any undesired byproduct formation was also confirmed. These data recommend NDBF as the most efficient thiol-protecting group explored to date.

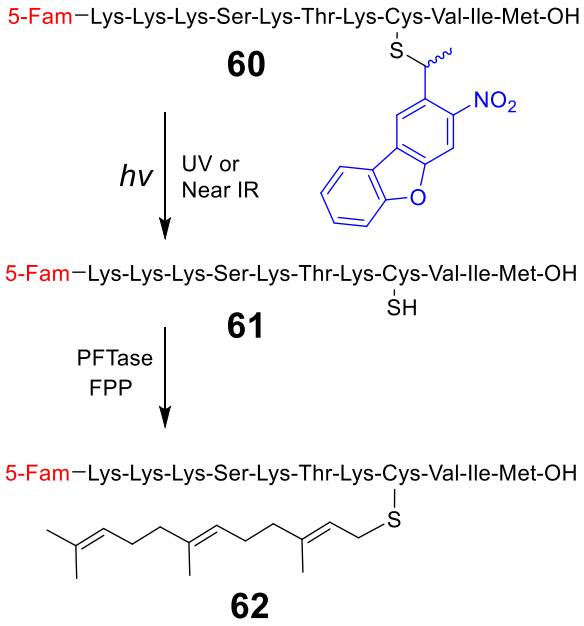

Figure 1-20 Photo-uncaging of KKKSKTKC(NDBF)VIM and subsequent farnesylation by PFTase enzyme. The figure was adapted from Mahmoodi et. al. [16] and reproduced.

In order to show the utility of this approach for peptide activation inside cells, they utilized this strategy for caging peptides such as Hex-CLC(Sfarnesyl)-OMe (Figure 1-21), which is a substrate for protein palmitoyl acyltransferase (PAT). Prior to palmitoylation of Hex-CLC(Sfarnesyl)-OMe, the peptide resides mainly in the cytosol and the Golgi; however, palmitoylation of the free cysteine by PAT inside

cells results in migration of the peptide to the plasma membrane. Therefore, a thiol-caged analogue of Hex-CLC(Sfarnesyl)-OMe cannot be a substrate for PAT and would thus localize in the cytosol/Golgi. Irradiation should uncage the peptide, revealing a free thiol which would become palmitoylated and result in peptide localization in the plasma membrane.

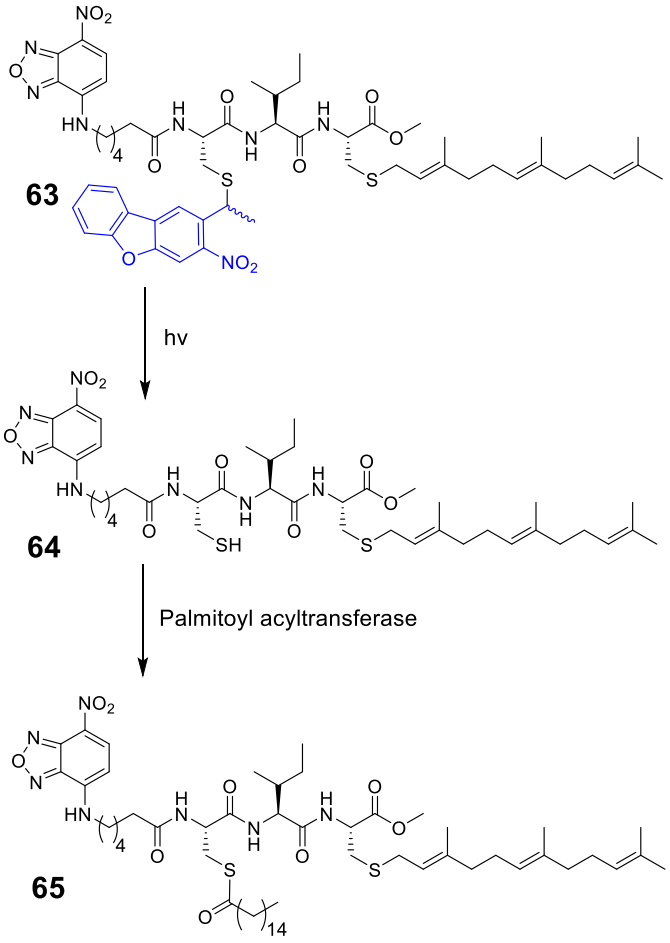

Figure 1-21 Schematic Representation of NBD-HexC(NDBF)LC-OMe uncaging and subsequent palmitoylation. The figure was adapted from Mahmoodi et. al. [16] and reproduced.

To test this hypothesis, a cysteine protected cell-penetrating peptide was developed and incubated with human ovarion carcinoma cells (SKOV-3). As

depicted in Figure 1-22, before any irradiation the peptide mainly localizes into cytosol; however, after irradiation the generated free peptide become palmitoylated and migrates to the plasma membrane. These results suggest that NDBF is an efficient thiol caging group for development of photo-activatable probes in cells and tissues useful for cell biology studies.

a

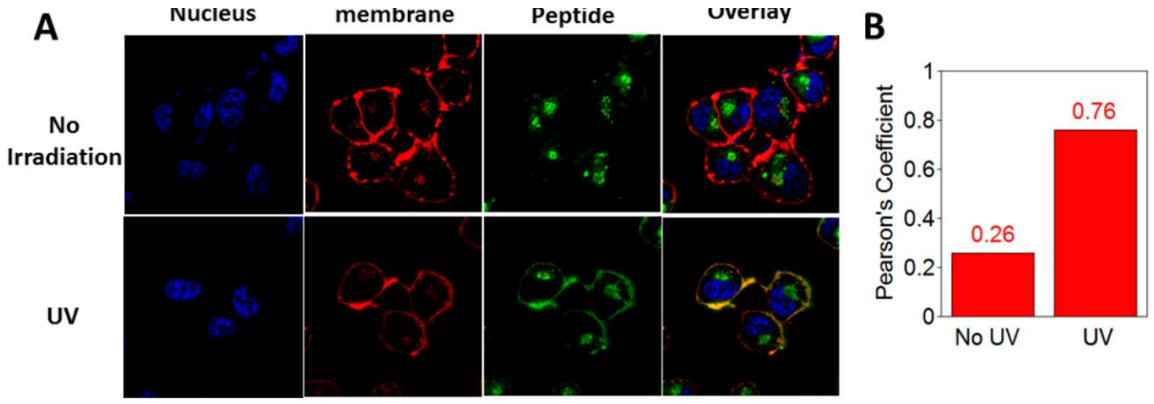

Figure 1-22 Live-cell experiments showing temporal control of enzymatic palmitoylation via NDBF-thiol caging. (A) Images obtained by fluorescence confocal microscopy illustrating intracellular localization of fluorescently labeled peptide 20 in SKOV3 cells, before (top) and after (bottom) UV exposure. (B) Quantification of colocalization of peptide and membrane dye via Pearson's coefficient analysis, indicating a significant increase in plasma membrane localization of peptide upon irradiation. The figure was adapted from Mahmoodi et. al. [16] and reproduced.

1.5 p-Hydroxyphenacyl Cages for Thiols

p-Hydroxyphenacyl (pHP) chromophores were introduced over a decade ago and have found a variety of applications as photo-removable protecting groups in enzyme catalysis, neurobiology and organic synthesis.[4] Among the advantageous properties of pHP groups are water solubility, ease of synthesis and high yield of

installment. Pei and coworkers reported the first usage of pHP for thiol caging in enzymes (Figure 1-23).[38] In their study, pHP was among various phenacyl derivatives that were used for generation of caged cysteine residues in tyrosine phosphatases. Direct treatment of the protein with pHP-Br (**66a,** Figure 1-23 A) resulted in selective modification of desired cysteine with high yield, confirmed by MS analysis. In order to evaluate the uncaging ability of the pHP compounds, caged enzymes were irradiated, and the restored activity was measured. According to enzymatic assays, photolysis at 350 nm restored 80% of the activity of the full enzyme (SHP-1), while only restored 30 % of the catalytic domain (SHP-1(ΔSH2)). No further photochemical analysis was carried out in this research.

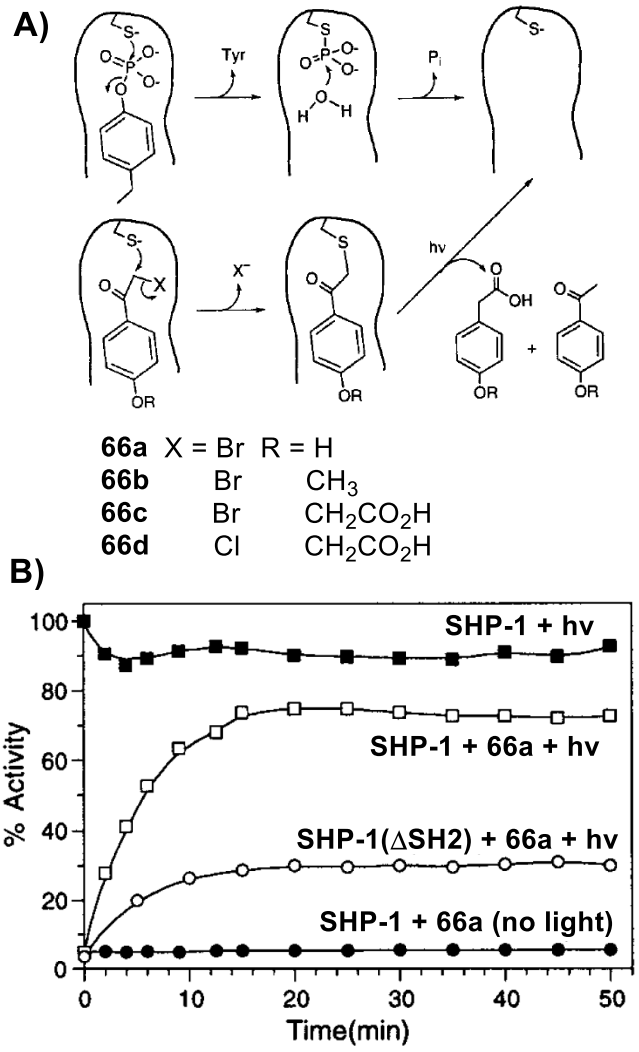

Figure 1-23 A) Mechanism of tyrosine phosphatase catalysis, and inactivation via pHP protection, B) In vivo enzymatic assays, showing restoration of tyrosine phosphatase activity upon UV irradiation which leads to pHP uncaging. The figure was adapted from Mahmoodi et. al. [38] and reproduced.

Specht et. al. carried out a more in-depth analysis of pHP properties for thiol caging.[39] They have utilized pHP for thiol protection in cysteine, thymidine nucleoside and glutathione derivatives (Figure 1-24 A). The caged biomolecules were synthesized with high yield due to the ease of installment of pHP as an α-bromo acetophenone. Caged molecules were photolyzed at 312 nm and analyzed

by HPLC, UV-vis spectroscopy and MS. As shown in Figure 1-24 B, photolysis of compound **69a** and **69b** resulted in generation of unmasked thiol together with small fraction of disulfide with overall yield of 65 and 70%, respectively. Besides formation of the free thiols, three other photolysis side-products were generated in all three reactions: the expected p-hydroxyphenylacetic acid together with p-hydroxy acetophenone as well as a new compound, the p-hydroxyphenylacetic thioester, derived from the biomolecules. Thioesters were produced in 30% yield, lowering the efficiency of thiol release. Uncaging quantum yield of **69b** was measured to be 0.08 which is lower than the valued obtained for caged carboxylates and phosphates.

A)

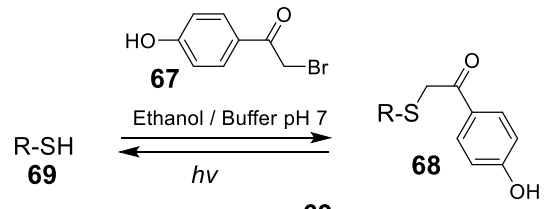

RSH = N-Bz-Cysteine-OMe **69a**
RSH = 3'-Thio-deoxythymidine Phosphate **69b**
RSH = 3'-Glutathione **69c**

B)

Compound Photolytic products	69a %	69b %	69c %
RSH (RSSR)	60 (5)	71	ND
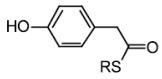	30	29	23
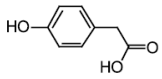	60	62	65
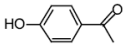	10	9	12

Figure 1-24 A) Thiol derivatives caged by pHP group. B) Product yields generated by 312 nm irradiation of pHP caged thiols. The figure was adapted from Mahmoodi et. al. [39] and reproduced.

1.6 Benzoin and Benzoyl Cages for Thiols

Benzoin- and Benzoyl-based groups have generally been utilized for carboxyl and alcohol protection. Application of these molecules for thiol caging is limited, with few reports in the literature. Hence, much needs to be explored regarding the efficiency and photo-physical properties of these chromophores for thiol protection. Bradley and Pirrung, utilized dimethoxy benzoin (DMB) for protection of benzyl thiol as a thiocarbonate.[40] Photolysis at 350 nm in benzene resulted in high yield (> 95%) of conversion to the free thiol. No additional experiments were carried out in this article to further establish the photo-physical properties of this chromophore.

Porter and coworkers utilized 2-benzoylbenzoic acid for masking organic thiols as thioesters.[41] To obtain efficient uncaging using this chromophore, photolysis reactions needed to be carried out in presence of proton donors (alcohols) or electron donors (amines) which imposes limitations on the utility of this caging group for biological applications. According to NMR analysis, photolysis of caged thiols in the presence of cyclohexyl amine resulted in conversion to the free thiol (60%) and the corresponding disulfide (20%). No further photophysical measurements were performed on these caged thiols.

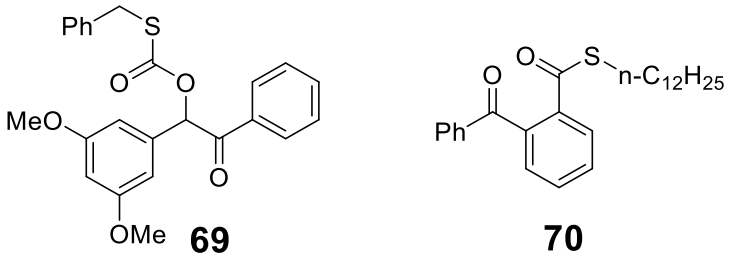

Figure 1-25 Structures of 3,5-dimethoxybenzoin (DMB) caged phenylmethylthiol and 2-benzoylbenzoic acid caged aliphatic thiol. The figures were adapted from [40] and [41].

1.7 Conclusion

Thiols play unique and important roles in various aspects of biology and chemistry and have strong potential for use in biomaterial applications. This is in part the result of their high reactivity and nucleophilicity. On the other hand, sulfhydryl is a relatively poor leaving group in comparison to carboxyl and phosphate. These properties pose specific challenges when choosing efficient and broadly applicable caging groups suitable for thiol caging. Therefore, several caging groups have been explored and developed for sulfhydryl protection. Table 1-1 summarizes

spectral and photochemical properties of photocleavable protecting groups covered in this review.

Thus far, ONB-based groups are the most commonly used approach for thiol protection. They are easy to install, possess modest quantum yield and high yield of photo-conversion. These compounds have been extensively used as orthogonal cysteine protecting group for peptide and protein synthesis as well as development of photoactivatable sulfhydryl-containing probes for biological studies. Unfortunately, ONBs generally have low one- and two-photon absorptivity, which limits their applicability in biological studies where photo-damage is a concern and uncaging in deeper tissues is necessary.

Alternatively, coumarin-based protecting groups possess longer absorption maxima, larger one- and two-photon absorptivity. Their quantum yield is relatively low; however, and more importantly their release efficiency is largely limited by the formation of an unwanted photo-isomerized by-product. Recent development of mBhc, which does not undergo photo-isomerization upon irradiation, significantly extends the utility of coumarin-based compounds for thiol protection. Additionally, the systematic design of mBhc which was guided by mechanistic studies of the photo-triggered isomerization of Bhc caged-thiols, sets the stage for further development of more efficient caging groups based on coumarin structure. Recently, several research groups have developed coumarin derivatives, with substitution at their C-3 endocyclic position, similar to mBhc. These compounds have been successfully used for alcohol and carboxyl release. Hence, they will be great candidates to be tested for sulfhydryl protections, as well.[42,43]

Phenacyl has shown to be easily installed on small molecules as well as proteins, and possess modest quantum yield. However, their release efficiency is limited by a formation of an unwanted thioester-based by-product. Their absorptivity is also comparatively low and moreover they are not two-photon active. More work is needed to fully evaluate the efficiency and reliability of benzoin and benzoyl cages for thiols. Dimethoxy benzoin has only been used for masking thiol as a thiocarbonate, but never used for direct thiol protection. Benzoyl group showed high yield of photo-release, although photolysis was supposed to be carried out in presence of amines, which is not ideal for biological studies.

To date, NDBF is the most promising photocleavable protecting group utilized for thiol caging. This compound possesses large absorptivity, high quantum yield, and large two-photon sensitivity, together with quantitative thiol photorelease. NDBF has been successfully utilized for sulfhydryl protection in both peptides and organic molecules and was shown to be cleaved via both one and two-photon irradiation. The only problematic feature of this protecting group is its comparatively low water solubility, particularly when used for caging poorly water soluble bio-agents. This necessitates development of more water soluble NDBF analogues. Additionally, the reliability of NDBF for thiol protection warrants further modification of this compound to generate even more efficient NDBF-based caging groups with longer λ_{max} and significantly improved two-photon sensitivity. This also suggests ONB-based groups with extended conjugation, such as ortho-nitrobiphenyl derivatives developed by Specht and coworkers,[44] and 2-(4-nitrophenyl)benzofuran

developed by Kobayashi and coworkers,[45] as great candidates to be evaluated for sulfhydryl protection.

Caging Groups	Spectral and Photo-chemical properties	Cons and Pros when used for thiol caging
Ortho-nitrobenzyl (ONB)	$\varepsilon(M^{-1}cm^{-1})$ = 2000 (**7**) - 4000(**9**) λ_{max}(nm) = 265 (**7**), 356 (**9**) Q_u = 0.04 – 0.16	- Modest uncaging yield. - Case sensitive uncaging yield. - Low one- and two- photon absorptivity
Coumarin	$\varepsilon(M^{-1}cm^{-1})$ = 11000 (**42**), 14000 (**44**), 18500 (**43**) λ_{max} (nm) = 324 (**42**), 365 (**43**), 384 (**44**) Q_u = 0.01 δ_u (GM) = 0.16 GM (at 800 nm)	- Low uncaging yield: Mainly photo-isomerizes upon uncaging except for mBhc-protected thiols. - Two-photon active.
Nitrodibenzofuran (NDBF)	$\varepsilon(M^{-1}cm^{-1})$ = 18400 λ_{max} = 330 nm Q_u = 0.2 δ_u (GM) = 0.13 GM (at 800 nm)	- Quantitative uncaging yield - High one- and two-photon sensitivity.
p-Hydroxyphenacyl (pHP)	$\varepsilon(M^{-1}cm^{-1})$ = 3000-12000 (highly pH dependent) λ_{max} = 278 - 340 nm Q_u = 0.08	- Modest uncaging yield: Formation of a thio-ether byproduct limits the yield. - Low one- and two-photon absorptivity.

Table 1-1 Overview of spectral and photo-chemical properties of thiol caging groups reviewed in this article.

2 Nitrodibenzofuran: A One- and Two-Photon Sensitive Protecting Group That Is Superior to Brominated Hydroxycoumarin for Thiol Caging in Peptides

2.1 Introduction

The ability of light to traverse various chemical and biological barriers and be modulated by time and amplitude makes light- regulated molecules unique tools for a plethora of applications in the areas of chemistry and biology.[1−4] Photoremovable protecting groups, also known as caging groups, are one of the most important light-regulated tools, which can be utilized to mask specific functional groups in molecules such that they can be cleaved on demand upon irradiation.[5,6] In biological applications, this typically involves masking a biomolecule with a caging group to produce a compound whose biological activity is either increased or decreased upon uncaging.[7−9] The recent development of two-photon-sensitive protecting groups, which allow uncaging using near-infrared (near-IR) irradiation, has resulted in significant improvements in the spatiotemporal resolution of uncaging as well as increased penetration with lower phototoxicity;[10−14] the latter attribute is of particular importance for the use of caged molecules in tissue samples or intact organisms that are essentially opaque to UV light. Due to inherent differences in the chemical reactivity of various functional groups, there is no single photocleavable protecting group that works efficiently for caging all functionalities. Hence, protecting group selection must be performed on a case by case basis.[15,16]

Thiol-containing compounds play vital roles in many aspects of biology (e.g., controlling cellular redox state),[17] protein chemistry (e.g., protein and peptide folding, native chemical ligation[18]), and enzymology.19 Hence, significant efforts have gone into the preparation of proteins and ligands/substrates containing caged thiols that can be triggered with light to reveal bioactive species;[20−24] for that purpose, several protecting groups have been explored.[25−29] The most widely used approach for thiol protection involves caging with o-nitrobenzyl (ONB) groups. Among the advantages of ONB groups are high one-photon quantum efficiency and high yield of free compound produced upon photolysis.30 However, they are poor chromophores with low two-photon sensitivities which limit their biological applications. To address this issue, coumarin-based protecting groups have been recently employed, which absorb light at longer wavelengths and possess significantly higher one- and two-photon absorptivity.[31] In one important study, Hagen and co-workers harnessed the chromatic orthogonality of ONB- and coumarin-based protecting groups to introduce a wavelength-selective thiol caging system.[32] Using a combination of those protecting groups, they were able to selectively uncage different thiols in a peptide sequence using different wavelengths for UV irradiation; however, no two-photon photochemistry was explored. In another novel study, Shoichet and co-workers incorporated brominated hydroxycoumarin (Bhc)-protected thiols into hydrogels that allowed them to perform light- induced protein patterning within those materials with high spatial control.[33,34] The high two-photon sensitivity of Bhc allowed them to create

3D protein patterns inside these polymeric scaffolds for tissue engineering applications.

In recent work, we demonstrated that Bhc could also be used for thiol protection of a peptidomimetic enzyme inhibitor.[35] The high one- and two-photon sensitivity of Bhc allowed efficient uncaging of the inhibitor inside cells for biological applications. Inspired by these results, we reasoned that Bhc could also be used for thiol protection of cysteine-containing peptides. In the work reported here, we first explored the use of Bhc-protected cysteine in peptides. While they are straightfor- ward to prepare using Fmoc-Cys(Bhc)-OH as a building block in solid-phase peptide synthesis (SPPS), irradiation of such caged peptides was complicated by the generation of an unwanted photoisomer instead of the free thiol. Using NMR analysis,we wereableto confirm the structure of the photoisomer to be a 4-methylcoumarin-3-yl thioether, in agreement with a previous prediction by Hagen and co- workers.[32] Further analysis of several different peptide sequences revealed that the photocleavage efficiency of Bhc- protected thiols is context dependent and typically leads to formation of a photoisomer as the major product. To circumvent this problem, we next explored using nitro- dibenzofuran (NDBF)36 as a thiol caging group since it manifests a two-photon cross-section comparable to that of Bhc. Thus, cysteine-containing peptides were prepared where the thiol was protected with an NDBF group. This was accomplished by preparing Fmoc-Cys(NDBF)-OH and incorporating it into peptides via standard SPPS. In contrast to that of Bhc-caged thiols, irradiation of NDBF-protected thiols at 365 nm resulted in clean conversion to the free mercaptan. Deprotection was

also obtained via irradiation at 800 nm, where the two-photon action cross-section was measured to be comparable to that of Bhc-protected acetate (Bhc-OAc). To probe the utility of this protecting group for biological experiments, thiol group uncaging was carried out using a K- Ras-derived peptide containing an NDBF-protected cysteine. Irradiation of that molecule in the presence of protein farnesyltransferase (PFTase) and farnesyl diphosphate (FPP) resulted in the formation of the free thiol form and subsequent enzymatic conversion to a prenylated species. Those experi- ments indicate that one- and two-photon deprotection can be performed under mild conditions that allow enzymatic activity to be retained. In order to illustrate the utility of this strategy for the development of caged peptides that can be activated via irradiation inside live cells, the thiol of a cell-penetrating peptide known to be a substrate for palmitoyl acyltransferase was protected as a NDBF thioether. Irradiation of human ovarian carcinoma (SKOV3) cells, preincubated with the probe, resulted in migration of the peptide from the cytosol/Golgi to the plasma membrane (visualized via confocal microscopy) due to enzymatic palmitoylation. These data suggest that the NDBF group should be useful for caging thiols in peptides and potentially larger proteins assembled via native chemical ligation[18] for biological applications. The high uncaging yield of NDBF-caged thiols upon one- and two-photon irradiation, together with the facile incorporation of caged cysteine via standard SPPS into peptides containing multiple cysteines, make this a highly versatile strategy for studying cysteine- containing peptides and proteins.

2.2 Results and Discussion

2.2.1 Synthesis and Studies of the Photolysis of Bhc- Protected Cysteine-Containing Peptides.

2.2.1.1 Synthesis of Bhc-Protected Fmoc-Cysteine and Incorporation into Peptides.

Previous studies in our laboratory have shown that Bhc can be used for photolabile thiol protection of a peptidomi- metic enzyme inhibitor. The caged molecule manifested efficient cleavage to yield a free thiol upon one- and two- photon irradiation, allowing it to be used for biological applications in cell culture. Therefore, in order to develop photolabile S-protected cysteine-containing peptides, we initially used Bhc as a caging group. Our strategy was to prepare Bhc-protected Fmoc-cysteine and incorporate that into a peptide of interest through SPPS; the synthesis of a form of cysteine suitable for SPPS is depicted in Scheme 2-1. The phenolic hydroxyl group of Bhc-chloride (**1**) was protected using chloromethyl methyl ether and triethylamine to give MOM-protected Bhc-Cl (**2**) in 89% yield. This chloride was subsequently used to alkylate Fmoc-cysteine methyl ester under mild acidic conditions, using Zn(OAc)2 as a catalyst,[38] to produce 3 in 80% yield. Saponification of the methyl ester using trimethyl tin hydroxide[39] under reflux generated the desired caged Fmoc-cysteine derivative (**4**) in 81% yield.

The general route for synthesis of caged peptides employed standard SPPS conditions, in which Fmoc-protected residues were added sequentially to a peptide anchored on Wang resin.

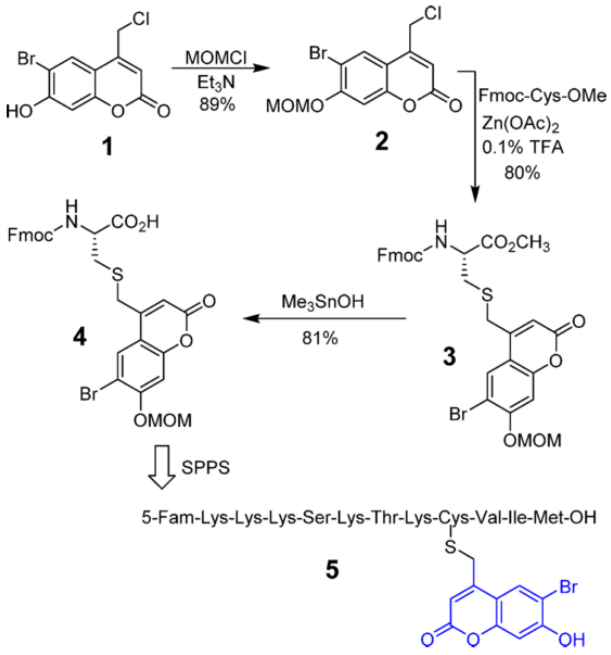

Scheme 2-1 Synthesis of Bhc-Protected Fmoc-Cys and Incorporation into a Peptide via SPPS.

The only exception involved the incorporation of the caged Fmoc-Cys residue, where the coupling time was increased to 6 h to ensure quantitative incorporation of the nonstandard residue. Final treatment of the resin-bound peptide with acid (standard conditions using Reagent K) removed all side-chain protecting groups, including the MOM group present on the Bhc moiety, and cleaved the polypeptide from the resin to generate the desired caged molecule. This strategy was successfully employed to synthesize a caged form of K-Ras peptide, **5**, that includes an N-terminal fluorescein group. While the uncaged form of that peptide is a known substrate for the enzyme, PFTase, the Bhc-protected form is not. The goal was to use light to uncage the peptide and restore its ability to be recognized by the enzyme and undergo farnesylation.

2.2.1.2 Photolysis of Bhc-Protected Cysteine-Containing Peptides.

Once the fluorescein-labeled caged peptide was successfully synthesized and purified, the next step was to verify its uncaging efficiency upon photolysis. Hence, solutions of caged peptide in photolysis buffer (1 mM DTT in 50 mM PB at pH 7.2) were irradiated using 365 nm light in a Rayonet photoreactor for varying amounts of time (Figure 2-1A). Each sample was analyzed by RP-HPLC and monitored by fluorescence. Inspection of the HPLC traces (Figure S1) revealed that the starting peptide peak disappeared over time, with concomitant formation of a new peak with a later retention time. Surprisingly, further analysis of the reaction mixture via ESI-MS revealed that the photolytic product and non-irradiated starting peptide had identical masses, indicating that irradiation causes isomerization instead of uncaging.

Extracted ion current (EIC) chromatograms obtained by LC- MS analysis (Figure 2-1B,C) clearly revealed the disappearance of the starting peptide (tR = 8.45 min, m/z = 635.26) upon photolysis and concomitant formation of a new peak with identical mass (tR = 8.70 min, m/z = 635.26) that corresponds to the photoisomerized product. To study whether any free (uncaged) peptide **6** was produced upon irradiation, **6** was synthesized by an independent route and subjected to LC-MS. Analysis of the LC-MS traces of the irradiated peptide showed no evidence for the presence of free peptide ions that match with the authentic standard (Figure 2-1C, D).

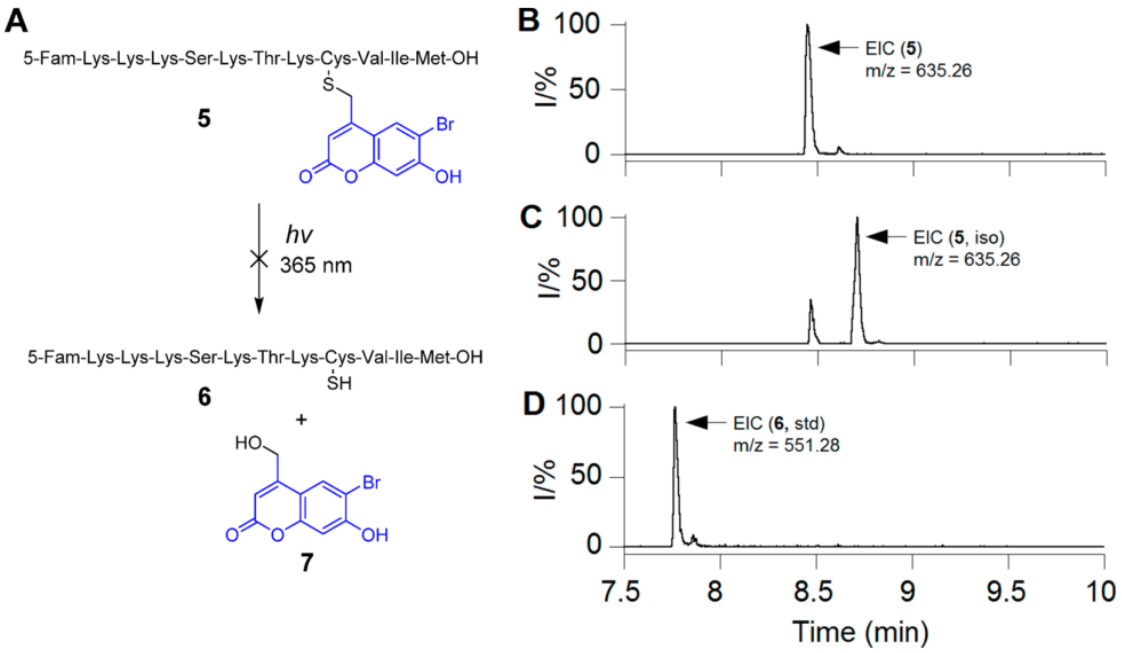

Figure 2-1 (A) Uncaging reaction of Bhc-protected cysteine-containing peptide **5** upon UV irradiation. LC-MS analysis of photolysis of peptide **5**: (B) EIC chromatogram (m/z = 635.20−635.30) of a sample of **5** in photolysis buffer, (C) EIC chromatogram (m/z = 635.20−635.30) of sample of **5** after 120 s photolysis showing the formation of a photoisomer, and (D) EIC chromatogram (m/z = 551.20−551.30) of a standard sample of free peptide **6b** showing that no uncaged product was detected upon photolysis of **5**.

We initially hypothesized that the observed isomerization might be due to photoinduced migration of the Bhc group to a side-chain amine group of a neighboring lysine residue. This hypothesis was tested by MS/MS fragmentation analysis, since migration of Bhc to other residues would change the fragmentation of the photoisomer relative to the starting peptide. Interestingly, MS/MS analysis revealed that the two isomers have the same backbone fragmentation pattern (Table S1). Of particular importance, two of the main fragments present in both the photoisomer and the caged peptide are the doubly charged X4 and B7 ions (Figure S2), which clearly indicate that the Bhc group remains connected to cysteine even

after irradiation. This observation is not consistent with the hypothesis of phototriggered Bhc migration to lysine residues and indicates that a rearrangement occurs directly on the caged cysteine residue.

The high extent of photoisomerization observed upon photolysis of compound 5 was somewhat contrary to our previous results with Bhc-protected inhibitors, where photolysis led to efficient (>85%) uncaging. Thus, we considered the possibility that the photocleavage of Bhc-caged thiols may be context dependent. To test this hypothesis, two additional peptides were synthesized in which the location of caged cysteine was moved by one residue along the peptide sequence. Each peptide was photolyzed separately, and the resulting products were analyzed by LC-MS. Based on the EIC data (Figures S3 and S4), photolysis of KKKSKTCC(Bhc)IM produced only the photoisomer and no detectable uncaged peptide. In contrast, photolysis of KKKSKTC(Bhc)CVIM generated a mixture of both the photoisomer and free peptide. This hypothesis was also tested with shorter peptides where C(Bhc)VLS showed formation both uncaged and isomerized product (Figure S5), whereas photolysis of dansyl-GC(Bhc)VLS did not produce any uncaged peptide (Figure S6). These data confirm that the efficiency of Bhc photocleavage is highly dependent on its surrounding chemical environment. It is worth noting that photoisomerization was also observed upon two photon excitation of C(Bhc)VLS (Figure S7).

Previously reported mechanistic studies have demonstrated that the photocleavage of coumarin-based protected carboxylic acids results in scission of the C−O bond to produce a reactive carbocation which is rapidly quenched by

water when the latter is used as the solvent.40 However, an alternative pathway could involve reaction of the cationic intermediate with an internal nucleophile via an intramolecular process; such a mechanism would give rise to an isomeric product consistent with the observations reported here. To examine this possibility, photolysis reactions were performed in the presence of high concentrations of thiols in order to increase the rate of trapping. Thus, aqueous solutions of 5 were irradiated in the presence of excess DTT (up to 200 mM), and analyzed by RP-HPLC. Interestingly, none of those experiments revealed any measurable change in the extent of photoisomerization. These results suggest that the photo-rearrangement may proceed through a concerted intramolecular mechanism; however, additional experiments are needed to thoroughly address this question.

2.2.1.3 NMR Analysis of Bhc Photo-rearrangement.

The possibility of photo-rearrangement of related amino-coumarin- protected cysteines has been previously suggested by Hagen and co-workers; however, in their publication, no analysis was performed to conclusively identify the structure of photoisomer generated.[32] Therefore, after first observing the photo-rearrangement of Bhc-caged thiols by mass-spectroscopy, we decided to determine the structure of the isomeric product using NMR methods. In order to obtain sufficient material for NMR analysis, a solution of caged peptide 5 was irradiated and the photoisomer was isolated via preparative RP-HPLC purification. ^{1}H NMR spectra were obtained using a sensitive cryoprobe instrument. As shown in Figure S8A,B for **5** and the photoisomer, respectively, both compounds have very similar spectra, with the exception of a distinctive peak at 6.2 ppm present in

the spectrum of **5** that is missing in the spectrum of the photoisomer; concomitantly, a new signal appears at 2.4 ppm in the spectrum of the isomer that is not present in the spectrum of **5**. Comparison of those spectra with the Bhc ^{1}H NMR spectrum[31] indicates that the signal at 6.2 ppm corresponds to the aryl proton at the 3 position of Bhc (Scheme 2-2). The disappearance of that peak and the appearance of the new signal at 2.4 ppm are consistent with a photoinduced 1,3 shift of the sulfur atom from the exocylic position to the 3 position to give intermediate **9** followed by tautomerization to yield a 4-methylbromohydroxycoumarin-3- yl thioether (**10**) as previously suggested by Hagen and co- workers.[32] In such a case, the resonance at 2.4 ppm could be attributed to the presence a methyl group in the final photoproduct **10**.

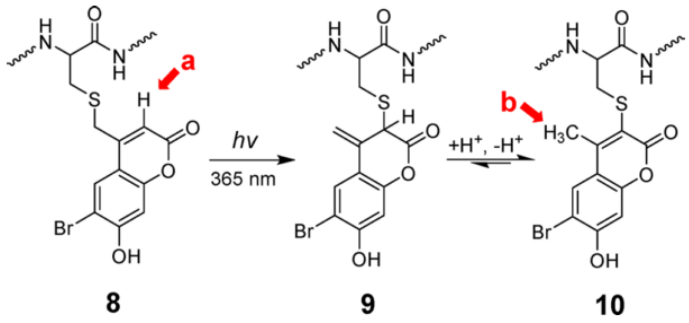

Scheme 2-2 Hypothesized Mechanism of Photoisomerization of Bhc-Caged Cysteine.

Due to the complicated ^{1}H NMR spectra of the peptides, we decided to validate the proposed hypothesis using a simpler model system. Hence, Bhc-protected cysteamine (**11**, Figure 2-2), which has a simple structure and a straightforward synthetic route, was chosen as the model system. Additionally, this specific

molecule has been previously used by Shoichet and co- workers for phototriggered uncaging of thiol functionality inside hydrogels.[28] Therefore, knowing all the complexities due to context dependence of Bhc photocleavage, we were also interested to see how efficient this compound could undergo uncaging.

Compound **11** was synthesized following a previously reported procedure.[33] Solutions of **11** were irradiated using 365 nm light in a Rayonet photoreactor for varying amounts of time followed by analysis via RP-HPLC with UV detection. That allowed the disappearance of **11** as well as the formation of the isomeric rearrangement product **12** and Bhc-OH (**7**) (formed from the desired uncaging reaction) to be monitored. Inspection of the HPLC data (Figure S9) indicates that the major product of photolysis of compound **11** under these conditions is the photoisomer **12**, the product with a higher retention time) with a smaller amount of the desired uncaged product formed, as indicated by the low intensity peak corresponding to **7**.

Compound 11 was synthesized following a previously reported procedure.[33] Solutions of **11** were irradiated using 365 nm light in a Rayonet photoreactor for varying amounts of time followed by analysis via RP-HPLC with UV detection. That allowed the disappearance of **11** as well as the formation of the isomeric rearrangement product 12 and Bhc-OH (**7**) (formed from the desired uncaging reaction) to be monitored. Inspection of the HPLC data (Figure S9) indicates that the major product of photolysis of compound **11** under these conditions is the photoisomer **12**, the product with a higher retention time) with a smaller amount of

the desired uncaged product formed, as indicated by the low intensity peak corresponding to **7**.

Reactions containing Bhc-cysteamine (**11**) and its corre- sponding photoisomer **12** were separated by RP-HPLC and the purified compounds analyzed by NMR spectroscopy. Compar- ison of the ^{1}H NMR spectrum of **11** with that of compound **12** revealed characteristic changes in the proton signals corre- sponding to those observed in the peptide experiment (Figure 2-2). Methylene (Hd) and aryl (He) protons present in the starting material are absent in the spectrum of the photoisomer. In addition, a new signal at 2.72 ppm (Hh) corresponds to the new methyl group that is generated. Also of note, the triplet signal (H′b), corresponding to the methylene protons of cysteamine, shifts downfield relative to that of the starting compound (Hb) as a result of thiol conjugation with double bonds which renders the thiol a stronger electron-withdrawing group; alternatively, this shift may be due to a ring current effect. These observations convincingly support the suggested mechanism for photo-rearrangement and the proposed structure of the photoisomer. A similar photolysis experiment was performed in D_2O. LC-MS analysis clearly indicates formation of a mono deuterated photoisomer (Figure S10). This data demonstrates that there is a solvent-derived proton incorporated in the product, consistent with the mechanism proposed for photo-rearrangement described in Scheme 2-2.

To obtain an accurate ratio of the extent of uncaging versus photo-rearrangement, a sample of compound **11** that had been subjected to irradiation, and thus contained both uncaged and photoisomerized product, was analyzed by ^{1}H NMR

spectros- copy (Figure S11). Using integration values obtained from characteristic protons from each product, a ratio for uncaging versus photoisomerization of 1:10 was calculated. Thus, while Shoichet and co-workers have used **11** (under different conditions) to successfully uncage a thiol upon photolysis, the experiments reported here revealed that the major product of this reaction is an unwanted photoisomer. Overall, the variability obtained using Bhc suggests that it is not generally applicable as a caging group for thiols and that there is a real need for an alternative caging group for general usage.

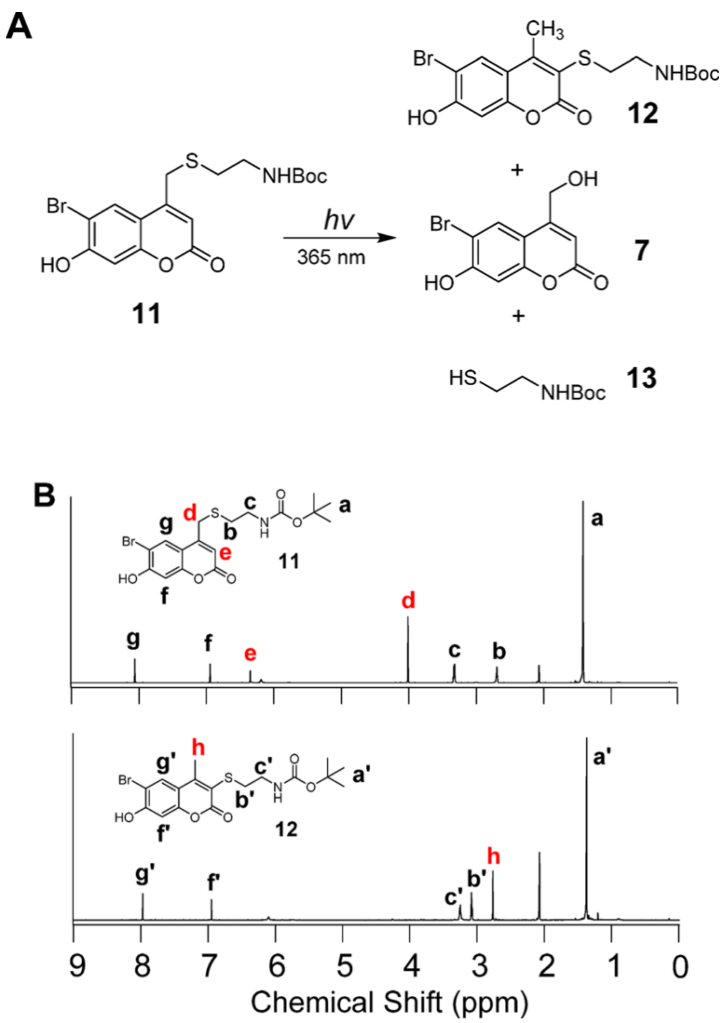

Figure 2-2 (A) Photolysis of Bhc-protected Boc-cysteamine and the resulting photolytic products. (B) 1H NMR spectrum of Bhc-protected Boc-cysteamine (top) and the corresponding photoisomer (bottom).

2.2.2 Use of Nitrodibenzofuran for Development of Caged Cysteine-Containing Peptides.

2.2.2.1 Alternative Strategy Using NDBF.

The initial goal of our work was to identify a protecting group that could be used to cage the thiol group of cysteine when present within a peptide that would be efficiently deprotected through UV irradiation as well as near- IR light via a two-

photon process. Although Bhc has shown reasonable one- and two-photon uncaging efficiencies for protection of various functionalities including carboxylates, phosphates and carbamates, the experiments described above revealed its photocleavage efficiency is unpredictable when used with thiols; moreover, the main product formed upon irradiation is often an unwanted rearrangement byproduct in lieu of the desired free thiol. To address these limitations, we elected to examine another type of caging group that undergoes uncaging via a process significantly different from coumarin- based compounds.

o-Nitrobenzyl (ONB)-based caging groups have been extensively used for thiol photocaging. Despite, their relatively slower uncaging rate (compared with coumarins), they undergo photolysis with minimal byproduct formation. However, ONB- based compounds suffer from low one-photon and especially low two-photon absorptivity which limits their applications in cellular media and live tissue. In 2006, Momotake et al. introduced NDBF, a more extensively conjugated form of ONB, as a new caging group with high one- and two-photon sensitivity.[36] This compound has previously been used for protection of hydroxyl functionalities and showed rapid and efficient uncaging upon one- and two-photon irradiation.[41] Due to its advantages over traditional ONB-based molecules, we decided to explore its applicability for photocaging of thiols in order to prepare peptides containing caged cysteine residues.

2.2.2.2 Synthesis of NDBF-Protected Fmoc-Cys-OH and Incorporation via SPPS.

Similar to the synthesis of Bhc- caged peptides, the strategy pursued here was to first synthesize Fmoc-cysteine containing an NDBF-protected thiol [Fmoc-Cys(NDBF)-OH] and then incorporate that into a peptide through standard SPPS. Starting from dibenzofuran, NDBF-Br (**13**) was synthesized in four steps (Scheme S1). Next, as described in Scheme 2-3, Fmoc-cysteine methyl ester was first reacted with NDBF-Br under acidic conditions, to produce compound 15 in 70% yield. The resulting methyl ester was then hydrolyzed using (CH3)3SnOH to yield Fmoc-Cys(NDBF)-OH (**16**) in 75% yield.

The resulting protected cysteine residue was successfully incorporated into several K-Ras-derived peptides (**17a,b**) via standard SPPS as described for the related Bhc-protected peptides noted above; the final products were characterized by ESI-MS-MS to confirm the presence of the NDBF group after the global deprotection step (Table S2). Since NBDF protection of cysteine involves a thioether bond, there was no evidence of any S-to-N shift or deprotection occurring during synthesis, a problem that does occur when thiocarba- mate-based protection strategies are used.[32]

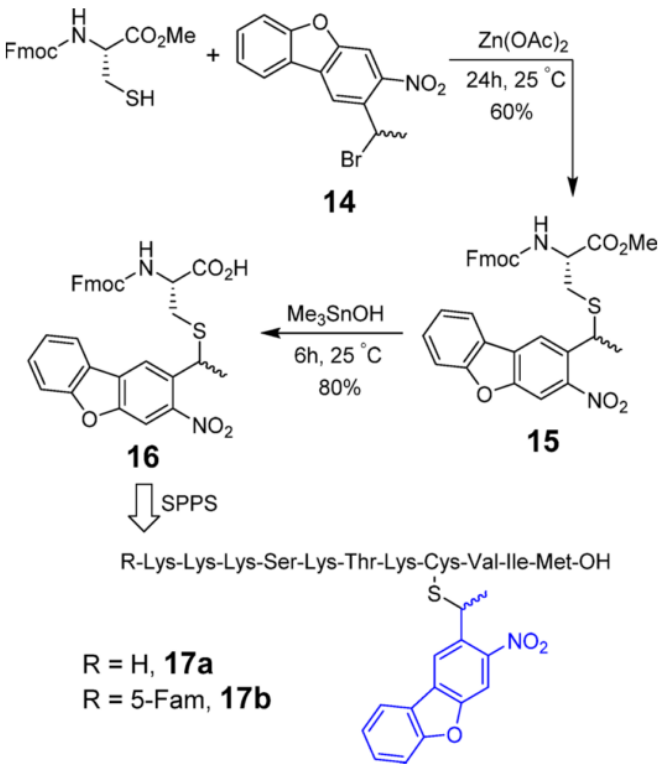

Scheme 2-3 Synthesis of NDBF-Protected Fmoc-Cys-OH and Incorporation into Peptide Sequence via SPPS.

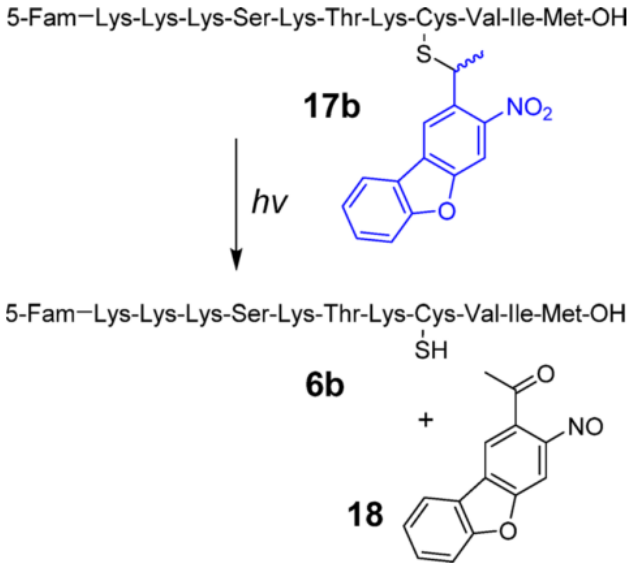

Scheme 2-4 Light-Triggered Uncaging of NDBF-Protected K- Ras Peptide (**17b**).

2.2.2.3 One- and Two-Photon Photolysis of NDBF-Caged Cysteine Peptides.

After completion of the synthesis of the fluorescently labeled caged peptide **17b**, photolysis experiments were conducted to probe for the formation of the uncaged peptide containing a free thiol upon photolysis (Scheme 2-4). In this experiment, a solution of **17b** was irradiated at 365 nm for 45 s and subjected to RP-HPLC. As can be seen from the chromatograms shown in Figure S12, photolysis resulted in the disappearance of the peak corresponding to the starting peptide **17b** and concomitant appearance of a new peak tentatively assigned as 6b. ESI-MS/MS analysis confirmed that the newly formed peak corresponds to the expected free peptide (Figure S12, Table S3). The absence of any unwanted photoproducts based on an HPLC trace devoid of any other significant products, suggests that that photolysis of NDBF-caged peptides undergo conversion to free peptide upon UV irradiation with high efficiency. In order to further evaluate the general applicability of this strategy, a second peptide, dansyl-GC(NDBF)VLS was also synthesized and studied. Analysis of a photolysis reaction containing that peptide showed complete conversion to the free peptide upon irradiation (Figure S13), unlike its Bhc-protected counterpart (compare with Figure S6). These data suggest that NDBF lacks the limitations and undesired reactivity manifested by Bhc for thiol caging.

One-photon uncaging kinetics of compound **17b** were evaluated by irradiating solutions of 17b for varying periods of time followed by analysis via RP-HPLC (Figure 2-3A). Based on those data, the uncaging quantum yield (εΦ) of peptide

17b was measured to be 0.2. The quantum yield measured in this experiment is somewhat lower than the value reported for NDBF used for caging hydroxyl functionality (0.7),36 which may be due to the light absorption of fluorescein attached to the peptide. However, due to the high molar absorptivity of NDBF, which results in a high εΦ value, the uncaging $t_{1/2}$ was quite short (25 s) under the photolysis conditions (standard Rayonet reactor).

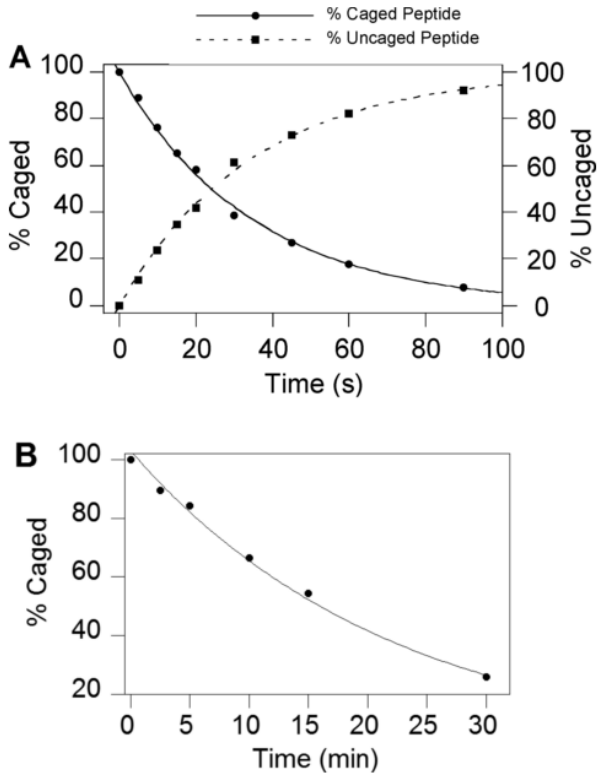

Figure 2-3 (A) HPLC quantification of disappearance of the starting peptide (**17b**) and formation of the uncaged peptide (**6b**) as a function of irradiation time at 365 nm. (B) HPLC quantification of uncaging of **17a** as a function of two-photon irradiation time (800 nm, pulsed Ti:Saphire laser, 210 mw, 80 fs pulse width). Photolysis reactions were performed in 200 and 300 μMsolutions of **17b** and **17a** respectively, containing 1 mM DTT in 50 mM PB, pH 7.5.

Since the NDBF-caged peptide showed useful uncaging properties upon one-photon irradiation, further experiments were performed to evaluate its two-photon

uncaging efficiency. Thus, solutions of **17a** were irradiated at 800 nm using a Ti:Saphire laser and the photolysis products were again analyzed by RP-HPLC and confirmed by LC-MS (Figure S14). The two-photon action cross-section of **17a** was measured using 6-bromo-7-hydroxycoumarin-4-ylmethyl acetate (Bhc-OAc) as a reference.[31] Even though the extinction coefficient of the NDBF chromophore at 400 nm is less than 10% of that at λmax (325 nm), a value of 0.13 GM for **17a** uncaging at 800 nm was calculated (Figure 2-3B). It should be noted that this value would be greater if the two-photon irradiation was performed at lower wavelengths where the extinction coefficient is closer to the maximum value although tissue penetration would be less. Overall, these results demonstrate that NDBF is an efficient thiol caging group that undergoes clean photocleavage to generate a free thiol upon one- or two-photon irradiation.

2.2.2.4 One- and Two-Photon-Triggered in Vitro Farnesylation of a Caged K-Ras Peptide.

Since the NDBF-caged peptide demonstrated good uncaging efficiency, we next sought to examine its utility in a more biologically relevant context. Protein prenylation is a critical process that affects key signaling mechanisms within cells involved in a plethora of functions from growth to differentiation.[42] Prenyl groups are appended to proteins via thioether linkages formed by alkylation of specific cysteine residues catalyzed by prenyltransferases including PFTase, which transfers a farnesyl (C15) group.[43] Thus, a K- Ras-derived peptide incorporating a caged cysteine residue at the site of prenylation should not be a substrate for PFTase; however, upon irradiation, the resulting peptide manifesting a free thiol

produced by photocleavage of the protecting group should be an efficient substrate and become farnesylated (Figure 2-4A). In order to test this, a series of experiments was conducted in which a caged peptide was treated with FPP in prenylation buffer (15 mM DTT, 10 mM MgCl2,50 μM ZnCl2, 20 mM KCl), with or without enzyme addition and UV light exposure.

As predicted, the caged peptide **17b** was not farnesylated when treated with yeast PFTase. LC-MS analysis of reaction mixture indicates only the presence of the caged peptide (m/z = 630.87, Figure 2-4A). Photolysis of **17b** for 60 s at 365 nm, in the absence of enzyme, generated the uncaged peptide, as confirmed by the formation of a new peak with the expected m/ z value (m/z = 551.21, Figure S15). However, photolysis of **17b** in the presence of PFTase led to the generation of a farnesylated peptide (**19b**). The new peak with the retention time of 10.55 min has a mass to charge ratio of 619.26 which is in good agreement with the calculated value ($C_{92}H_{145}N_{16}O_{20}S_{23}^{+}$, 619.34) for the farnesylated peptide. This observation clearly illustrates that the peptide undergoes UV-dependent farnesylation which could make it a useful probe for studying prenylation reactions in a spatiotemporally controllable manner.

Since, it would be useful to employ such caged peptides for studies in tissue or whole organisms where UV light cannot efficiently penetrate, the ability of **17a** to undergo farnesylation by irradiation at longer wavelengths via two-photon excitation was examined. Accordingly, in vitro farnesylation reactions, similar to those described above for UV irradiation, were conducted using an 800 nm laser light source. As was noted before, treatment of the caged peptide with enzyme in

the presence of FPP without irradiation did not alter the starting peptide (Figure 2-4). Irradiation of **17a** (m/z = 511.62) at 800 nm for 2.5 min in the absence of enzyme, generated the free peptide 6a, as confirmed from the EIC chromatogram (m/z = 431.95, Figure 2-4C). Treatment of **17a** with the enzyme along with 2.5 min two-photon irradiation generated the farnesylated peptide **19a**, as shown by the appearance of an ion of m/z = 499.99 (Figure 2-4D). In summary, these data demonstrate that an NDBF-caged K-Ras peptide (**17a**) is capable of undergoing farnesylation triggered by 800 nm light via two-photon excitation (also see Figure S16).

2.2.3 Light Activation of a Caged Peptide inside Live Cells.

One of the important goals for photocaging of bioactive molecules, including peptides, is to modulate their activity by irradiation inside cells in order to study biological processes. Since farnesylation of NDBF-caged K-Ras peptide was efficiently and rapidly triggered by UV and IR irradiation in vitro, we decided to explore the same strategy to develop peptides that can be efficiently activated upon irradiation inside live cells.

Protein palmitoylation is a post-translational modification that plays critical roles in subcellular protein localization. In this process, palmitoyl acyltransferases (PATs) covalently attach a C16 palmitate group via thioesterification to one or more specific cysteine residues present in protein targets.[44] This modification causes proteins to be more hydrophobic and migrate to the plasma membrane where they are active;45 prenylated proteins including H-Ras and N-Ras are commonly

palmitoylated. Draper et al. have developed several fluo- rescently labeled cell-penetrating peptides including NBD-Hex-CLC(S-farnesyl)-OMe (**21**, Scheme 2-5), which they have used to study palmitoylation inside cells.[46] When the free cysteine in the peptide is not modified, it localizes mainly in the cytosol and the Golgi; however, palmitoylation of the free cysteine by PATs inside cells results in the migration of the peptide to the plasma membrane. Therefore, a caged version of Hex-CLC(S-farnesyl)-OMe (**20**), cannot be a substrate for PAT and would thus localize in the cytosol/Golgi; however, irradiation should uncage the peptide, revealing a free thiol that would become palmitoylated and hence gradually migrate to plasma membrane. While peptide **21** has previously been shown to traffic to the plasma membrane, it was impossible to temporally control that process since cellular uptake and trafficking could not be uncoupled. However, the availability of a caged form makes this possible.

Peptide **20** was prepared using a cysteine anchoring method developed by our group for the synthesis of C-terminal methyl esters (Figure S17).[47] Trityl chloride resin was first treated with Fmoc-Cys-OMe and DIEA in CH2Cl2 overnight to afford Fmoc-cysteine-loaded resin. The peptide was extended on the resin through standard SPPS employing Fmoc-based chemistry. Reagent K treatment cleaved the peptide from the resin which was then farnesylated via treatment with farnesyl bromide and Zn(OAc)2 under acidic conditions.

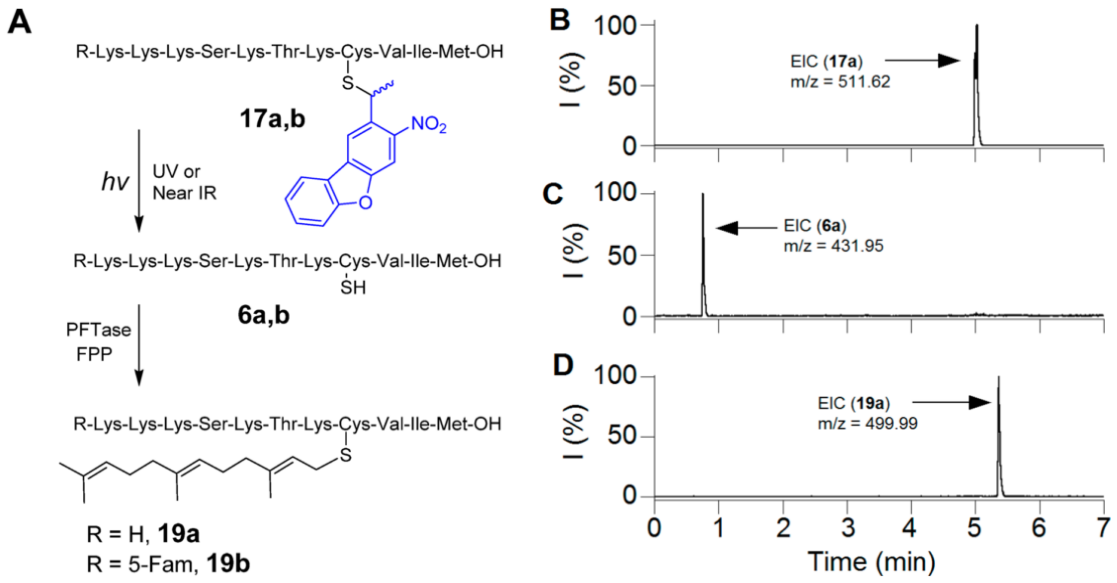

Figure 2-4 (A) Photo-uncaging of **17** and its subsequent farnesylation by enzyme. (B) EIC chromatogram (m/z = 511.62) of a 7.5 µM solution of **17a** in prenylation buffer containing PFTase without irradiation. (C) EIC chromatogram (m/z = 431.95) of a solution of **17a** after 2.5 min irradiation at 800 nm (Ti:sapphire laser, 170 mW, 90 fs) in prenylation buffer without PFTase. (D) EIC chromatogram (m/ z = 499.99) of **17a** after 2.5 min irradiation at 800 nm (Ti:sapphire laser, 210 mW, 90 fs) in the presence of PFTase, showing the formation of farnesylated peptide **19a**.

The final caged peptide was purified by preparative RP-HPLC. Despite the presence of two cysteines in the sequence, there was no evidence of NDBF scrambling between the two thiols during the synthesis, consistent with the stability afforded by the NDBF thioether linkage. Those results are in contrast to those obtained when thiocarbonate strategies are used for thiol protection in peptides containing multiple cysteines where migration via acyl transfer readily occurs. Moreover, studies have shown that carbonates and thiocarbonates are prone to hydrolysis via esterases, thus limiting their applicability in living systems.[48] In general, the efficient assembly of caged peptide **20** highlights the utility of NDBF-protected cysteine and how it can be employed for the synthesis of a variety of

caged peptides including those containing multiple cysteines, with no risk of caging group migration.

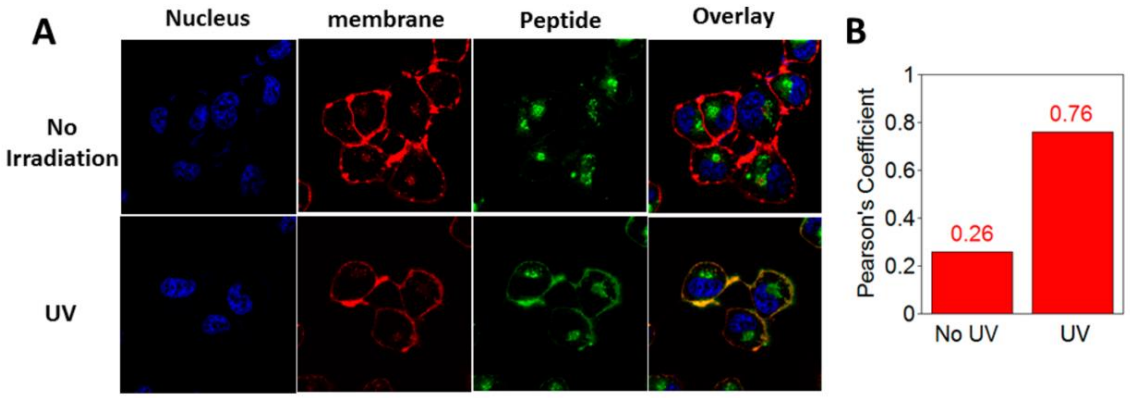

Figure 2-5 Live-cell experiments showing temporal control of enzymatic palmitoylation via NDBF-thiol caging. (A) Images obtained by fluorescence confocal microscopy illustrating intracellular localization of fluorescently labeled peptide 20 in SKOV3 cells, before (top) and after (bottom) UV exposure. (B) Quantification of colocalization of peptide and membrane dye via Pearson's coefficient analysis, indicating a significant increase in plasma membrane localization of peptide upon irradiation.

Next, light-triggered intracellular palmitoylation of caged peptide **20** was studied using human ovarian carcinoma SKOV3 cells. Cells were incubated with **20** in for 3 h at 37 °C to allow cellular uptake. The cells were then divided into two groups and one was subjected to 5 min of UV irradiation at 330 nm. Both irradiated and non-irradiated cells were incubated for an additional 120 min at 37 °C, stained with nuclear and membrane markers and imaged by confocal microscopy. As observed in the fluorescence microscopy images (Figure 2-5A), before irradiation, the peptides reside primarily in the cytosol and Golgi. However, after UV exposure, the peptides trafficto the plasma membrane where they colocalize with the membrane dye; this change in colocalization occurs due to enzymatic palmitoylation. The degree of colocalization of the peptide and plasma membrane dye was quantified

by calculating Pearson's coefficients for both the non-irradiated (0.26) and irradiated cells (0.76) which clearly indicates a significant increase in membrane localization of the peptide after irradiation (Figure 2-5B). It is important to note that while all of the peptide did not localize to the membrane upon photolysis, this is unlikely to be due to incomplete uncaging since UV-mediated uncaging is quite fast and efficient (see Figure 2-3). In their original work, Draper et al.[46] reported incomplete localization even when starting with the fully deprotected form of the peptide used here.[46] Similar results (only partial localization in pulse-chase labeling experiments) have been reported in work with fluorescent proteins that are prenylated and palmitoylated and have been attributed to competing pathways involving degradation versus membrane targeting.[49]

To study the localization process in more detail, samples of the caged peptide were allowed to internalize for 3 h and then uncaged by UV exposure. Analysis of the cellular distribution of the peptide in those samples at different times ranging from 30 to 120 min showed that the membrane colocalization reached a peak after 30 min followed by a slow decrease (Figure S18). Such behavior is consistent with observations made with fluorescent proteins that have been shown to undergo dynamic cycling involving palmitoylation and concomitant membrane localization followed by depalmitoylation and internaliza- tion.[50,51] Overall, these live cell experiments illustrate how NDBF caging of cysteine allows an enzyme substrate for palmitoylation to be temporally activated, thus permitting the processes of cellular entry and subsequent enzymatic modification to be deconvoluted.

Finally, in order to highlight the improved uncaging efficiency of NDBF and its utility in live cell experiments, a comparison was made between the uncaging efficiency of NDBF versus the 6-nitroveratryl (NV) group which is one of the most frequently used caging groups.[15] We elected to study this experimentally since a range of values for the quantum yield of NV have been reported.15 Thiol-protected forms of Fmoc-Cys-OMe were prepared using the two caging groups which were then subjected to UV irradiation (365 nm) and the extent of deprotection was monitored. Uncaging data obtained by HPLC analysis shown in Figure S19, shows that the NDBF uncaging efficiency is greater than 10-fold higher than that of NV. This difference reflects the high molar absorptivity (ε = 15 300 M^{-1} cm^{-1}) and high quantum yield (Φ = 0.2) of NDBF leading to a high $\varepsilon\Phi$ (~3060) value versus that of NV ($\varepsilon\Phi \approx 6000 \times 0.01 = 60$).[52] Thus, the lower uncaging efficiency manifested by NV requires longer irradiation times to obtain comparable levels of uncaging. When SKOV3 cells were subjected to 50 min of irradiation (10-fold longer than was used to uncage **20**), a significant decrease in cell viability was observed. Figure S20 shows a 5% loss of viability after 5 min of irradiation and a 57% decrease after 50 min. Clearly this excessive loss of viability precludes the use of NV protection in this experiments and serves to underscore the increased efficiency and utility of NDBF. However, it should be noted that the two-photon action cross-section of NDBF thiol uncaging is comparable to those manifested by Bhc- carboxylates31 and NDBF-alcohols.[36] To date, two-photon activation of such caged molecules has been restricted to experiments where only a small fraction of uncaging is required to obtain a biological response. At present, it is unclear whether a large fraction of

an NDBF-caged bioactive thiol can be released via two-photon excitation in cells since longer irradiation times may result in IR heating or phototoxicity; cell-based experiments to answer these questions are currently in progress. Nevertheless, the results reported here highlight the utility of NDBF caging for a variety of different biological applications. Coupled with its utility for the synthesis of peptides containing multiple cysteines, the data described here make it clear why NDBF is a superior choice for thiol caging.

2.3 CONCLUSION

In this work, we analyzed the photolysis of several Bhc- protected thiol-containing peptides and small molecules. Those experiments revealed that Bhc-caged thiols exhibit variable uncaging yields and that their photolysis frequently leads to the formation of an unwanted rearrangement product. Using NMR analysis, the structure of the photochemically produced isomer was established to be a 4-methylcoumarin-3-yl thioether.

The poor uncaging yield of Bhc-caged thiols led us to search for a more efficient thiol caging group that would be useful for biological applications; accordingly, NDBF caging, which has previously been shown to be effective for hydroxyl group protection, was explored. NDBF-protected Fmoc-cysteine was synthesized and successfully incorporated into a K-Ras-derived peptide via standard solid-phase synthesis. The resulting caged peptide was photolyzed and completely converted to free peptide with a photolysis quantum yield of 0.2. The two- photon action cross-section of the caged peptide was measured to be 0.13 GM at 800 nm

comparable to that of Bhc-OAc. The one- and two-photon photolysis of a caged K-Ras peptide in the presence of PFTase revealed that the free peptide formed upon irradiation is efficiently converted by the enzyme to its biologically relevant prenylated form. The NDBF-protected cysteine was also used to develop a light-activatable, cell- penetrating peptide containing a caged and a farnesylated cysteine. Confocal microscopy analysis showed that the caged peptide could be activated inside cells upon light exposure which resulted in intracellular migration due to enzymatic palmitoylation. Taken together, this work for the first time reports an efficient, robust, and broadly applicable strategy for the synthesis of a variety of peptides and related small molecules containing caged thiols that can be activated by both one- and two-photon processes in live cells. These results set the stage for a variety of studies where spatiotemporal control of thiol reactivity is required, including a diverse span of applications ranging from chemical biology to material science.

2.4 Experimental Section

General Details. All reagents needed for SPPS were purchased from Peptide International (Louisville, KY). All other solvents and reagents used for synthesis and other experiments were purchased from Sigma-Aldrich (St. Louis, MO). High-performance liquid chromatography (HPLC) analysis (analytical and preparative) was performed using a Beckman model 125/166 instrument, equipped with a UV detector and C18 columns (Varian Microsorb-MV, 5 μm, 4.6 × 250 mm and Phenomenex Luna, 10 μm, 10 × 250 mm, respectively). 1H NMR data of synthetic compounds were recorded at 500 MHz on a Varian Instrument at 25 °C. 1H NMR

data for the products of photolysis reactions were recorded using a Bruker Advance III 700 MHz spectrometer with 1.7 mm TCI cryoprobe.

General Procedure for Solid-Phase Peptide Synthesis (SPPS). Peptides were synthesized using an automated solid-phase peptide synthesizer (PS3, Protein Technologies Inc., Memphis, TN) employing Fmoc/HCTU-based chemistry. Fmoc-Met-Wang resin (0.25 mmol) was transferred into a reaction vessel, and peptide chain elongation was performed using HCTU and N-methylmorpho- line. Standard amino acid coupling was performed by incubation of 4 equiv of both HCTU and Fmoc-protected amino acid with the resin for 30 min. Coupling of Fmoc-Cys(Bhc)-OH or Fmoc-Cys(NDBF)-OH was performed by incubation of 1.5 equiv of both the amino acid and HCTU with the resin for 6 h. Peptide chain elongation was completed by N-terminus deprotection using 10% piperidine in DMF (v/v). 5-Fam coupling was conducted by incubation of 1.2 equiv of 5-Fam, 1.2 equiv of HCTU, and 2 equiv of N,N-diisopropylethylamine (DIEA) with the resin for 8 h. Resin was then transferred into a syringe filter, washed three times with DCM, and dried in vacuo. Global deprotection and resin cleavage were accomplished via treatment with Reagent K. Peptides were then precipitated with Et2O and pelleted by centrifugation, and the residue was rinsed twice with Et2O. The resulting crude peptide was dissolved in MeOH and purified by preparative reversed-phase (RP)-HPLC.

General Procedure for Synthesis of Peptides Containing C-Terminal Methyl Esters. Trityl chloride resin (1 equiv) was transferred into a fitted syringe and washed three times with DMF. In a separate flask, Fmoc-Cys-OMe (3 equiv) was

treated with DIEA (6 equiv) in DCM, transferred into the resin-containing fitted syringe, and then mixed overnight using a rotisserie. Resins were treated with MeOH to cap any unreacted trityl moiety, followed by washing three times with DMF. The prepared Fmoc-Cys-OMe-loaded resins were used to synthesize peptides containing C-terminal methyl esters via traditional Fmoc/HCTU-based chemistry as described in “General Procedure for Solid-Phase Peptide Synthesis”.

5-Fam-KKKSKTKC(Bhc)VIM (5): ESI-MS calcd for $[C_{87}H_{126}BrN_{16}O_{23}S_2 + 3H]^{3+}$ 635.2597, found 635.2568.

5-Fam-KKKSKTKC(NDBF)VIM (17b): ESI-MS calcd for $[C_{91}H_{130}N_{17}O_{23}S_2 + 3H]^{3+}$ 630.9650, found 630.9658.

C(Bhc)VLS: ESI-MS calcd for $[C_{27}H_{37}BrN_4O_9S+ H]^+$ 673.1537, found 673.1575.

Dansyl-GC(Bhc)VLS: ESI-MS calcd for $[C_{41}H_{51}BrN_6O_{12}S_2 +H]^+$ 963.2363, found 963.2302.

Dansyl-GC(NDBF)VLS: ESI-MS calcd for $[C_{45}H_{55}N_7O_{12}S_2 + Na]^+$ 972.3248, found 972.3280.

KKKSKC(Bhc)CVIM (5): ESI-MS calcd for $[C_{63}H_{109}BrN_{15}O_{17}S_3 + 3H]^{3+}$ 507.5485, found 507.5497.

Fmoc-Cys(MOM-Bhc)-OCH3 (3). Chloride **2** (93 mg, 0.28 mmol) and Fmoc-Cys-OCH3 (200 mg, 0.56 mmol) were dissolved in 3 mL of a solution of 2:1:1 DMF/CH3CN/H2O/0.1% TFA (v/v). $Zn(OAc)_2$ was then added (154 mg, 0.70 mmol) and the reaction monitored by thin-layer chromatography (TLC) (1:1

Hex/EtOAc). After 2 days, the solvent was removed and the reaction purified via column chromatography (1:1 Hex/EtOAc) to give 149 mg of **3** as a yellow powder (81% yield): ^{1}H NMR (CDCl3) δ 7.83 (1H, s) 7.76 (2H, d, J = 7.5), 7.6 (2H, d, J = 7.5 Hz), 7.38 (2H, m), 7.29 (2H, m), 7.13 (1H, s), 6.36 (1H, s), 5.74 (2H, s), 4.68 (1H, m), 4.38−4.48 (2H, m), 4.20 (1H, t), 3.74 (3H, s), 3.50 (3H, s); HR-MS (ESI) m/z calcd for $(C_{31}H_{28}BrNO_8S + Na)^+$ 676.0611 (^{79}Br) and 678.0596 (^{81}Br), found 676.0639 (^{79}Br) and 678.0636 (^{81}Br).

Fmoc-Cys(MOM-Bhc)-OH (4). Ester **3** (100 mg, 0.15 mmol) and Me_3SnOH (69 mg, 0.38 mmol) were dissolved in CH2Cl2 (5 mL) and brought to reflux. After 7 h the reaction was judged complete by TLC (1:1 Hex/EtOAc). The solvent was removed in vacuo and the resulting oil redissolved in EtOAc (20 mL). The organic layer was washed with 5% HCl (3 × 10 mL) and brine (3 × 10 mL), dried with Na_2SO_4, and evaporated to give 92 mg of **4** as a yellow powder (90% yield): ^{1}H NMR (d6-acetone) δ 8.12 (1H, s), 7.86 (2H, d, J = 7.5), 7.73 (2H, t, J = 7), 7.41 (2H, t, J = 7.5), 7.33 (2H, m), 7.16 (1H, s), 6.42 (1H, s), 5.64 (1H, s), 5.42 (2H, s), 4.51 (1H, b), 4.37−4.41 (2H, m), 4.32 (1H, t), 4.25 (1H, t), 4.07 (2H, d), 3.49 (3H, s); HR-MS (ESI) m/z calcd for $[C_{30}H_{26}BrNO_8S + Na]^+$ 662.0455 (^{79}Br) and 664.0439 (^{81}Br), found 662.0472 (^{79}Br) and 664.0428 (^{81}Br).

Fmoc-Cys(NDBF)-OCH3 (15). NDBF-Br (1.00 g, 3.12 mmol) and Fmoc-Cys-OCH_3 (2.2 g, 6.25 mmol) were dissolved in 60 mL of a solution of 2:1:1 DMF/ACN/0.1% TFA in H2O (v/v/v). A 0.5 M aqueous solution of $Zn(OAc)_2$ was prepared in 0.1% TFA (v/v), and 25 μL of that solution was added to the reaction mixture. The reaction was monitored by TLC (1:1 Hex/Et_2O) and stopped after 36

h of stirring at room temperature. Solvent was evaporated in vacuo, and the final product was purified via column chromatography (1:1 Hex/ Et_2O) to give 0.90 g of a diastereomeric mixture of **15** as a yellow oil (48% yield): 1H NMR ($CDCl_3$) δ 8.38−8.40 (1H), 8.01−8.06 (2H, m), 7.77 (2H, m), 7.54−7.63 (4H, m), 7.30−7.45 (5H, m), 5.58−5.59 (1H, m), 4.84−4.88 (1H, m), 4.53−4.59 (1H, m), 4.14−4.40 (3H, m), 3.72−3.78 (3H), 2.84−3.03 (2H, m), 1.72−1.74 (3H, m); HR-MS (ESI) m/z calcd for $[C_{33}H_{28}N_2O_7S + Na]^+$ 619.1515, found 619.1537.

Fmoc-Cys(NV)-OMe. This compound was synthesized following the same procedure described above for synthesis of **15**, except NDBF-Br was replaced with 1-(bromomethyl)-4,5-dimethoxy-2-nitrobenzene (NV-Br, 80% yield): ^1H NMR ($CDCl_3$) δ 7.78 (2H, d, J = 7.5), 7.68 (1H, s), 7.62 (2H, t, J = 8.0 Hz), 7.42 (2H, t, J = 7.5 Hz), 7.33 (2H, t, J = 8 Hz), 6.89 (1H, s), 5.66 (H, d, J = 8.0 Hz), 4.64 (1H, q, J = 7.5 Hz), 4.42 (2H, d, J = 7.0 Hz), 4.25 (1H, t, J = 7.5 Hz), 4.00 (3H, s), 3.94 (3H, s), 3.81 (3H, s), 3.00 (2H, m); HR-MS (ESI) m/z calcd for $[C_{28}H_{28}N_2O_8S + Na]^+$ 575.1464, found 575.1493.

Fmoc-Cys(NDBF)-OH (16). Ester **15** (900 mg, 1.50 mmol) was dissolved in 25 mL of CH2Cl2, and Me3SnOH (678 mg, 3.75 mmol) was added. The reaction was refluxed for 7 h and monitored by TLC (1:1 Hex/EtOAc), at which point the solvent was removed in vacuo and the resulting oil dissolved in EtOAc (30 mL). The organic layer was washed with 5% HCl (3 × 10 mL) and brine (3 × 10 mL), dried with Na2SO4, and evaporated to give 786 mg of **16** as a yellow powder (90% yield) as a diastereomeric mixture: ^1H NMR (CDCl3) δ 8.36− 8.39 (1H), 7.97−8.03 (2H, m), 7.75−7.77 (2H, m), 7.53−7.62 (4H, m), 7.30−7.42 (5H, m), 5.58−5.62 (1H, m),

4.88−4.91 (1H, m), 4.54−4.66 (1H, m), 4.16−4.40 (3H, m), 2.88−3.04 (2H, m), 1.71− 1.74 (3H, m); ^{13}C NMR ($CDCl_3$) δ 174.42, 158.28, 155.88, 153.66, 147.66, 143.75, 141.31, 133.37, 129.45, 128.95 127.73, 127.11, 125.21, 123.77, 122.41, 121.87, 120.99, 119.97, 112.18, 108.25, 67.49, 53.48, 47.02, 39.60, 33.70, 23.66; HR-MS (ESI) m/z calcd for $[C_{32}H_{26}N_2O_7S + Na]^+$ 605.1358, found 619.1335.

General Procedure for UV Photolysis of Caged Molecules. The caged compound was dissolved in photolysis buffer (50 mM phosphate buffer (PB), pH 7.4 containing 1 mM DTT) at a final concentration of 25−250 μM. The solutions were transferred into a quartz cuvette (10 × 50 mm) and irradiated with 365 nm UV light using a Rayonet reactor (2 × 14 W RPR-3500 bulbs). After each reaction the samples were analyzed by RP-HPLC or liquid chromatography−mass spectrometry (LC-MS).

General Procedure for LC-MS Analysis. Aliquots (100 μL) containing 5−20 μM caged compound in photolysis buffer were irradiated in a Rayonet UV photoreactor or using an 800 nm laser (see below for description). Each irradiated sample was then analyzed by LC-MS. The general gradient for LC-MS analysis was 0−100% H2O (0.1% HCO_2H) to CH_3CN (0.1% HCO_2H) in 25 min.

Photolysis Study of Bhc-Protected Boc-Cysteamine (11) and NMR Analysis of the Photoisomerization Reaction. Aliquots (200 μL) containing compound **11** (200 μM in photolysis buffer) were irradiated at 365 nm for 80 and 400 s. After each illumination, samples were analyzed via RP-HPLC by monitoring the absorbance at 220 nm. To obtain sufficient photoisomer for NMR analysis, 10 mL of a 300 μM solution of **11** was irradiated for 6 min and purified via preparative RP-

HPLC. The collected eluate was lyophilized to yield ~1 mg of the desired compound, which was then dissolved in 500 μL of d_6-acetone and subjected to ^{1}H NMR analysis.

Photolysis Rate and Quantum Efficiency of 17b Using UV Excitation. Aliquots (100 μL) containing **17b** (200 μM in photolysis buffer) were irradiated at 365 nm in a Rayonet UV reactor. The duration of irradiation ranged from 5 to 90 s. After each irradiation interval, 80 μL of the sample was analyzed by RP-HPLC. The reaction samples were eluted with a gradient of 0.1% TFA in H_2O (Solvent A) and 0.1% TFA in CH_3CN (Solvent B) (gradient of a 3% increase in Solvent B/min, flow rate 1 mL/min) and monitored by fluorescence (λex = 492 nm, λem = 518 nm). Reaction progress data were plotted in KaleidaGraph 3.0 and fitted via nonlinear regressional analysis to a first-order process. The quantum efficiency (Qu) was calculated using the formula $Qu = (I\sigma t90\%)^{-1}$, where I is the irradiation intensity in einstein cm^{-2} s^{-1}, σ is the decadic extinction coefficient ($10^3 \times \varepsilon$, molar extinction coefficient) in cm^2 mol^{-1}, and t90% is the irradiation time in seconds for 90% conversion to the product.[31] The UV intensity of the lamps (I) in the photoreactor was measured using potassium ferrioxalate actinometry.[37]

Laser Apparatus for Two-Photon Irradiations. The light source that was utilized for two-photon irradiation is a home-built, regeneratively amplified Ti:sapphire laser system. This laser operates at 1 kHz with 210 mW pulses centered at a wavelength of 800 nm. The laser pulses have a Gaussian full width at half-maximum of 80 fs. Samples were irradiated in a 15 μL quartz cuvettes (Starna Cells Corp.).

Two-Photon Uncaging Cross-Section (δu) of 17a at 800 nm. The two-photon action cross-section for **17a** was measured by comparing the photolysis rate of 17a with that of Bhc-OAc as a reference (δu = 0.45 at 800 nm). Aliquots (100 μL) containing **17a** (300 μM in photolysis buffer) were irradiated with the 800 nm laser system for varying amounts of time, ranging from 2.5 to 30 min. Each sample was analyzed by HPLC using the method described above. Similar photolysis experiments were conducted using 100 μL aliquots of Bhc-OAc (100 μM in 50 mM PB, pH 7.2). Photolyzed Bhc-OAc solutions were also analyzed by RP-HPLC. The compounds were eluted with a gradient of Solvent A and Solvent B (gradient of a 1% increase in Solvent B/min, flow rate 1 mL/min) and monitored by absorbance at 220 nm. Reaction progress data were analyzed as described above, and the first-order decay constants for the two compounds were used in the formula δuΦu(**17a**)= δuΦu(reference) × Kobs(**17a**)/Kobs(reference) to calculate the value of δu for **17a**, where δuΦu(reference) = 0.45 GM.

UV- and Two-Photon-Triggered Farnesylation of 17. A 7.5 μM solution of compound 17 was prepared in prenylation buffer (15 mM DTT, 10 mM $MgCl_2$,50 μM $ZnCl_2$, 20 mM KCl, and 22 μM FPP) and divided into three 100 μL aliquots. Yeast PFTase was added to the first aliquot to give a final concentration of 30 nM, but the resulting sample was not subjected to photolysis. The second aliquot was irradiated in the absence of yeast PFTase, while the third sample was supplemented with yeast PFTase (50 nM) and then photolyzed with either UV or laser light. UV photolysis was conducted for 1 min at 365 nm, while two-photon

irradiation was performed for 2.5 min at 800 nm. Each sample was incubated for 30 min at room temperature and then analyzed by LC-MS as described above.

Cell Culture and Microscopy. SKOV3 cells were grown in Mcoy's 5a medium containing 10% FBS at 37 °C under CO2 (5.0%). For microscopy experiments, cells were seeded into 35 mm glass-bottomed dishes at a density of 8×10^3 cells/cm^2. To monitor the trafficking of 20 before and after UV irradiation inside cells, SKOV3 cells were incubated with 5 μM 20 for 3 h. The medium was then replaced with RPMI (10% FBS) medium without phenol red. Half of the plates were irradiated at 330 nm for 5 min using a transilluminator (Fotodyne Inc.), and then all of the plates were incubated for 120 min at 37 °C under CO2 (5.0%). Cells were then incubated with Hoecht 33342 (2 μg/mL) and AF488-WGA (15 μg/mL) in Mcoy's 5a (10% FBS) medium for 10 min. The medium was removed, and cells were washed three times with warm phosphate-buffered saline (PBS), followed by RPMI medium (10% FBS, no phenol red). Cells were directly imaged using an Olympus FluowView IX2 inverted confocal microscope with a 60× objective. Colocalization of the peptide with the plasma membrane, in the presence and absence of UV exposure, was statistically quantified using Pearson correlation coefficient analysis calculated using FIJI software.

Cell Viability Assay. SKOV3 cells were grown and irradiated for 0,5, and 50 min following the same procedure described above. In each sample, medium was replaced with 1 mL of Mcoy's 5a medium (10% FBS) containing 0.5 mg/mL 3-(4,5-dimethylthiazol-2-yl)-2,5-diphenyltetrazolium bromide (MTT) and incubated for 1 h at 37 °C under CO2 (5.0%). Medium was removed from each plate, and cells were

washed once with warm PBS. Next, 1.5 mL of DMSO was added to each plate to lyse the cells. The cells were placed on an orbital shaker for 15 min until they were completely dissolved. Absorbance was obtained at 570 nm using a UV spectrometer. Data were normalized such that cells that were not exposed to irradiation had a cell viability of 100%.

3 6-Bromo-7-hydroxy-3-methyl coumarin (mBhc) is an efficient multi-photon labile protecting group for thiol caging and three-dimensional chemical patterning

3.1 Introduction

Photo-removable protecting groups (also known as caging groups) allow spatio-temporally controlled release or activation of a variety of biomolecules, including peptides and inhibitors inside living systems.[1,2] These protecting groups can be used to mask specific functionalities present in bioactive agents (generating caged inactive molecules) such that they can be cleaved on-demand upon irradiation and release the bioactive species.[3,4] Recent advances in the development of two-photon cleavable protecting groups allow uncaging using near IR irradiation instead of UV light, with remarkably improved spatial resolution and increased penetration while causing significantly lower photo-toxicity.[5,6] This has broadened the application of the caging strategy for photo-triggered release of biomolecules inside tissues or organisms useful for a variety of biological studies.[7] Additionally, two-photon uncaging approaches have proved to be extremely useful for creating novel biomaterials; in that strategy, laser irradiation is used to unmask a specific caged functionality pre-incorporated into a hydrogel or matrix, such that it can be used to immobilize peptides, proteins or cells in a three dimensionally controlled fashion.[8–10] Such highly tuned matrices allow artificial extracellular environments to be created that can be used to study cell migration, differentiation and cell-cell interactions.[11]

Differences in the chemical reactivity of various functional groups means that there is no single protecting group that can be universally employed for caging applications.[1] Sulfydryl-containing compounds play critical roles in various aspects of cellular function.[12,13] Hence, significant effort has gone into development of photo-activatable thiol-containing peptides or small molecule substrates as tools to elucidate or dissect cellular pathways;[14,15] under many conditions, thiols are the most reactive nucleophiles present in biological systems. Importantly, they are prone to oxidation and are also relatively poor leaving groups compared with phosphates and carboxylates.[16] Those features render the design of photoremovable thiol protecting groups challenging.

Ortho-nitrobenzyl (ONB) compounds are the most commonly used caging groups for sulfhydryl-protection.[17] ONB groups provide free thiols in high yield upon photolysis, however, they are poor chromophores and they generally lack two-photon sensitivity. To address these limitations, coumarin-based protecting groups have been utilized due to their high one- and two-photon sensitivity. The fluorogenic character of coumarins can also be used as a tool to track the caged probes inside cells, tissue or in a polymeric matrix.[18] Despite several reports that showed successful application of brominated hydroxy-coumarin (Bhc, **1**) for thiol-protection,[9,19,20] a recent study showed photolysis of Bhc-protected thiols often leads to the generation of unwanted photo-isomeric by-products.[21] The two-step mechanism of this photo-rearrangement process was studied in detail by Distefano and coworkers, which set the stage for further modification of the Bhc structure to engineer reduced photoisomerization.

In this report, guided by mechanistic studies of the photo-triggered isomerization of Bhc-thiols, we developed 6-bromo-7-hydroxy-3-methyl coumarin-4-ylmethyl (mBhc, **3**) as an alternative coumarin-based caging group that can afford efficient thiol release upon one- and two-photon irradiation. To test the efficiency of mBhc for thiol-protection in peptides, we have synthesized an mBhc-protected form of cysteine (Fmoc-Cys(mBhc)-OH) suitable for incorporation via solid phase peptide synthesis and subsequently used it to prepare a K-Ras-derived peptide. One- and two-photon photolysis of the caged peptide resulted in clean conversion to the free compound with no photo-isomerization. Irradiation of the caged peptide using a near-IR laser in the presence of an enzyme (protein farnesyltransferase, PFTase) resulted in the generation of a free thiol-containing peptide which was then enzymatically farnesylated. To further evaluate the utility of this novel caging group for biomaterial applications, an mBhc-protected thiol was covalently incorporated into a hydrogel. Using a 740 nm two-photon laser from a confocal microscope, patterns of free thiols were generated inside the matrix and visualized by reaction with maleimide functionalized fluorophores. Such 3D patterns could be useful for a variety of applications in tissue engineering.[10,11]

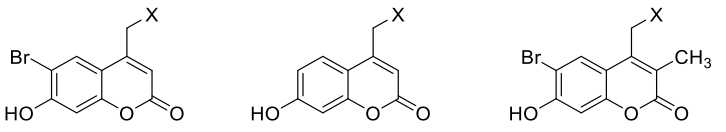

Scheme 3-1 Coumarin-based caging groups discussed in this work.

3.2 Results and Discussion

3.2.1 Design and synthesis of a coumarin-based caging group for efficient thiol protection

In previous work, we demonstrated that the major product of photolysis of Bhc-protected thiols (**4**) is not the free thiol, but rather an isomeric product (**6**) that is formed via the two step process illustrated in Scheme 3-2. We proposed that the first step of that mechanism involves a photo-induced 1,3 shift of the thiol from the exocyclic position to the endocyclic 3 position yielding intermediate **5** that undergoes tautomerization to produce the final photo-rearranged product **6**. Those results illustrate why Bhc is not an efficient caging group for thiol protection. To address this limitation, we have reported nitrodibenzofuran (NDBF) as an alternative caging group for thiol protection, which showed remarkably high uncaging efficiency in both one- and two-photon processes.[21]

Despite the efficiency of NDBF for thiol caging, using coumarin-based caging groups for thiol protection is still advantageous due to their comparatively straightforward synthesis, higher water solubility (relative to NDBF) and the fluorogenic character of coumarin which is useful to track probes inside cells. Hence, we elected to investigate the development of an alternative coumarin-based caging group for thiol protection in small molecules and peptides.

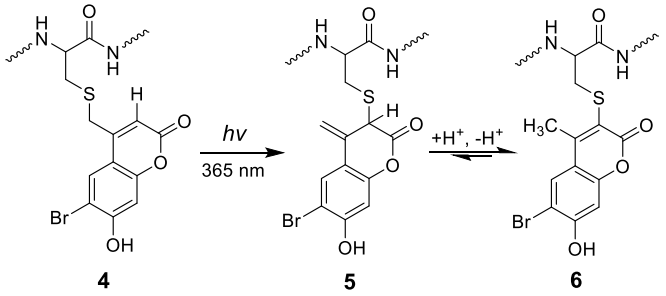

Scheme 3-2 Photo-rearrangement mechanism of Bhc protected cysteine.

We initially hypothesized that changing the substituents on the phenolic ring of Bhc could be used to decrease the extent of photo-rearrangement over uncaging. Therefore, we decided to study the photolysis of a thiol protected by hydroxycoumarin (Hc, **2,** Scheme 1) lacking the bromine on the phenolic ring. Hence, Hc-protected Boc-cysteamine (**7**, Figure 3-1A) was synthesized following a previously reported procedure[22] and studied as a model caged thiol for photolysis experiments. Solutions of compound **7** in buffered aqueous solution were irradiated using 365 nm light for varying times. Analysis of the photolysis reactions via LC-MS using extracted ion current data (EIC) clearly indicates the formation of the undesired photo-isomer upon photolysis as evidenced by the appearance of a new peak (t_R = 7.71 min) with an m/z ratio identical to that of the starting material (Figure 3-1B, C); no Hc-OH (**9**, m/z = 231) generation was observed in the corresponding EIC chromatogram suggesting minimal uncaging occurred upon irradiation.

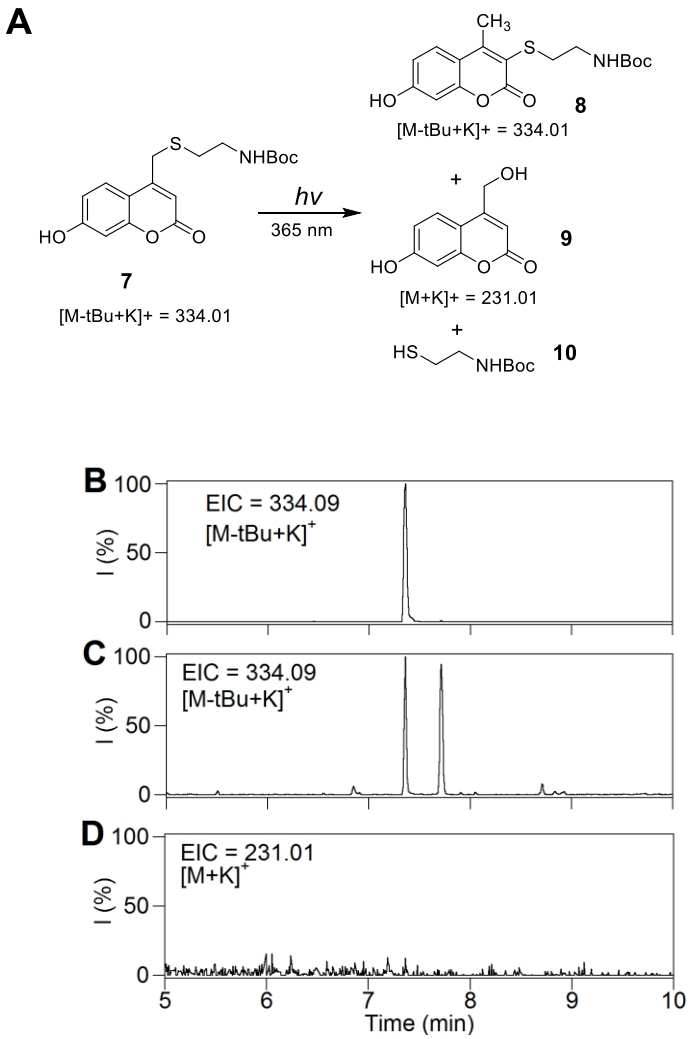

Figure 3-1 Photolysis reaction of Hc-protected Boc-cysteamine. (A) Structures used in this study. (B) EIC chromatogram (m/z = 334.09, calcd for [M(**7**)-tBu+K]$^+$ = 334.01) of a 50 µM solution of **7** in photolysis buffer (50 mM phosphate buffer, pH 7.4 containing 1 mM DTT) before irradiation, (C) EIC chromatogram (m/z = 334.09, calcd for [M(**7**)-tBu+K]$^+$ = 334.01) of a 50 µM solution of **7** in photolysis buffer after 6 min irradiation at 365 nm, this data clearly indicates generation of the photo-isomer, (D) EIC chromatogram (m/z = 231.01, calcd for [M(**9**) +K]$^+$ of **7** after 6 min irradiation showing no evidence of generation of **9**, this indicates photolysis leads predominantly to photo-isomerization rather than uncaging.

In addition to these data, it should be noted that Kotzur et al. previously reported photo-rearrangement occurring upon photolysis of 7-amino and 7,8-bis(carboxymethoxy) coumarin protected thio-carbamates.[19] These results and observations indicate that photoisomerization is widespread in coumarin

photochemistry and that simple alteration of the substituents on the phenolic ring would not be sufficient to shut down the photoisomerization reaction manifold. Given those results, we next elected to modify the endocyclic 3 position which is directly involved in the photo-rearrangement mechanism. We hypothesized that replacing the hydrogen atom at that position with an alkyl moiety should attenuate photo-isomerization due to several factors. First, the presence of an alkyl group on C-3 would block photoisomer formation since intermediate **12** cannot re-aromatize due to the absence of a hydrogen at the 3 position. Second, the syn pentane type interaction between the sulfur and the C-3 methyl group shown in Scheme 3-3 should make it sterically more difficult for the sulfur atom to migrate to the C-3 position. Computational analysis of the model compounds mBhc-SCH_3 and Bhc-SCH_3 shows that the lowest energy conformers for both molecules position the thiomethyl group 90° out of the coumarin plane (see Figure S1). However, the steric hindrance noted above is highly destabilizing for mBhc-SCH_3 as evidenced by the large increase in conformational energy that occurs when the thiomethyl group is moved towards the coumarin plane; such a movement would be required in the thiol migration step.

Based on this hypothesis, we decided to synthesize 6-bromo-7-hydroxy-3-methyl coumarin-4-ylmethyl bromide (mBhc-Br, **3a**) and examine its utility for thiol protection, particularly for S-protection of cysteine containing peptides. The synthesis of mBhc-Br is depicted in Scheme 3-4. Dropwise addition of Br_2 to an ice cold solution of ethyl-2-methylacetoacetate in $CHCl_3$ followed by overnight stirring at room temperature gave 4-bromo-2-methylacetoacetate (**14**, 70%

yield).[23] That compound was subsequently treated with 4-bromoresorcinol in CH_3SO_3H overnight at room temperature to afford the desired bromide (**3a**) in 35% yield. After successful synthesis of mBhc-Br, we next sought to utilize this caging group for thiol protection in cysteine containing peptides to evaluate its uncaging efficiency in the context of biologically useful molecules.

Our strategy for creating caged peptides was to prepare mBhc-protected Fmoc-Cys-OH and incorporate that into a peptide of interest through solid phase peptide synthesis (SPPS). The synthesis of the desired mBhc S-protected cysteine suitable for SPPS is illustrated in Scheme 3-4. The phenolic hydroxyl group of mBhc was protected as a MOM ether via treatment with MOM-Cl and TEA to give compound **15** in 95% yield. That species was then used to alkylate Fmoc-Cys-OCH_3 under mild acidic conditions using $Zn(OAc)_2$ as a catalyst to produce **16** in 90 % yield. The resulting methyl ester was hydrolyzed via treatment with $(CH_3)_3SnOH$ [24] in refluxing CH_2Cl_2 to generate a caged form of Fmoc-cysteine (Fmoc-Cys(mBhc)-OH **17**) in 85 % yield.

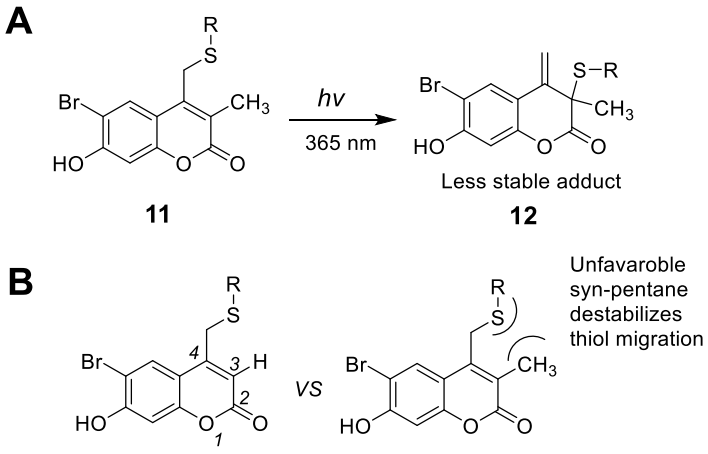

Scheme 3-3 Illustration of potential effects of C-3 substitution on photoisomerization process.

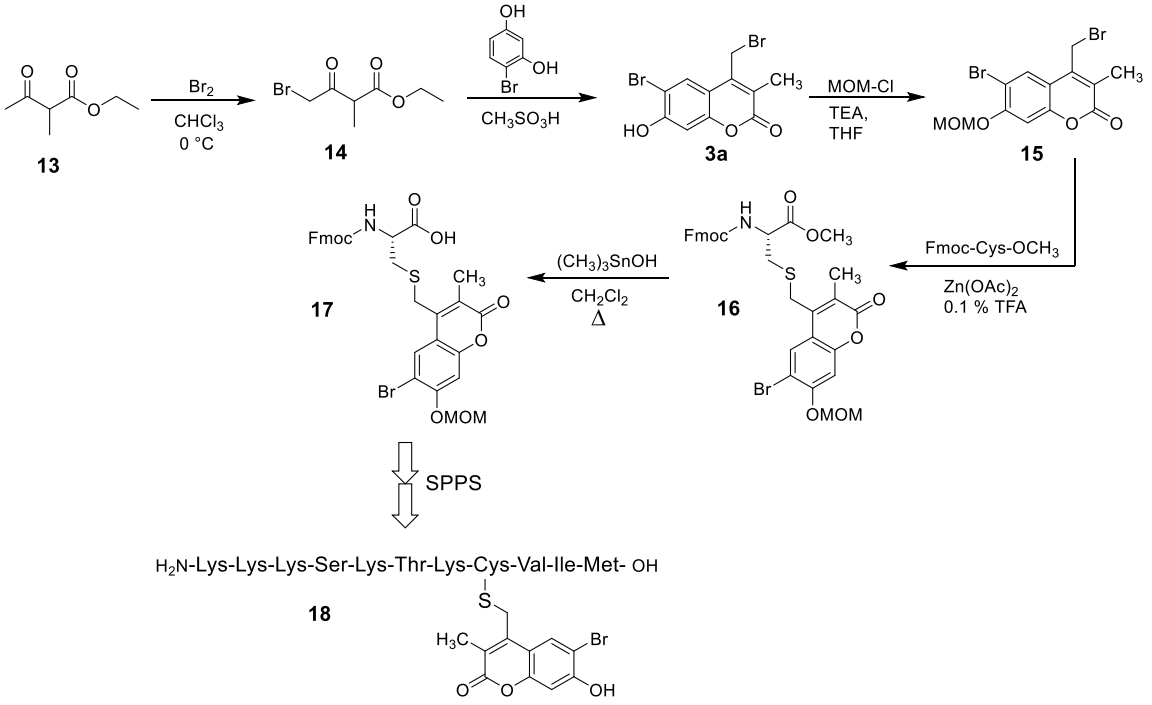

Scheme 3-4 Synthesis of Fmoc-Cys(mBhc)-OH and its incorporation into a K-Ras-derived peptide via SPPS.

Synthesis of the desired caged peptide was performed via SPPS, in which Fmoc-protected amino acids were added sequentially to the growing chain anchored on Wang resin. Standard coupling conditions were used throughout the synthesis except for the incorporation of Fmoc-Cys(mBhc)-OH where the coupling time was increased to 6 hours to ensure quantitative incorporation. Final acidic treatment of the resin-bound peptide with Reagent K ensured removal of all side-chain protecting groups including the MOM group present on the mBhc moiety, and cleavage of the peptide from the resin to produce the desired caged molecule. The above procedure was successfully used to generate a caged form of a K-Ras-derived peptide (**18**) that was subsequently used to study the uncaging reaction and the utility of this new protecting group.

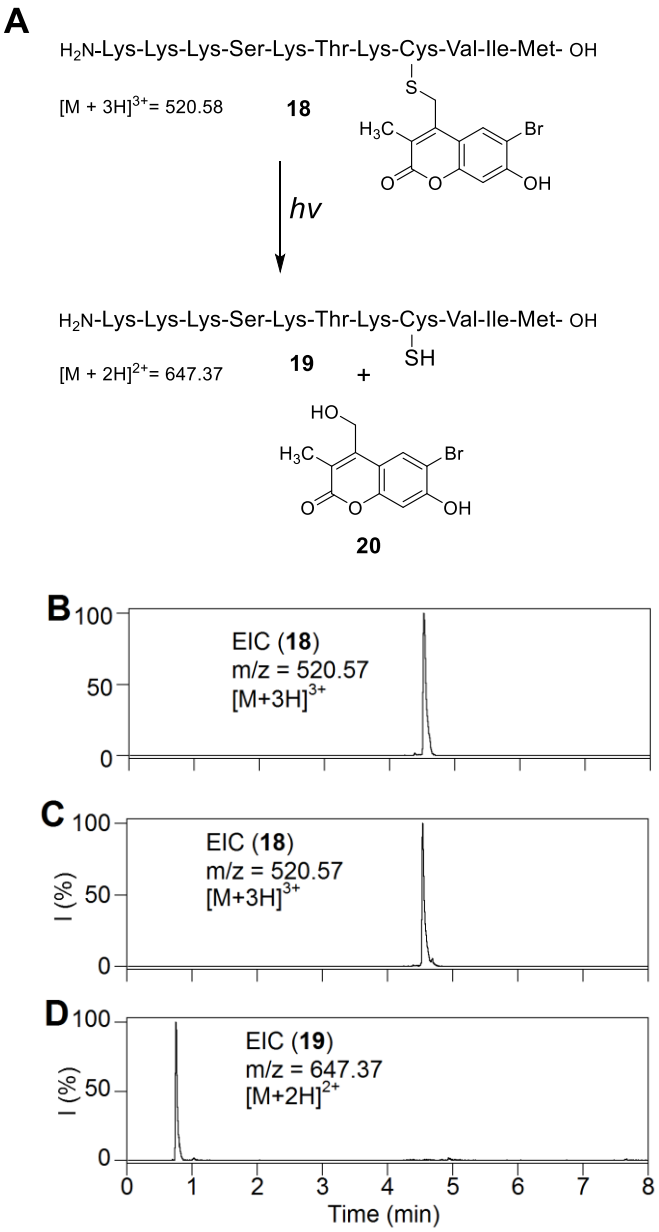

Figure 3-2 Uncaging studies using a peptide with a mBhc-protected thiol. (A) Photo-triggered uncaging of mBhc-protected K-Ras peptide (**18**). (B) EIC chromatogram (m/z = 520.57, calcd for $[M + 3H]^{3+}$= 520.58) of a 100 µM solution of **18** before irradiation, (C) EIC chromatogram (m/z = 520.57, calcd for $[M + 3H]^{3+}$= 520.58) of a 100 µM solution of **18** after 60 s irradiation at 365 nm suggesting that no photo-isomer is generated and only the remaining starting peptide peak is present, (D) EIC chromatogram (m/z = 647.37, calcd for $[M + 2H]^{2+}$= 647.37) of a 100 µM of **18** after 60 s irradiation at 365 nm which clearly indicates formation of free peptide **19**.

After synthesis and purification of the mBhc S-protected peptide, photolysis experiments were carried out to probe for the formation of free peptide and any possible photo-isomer. Thus, a solution of **18** was irradiated using 365 nm light and subsequently analyzed by LC-MS. As confirmed by the extracted ion-current (EIC) data shown in Figure 3-2, photolysis resulted in the generation of the desired uncaged peptide as evidenced by the appearance of the corresponding peak with the expected mass (t_R = 0.75 min, m/z = 647). However, apart from the remaining caged peptide peak (**18**, m/z = 520), there was no evidence of any new peak bearing the same mass suggesting that no photo-isomer was generated upon photolysis. Photolysis experiments were carried out in presence of 1mM DTT to block possible disulfide formation, thus simplifying analysis of the crude reaction mixture. (see Figure S2). Similar photolysis experiments, previously reported by our group using the analogous Bhc-protected (lacking the methyl group at C-3) peptide, resulted in the photo-isomer being the predominant product with only low amounts of the desired uncaged peptide formed. Overall, the data presented here indicates that an mBhc caged thiol, unlike its Bhc-protected counterpart, undergoes clean conversion to the uncaged peptide with no significant formation of undesired photo-rearranged byproducts.

3.2.2 Photo-physical properties of an mBhc protected thiol

The observations noted above suggest that mBhc should be useful as a caging group for thiol protection in peptides and other biomolecules. Accordingly, the spectral and photochemical properties mBhc were studied in detail in order to compare them with Bhc and other established caging groups. Perusal of the data

summarized in Table 3-1 shows that $\lambda_{max(ex)}$ and $\lambda_{max(em)}$ of mBhc at pH 7.2, are minimally (~ 5 nm) red-shifted relative to those of Bhc due to the electronic effect of the methyl substituent. The molar absorptivity of mBhc was measured to be 14,500 $M^{-1}cm^{-1}$ which is comparable to that of Bhc. The one- and two-photon uncaging efficiencies of an mBhc -protected thiol were also quantified by irradiating solutions of **18** followed by analysis via RP-HPLC (Figure 3-3). For one-photon measurement, solutions of **18** were irradiated using 365 nm light in a Rayonet reactor for varying amounts of time ranging from 5 to 60 sec and analyzed by RP-HPLC to monitor the disappearance of **18** over time. The one-photon quantum yield for thiol uncaging of **18** was measured to be 0.01 by following the disappearance of caged peptide over different irradiation times and using 6-bromo-7-hydroxycoumarin-4-ylmethyl acetate (Bhc-OAc) as a reference, which was photolyzed under the same conditions (Fig 3B). In order to fully evaluate the photo-conversion yield of mBhc protected thiols to the free thiols, a fluorophore-labeled homolog of the caged peptide **18** (Figure S4) and also an mBhc-protected form of cysteamine (Figure S3) were prepared. Having the fluorophore group remain associated with the thiol moiety after photolysis allowed us to fully monitor the release of the free thiol or any other possible byproducts using analytical RP-HPLC via fluorescence detection That HPLC data shows essentially clean conversion of the caged compounds to the corresponding free thiols with no photo-isomer or byproduct formation. Further experiments were carried out to evaluate the two-photon uncaging efficiency of mBhc. For those measurements, solutions of **18** were irradiated at 800 nm using a pulsed Ti:Saphire laser and the photolysis

products were again analyzed by RP-HPLC and confirmed by LC-MS (Figure 3-3C). The two-photon action cross-section of mBhc was measured to be 0.16 GM at 800 nm again using Bhc-OAc as a reference. The two-photon action cross-section and quantum yield for mBhc are comparatively high considering that thiols are poorer leaving groups relative to carboxylates and phosphates.

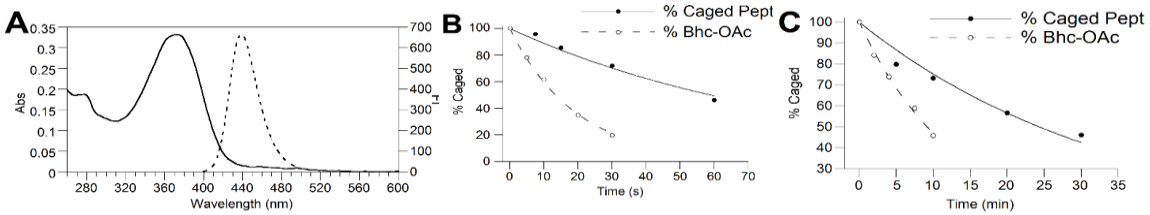

Figure 3-3 Photophysical properties of mBhc. (A) Absorption and emission spectra of mBhc (**3**) in 50 mM PB, pH 7.4. (B) Time course of photolysis of **18** and Bhc-OAc as a reference at 365 nm and (C) Time course of photolysis of **18** and Bhc-OAc as a reference at 800 nm (pulsed Ti:Saphire laser, 210 mw, 80 fs pulse width) quantified by RP-HPLC. Photolysis reactions were performed in 100 µM (for UV), and 300 µM (for TP) solutions of **18** containing 1 mM DTT in 50 mM PB, pH 7.4.

	λmax (ex) (nm)	λmax (em) (nm)	ε (λmax) ($M^{-1}cm^{-1}$)	Q_u (365 nm)	δ_u (800 nm)
mBhc-thiol (**18**)	374	480	14,500	0.01	0.16
Bhc-OAc	370	474	15,000	0.04	0.42
λmax (ex) and λmax (em): absorption and emission maximum in nm, respectively, ε: extinction coefficient in $M^{-1}cm^{-1}$ at wavelength indicated, Q_u: quantum yield of one-photon uncaging at 365 nm, δ_u two-photon action cross-section in $10^{-50}cm^4s$/photon (GM) for uncaging at 800 nm.					

Table 3.1 Photophysical properties of mBhc-thiol versus Bhc-OAc.

3.2.3 One- and two-photon activation of protein prenylation

Since an mBhc protected thiol demonstrated good uncaging efficiency toward one- and two-photon excitation, we next sought to study its utility for photo-triggered activation of a peptide in a more biologically relevant context. Protein prenylation is a ubiquitous post-translational modification that plays critical roles in a variety of cellular functions including the regulation of cell growth, differentiation and cytoskeletal integrity. Prenylation involves the enzymatic attachment of a prenyl group through a thioether linkage to a conserved cysteine residue near the C-terminus of various proteins.[25] This process is catalyzed by protein prenyltransferases including protein farnesyltransferase which transfers a farnesyl (C_{15}) group. Among the proteins that undergo prenylation is Ras, which upon farnesylation migrates to plasma membrane where it participates in key cell signaling pathways including cell division. Mutations in the Ras protein have been linked to numerous types of cancers.[26]

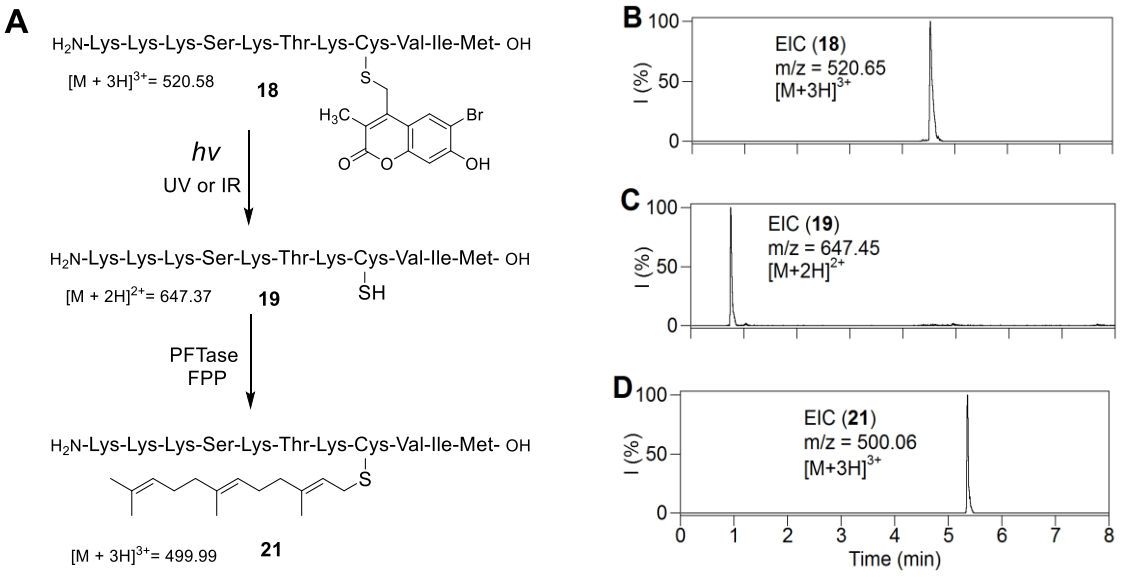

Figure 3-4 Photo-triggered farnesylation of an mBhc-protected K-Ras peptide. (A) Structures of peptides and products relevant to this study. (B) EIC chromatogram (m/z = 520.65, calcd for $[M + 3H]^{3+}$= 520.58) of a 7.5 µM solution of **18** in a prenylation buffer containing PFTase with no irradiation. (C) EIC chromatogram (m/z = 647.45, calcd for $[M + 2H]^{2+}$= 647.39) of a 7.5 µM solution of **18** after 60 s irradiation at 365 nm in prenylation buffer without PFTase showing the formation of free peptide **19**. (D) EIC chromatogram (m/z = 500.06, calcd for $[M + 3H]^{3+}$= 499.99) of a 7.5 µM of **18** after 60 s irradiation at 365 nm in presence of PFTase showing the formation of farnesylated peptide **21**.

To investigate the utility of mBhc, the K-Ras derived peptide described above was studied in *in vitro* prenylation reactions. It should be noted peptide **18** incorporates an mBhc-protected cysteine residue at the natural site of prenylation and hence should not be a substrate for protein farnesyltransferase in its caged state. However, upon irradiation, photo-cleavage of the protecting group should generate a peptide manifesting a free thiol suitable for prenylation by PFTase (see Figure 3-3A). To test this, *in vitro* farnesylation reactions using the caged K-Ras derived peptide **18** were performed under several different conditions. As predicted,

incubation of the caged peptide with the enzyme and FPP did not result in the generation of any farnesylated peptide. LC-MS analysis of the mixture indicates only the presence of the caged peptide (m/z = 520.65, Figure 3-3B). Photolysis of **18** for 60 seconds at 365 nm in the absence of the enzyme, produced the free-thiol containing peptide (**19**) as evidenced by the appearance of a new peak with a lower retention time exhibiting the expected mass (m/z = 647.45). Importantly, photolysis of **18** in the presence of PFTase resulted in generation of a different peak corresponding to the expected farnesylated peptide (**21**). This was confirmed by the detection of a new peak eluting at 5.36 min with an m/z ratio of 500.06 which is in good agreement with the calculated value (m/z for $[M+3H]^{3+}$ = 499.99).

Since, photo-triggered activation of the mBhc-protected peptide was successful using a one-photon (UV) process, we next sought to further evaluate its ability to be uncaged via two-photon excitation where IR light is used as the trigger in lieu of UV irradiation. This would open the door for employing such caged peptides in studies performed inside tissue or whole organisms where UV light has low penetration and causes phototoxicity. Accordingly, *in vitro* farnesylation experiments, similar to those described above for UV irradiation, were carried out using an 800 nm laser light source. Irradiation of **18** using 800 nm laser light for 5 min in the absence of PFTase resulted in the generation of free peptide (Figure S5). However, two-photon irradiation of caged peptide in the presence of FPP and PFTase generated the farnesylated peptide as confirmed by LC-MS analysis (Figure S5). This data clearly illustrates that mBhc-protected K-Ras peptide can

be being activated and undergo farnesylation upon near IR irradiation, setting the stage for future studies in whole cells and tissue samples.

3.2.4 Two-photon patterning using a mBhc-caged thiol

In addition to their use for triggering biological activity as noted above, caged thiols are also useful for creating patterns of thiols that can be further functionalized for various material science applications. In particular, since the above experiments demonstrated that mBhc could be efficiently removed by two-photon excitation with 800 nm light, we reasoned that it should be possible to use an mBhc-protected thiol to create 3D patterns within a hydrogel matrix. This has been previously accomplished using a Bhc-protected thiol.[9,27] However, the improved efficiency of thiol-uncaging obtained with mBhc relative to Bhc due to elimination of the photoisomerization pathway should increase the utility of this approach; in theory, higher levels of thiol uncaging should be obtained with mBhc for a given amount of irradiation. Accordingly, we sought to compare the thiol patterning obtained using mBhc versus Bhc. Hyaluronic acid (HA) hydrogels were modified with mBhc- or Bhc-protected thiols by coupling mBhc/Bhc-protected cysteamine with the carboxylate groups of HA, and furan functional groups, which are crosslinked with poly(ethylene glycol) (PEG)-bismaleimide (Scheme 3-5, Figure 3-5A). Unreacted furan groups are quenched with N-hydroxyethyl maleimide and then the functionalized, crosslinked hydrogels are extensively washed. The resulting material was then infused with sulfhydryl-reactive AlexaFluor546-maleimide to allow visualization of any uncaged thiols formed followed by two-photon irradiation at 740 nm using a confocal microscope. Square tile patterns were created by

scanning a square region of interest 5-20 times in the x-y plane at a fixed z-dimension. The overall dimensions for each square tile were 80x80 µm, with the plane of the patterned tile positioned 150 µm from the base of the hydrogel. After uncaged thiols react with the Alexa Fluor reagent, the patterns were imaged and quantified by confocal microscopy. Images from those experiments (Figure 3-5B) illustrate how clean patterns can be prepared using this approach. As expected, the intensity of thiol labeling was greater in hydrogels prepared using mBhc compared with Bhc due to the greater uncaging efficiency of the former. Quantitative image analysis of the immobilized Alexa Fluor 546 dye (Figure 3-5C) shows that the uncaging efficiency of the mBhc-functionalized hydrogel is approximately 4-fold higher than that obtained using the Bhc-containing material. Overall, these results further highlight the utility of the mBhc group for thiol protection.

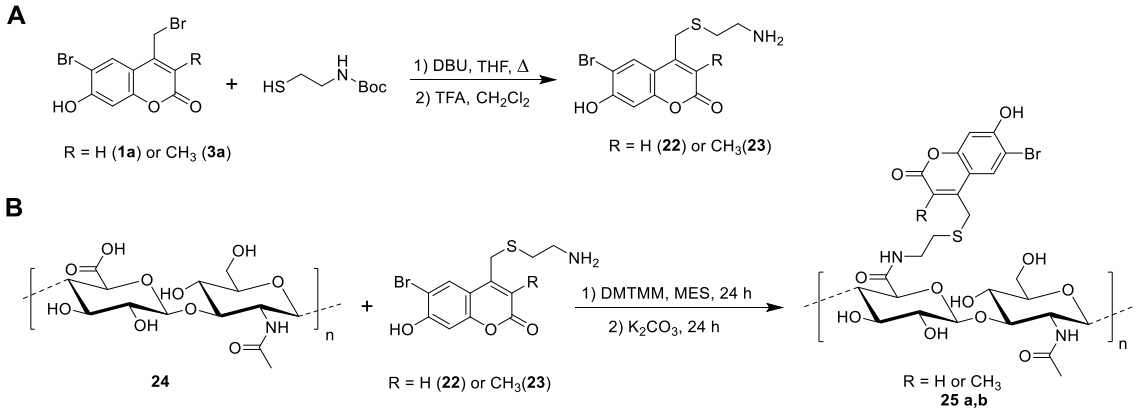

Scheme 3-5 Schematic representation of (A) synthesis of mBhc and Bhc protected cysteamine, followd by (B) conjugation to HA-carboxylic acids using DMT-MM prior to crosslinking HA-furan with PEG-bismaleimide.

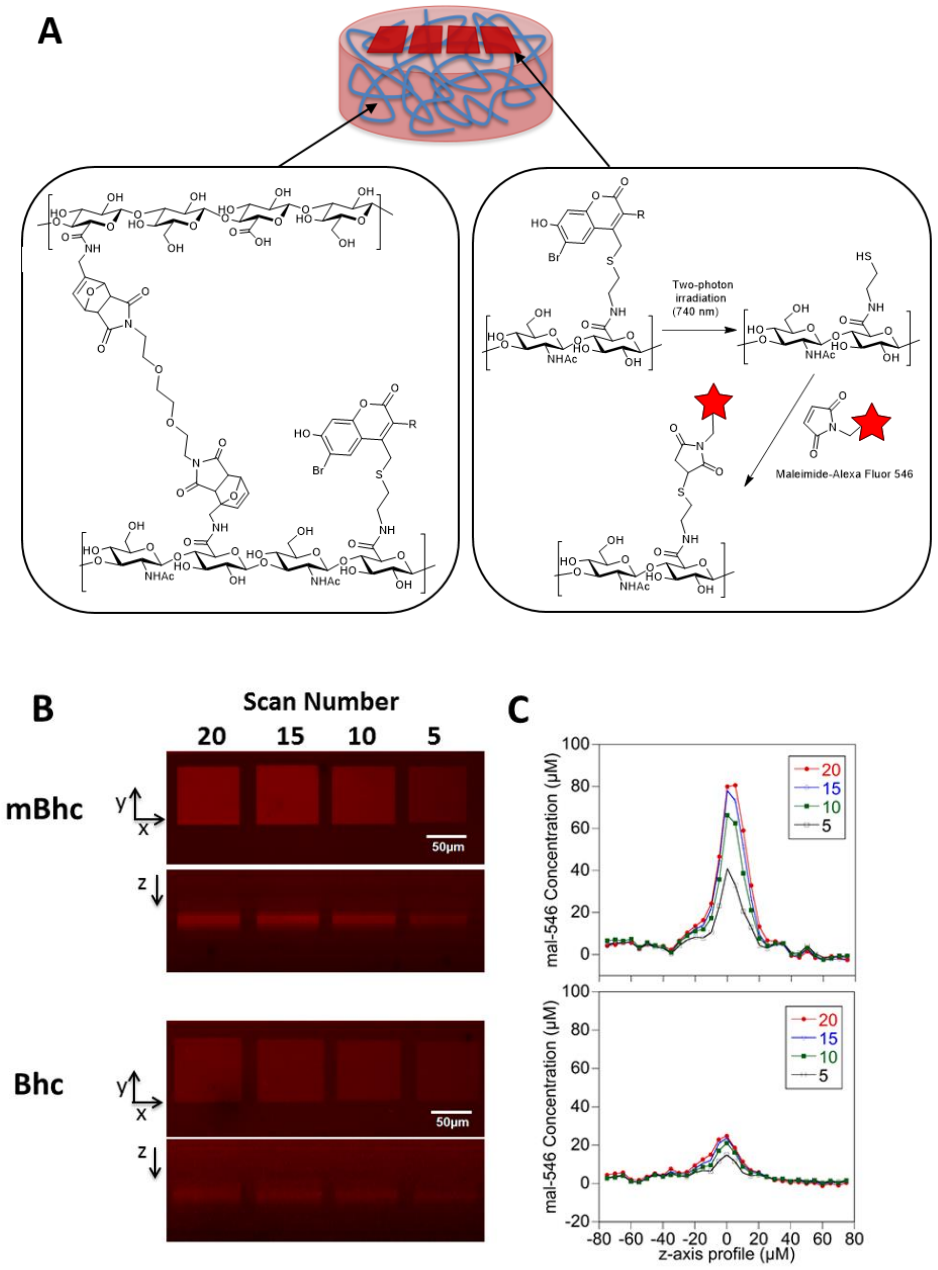

Figure 3-5 Comparison of two-photon patterning using Bhc- and mBhc-caged thiol. (A) Bhc or mBhc to is conjugated to HA-carboxylic acids using DMT-MM prior to crosslinking HA-furan with PEG-bismaleimide. (B) Schematic representation of two-photon patterning in Bhc or mBhc-conjugated HA hydrogels. A 3D hydrogel scaffold (i) is formed when Bhc/mBhc-modified HA-furan is chemically crosslinked with PEG-bismaleimide (ii).. The resulting photo-labile hydrogel undergoes photolysis of the Bhc/mBhc groups using two-photon irradiation to liberate free thiols in discrete regions of the hydrogel, which then react with maleimide-bearing Alexa Fluor 546 (mal-546) (iii) (C) Visualization of mal-546 patterns in the x-y plane and z-dimension in mBhc and Bhc conjugated HA hydrogels. Regions of

interest were scanned 5 to 20 times at a fixed z-dimension. The concentrations of mBhc and Bhc were matched based on UV absorbance. Patterns in mBhc and Bhc conjugated HA hydrogels were imaged at different confocal settings due to Bhc patterns being so faint in comparison to mBhc patterns. (D) The z-axis profile of immobilized mal-546 in mBhc and Bhc conjugated HA hydrogels was quantified with the maximum intensity was centered at 0 μm.

3.3 Conclusion

In this work, we have developed mBhc as an alternative, coumarin-based caging group capable of mediating thiol photo-release through both one- and two-photon irradiation. The design of mBhc was guided by recently reported mechanistic experiments that showed that photo-isomerization of Bhc-caged thiols leads to a low uncaging yield. Studies of the spectral properties of mBhc show minimal variations from those of Bhc suggesting that mBhc should be a useful chromophore with high fluorogenic character. A form of mBhc [Fmoc-Cys(MOM-mBhc)-OH] suitable for solid phase synthesis was prepared and used to assemble a K-Ras derived peptide incorporating a caged cysteine residue. One-photon photolysis of the caged peptide at 365 nm resulted in clean conversion to the free peptide with a photolysis quantum yield of 0.01. The two-photon action cross-section of the caged peptide was also measured to be 0.13 GM at 800 nm, comparable to that of Bhc-OAc. The one-and two-photon uncaging of the caged peptide in the presence of PFTase and FPP generated a farnesylated peptide indicating that the free peptide which resulted from photolysis can be recognized by PFTase and become enzymatically modified. The high two-photon uncaging efficiency of mBhc protected thiols was also harnessed to create 3D patterns of thiols inside hydrogels for material science applications. Overall, this work sets the stage for future work requiring caged sulfhydryl groups. Given the unique reactivity

of thiols, the mBhc protecting group developed here should be useful for a variety of applications in biology and material science.

3.4 Experimental Section

General. All reagents needed for solid phase peptide synthesis were purchased from Peptide International (Louisville, KY). All other solvents and reagents used for synthesis and other experiments were purchased from Sigma Aldrich (St. Louis, MO) or Caledon Laboratory Chemicals (Georgetown, ON, Canada). Lyophilized sodium hyaluronate (HA) was purchased from Lifecore Biomedical (2.15×10^5 amu) (Chaska, MN, USA). Dimethyl sulfoxide (DMSO), 4-(4,6-dimethoxy-1,3,5-triazin-2-yl)-4-methylmorpholinium chloride (DMT-MM), 1-methyl-2-pyrrolidinone (NMP), furfurylamine, and Dulbecco's phosphate buffered saline (PBS) were purchased from Sigma-Aldrich (St. Louis, MO, USA). N-(2-hydroxyethyl)maleimide was purchased from Strem Chemicals (Newburyport, MA, USA). 2-(N-mortholino)ethanesulfonic acid (MES) were purchased from BioShop Canada Inc. (Burlington, ON, Canada). Dialysis membranes were purchased from Spectrum Laboratories (Rancho Dominguez, CA, USA). Alexa Fluor 546 maleimide (mal-546) was purchased from Thermo Scientific (Waltham, MA, USA). HPLC analysis (analytical and preparative) was performed using a Beckman model 125/166 instrument, equipped with a UV detector and C18 columns (Varian Microsorb-MV, 5 µm, 4.6 x 250 mm and Phenomenex Luna, 10 µm, 10 x 250 mm respectively). ^{1}H NMR data of synthetic compounds were recorded at 500 MHz on a Varian Instrument at 25 °C, unless noted. ^{13}C NMR data of synthetic compounds were recorded at 125 MHz on a Varian Instrument at 25 °C, unless noted.

Procedure for solid phase peptide synthesis. Peptides were synthesized using an automated solid-phase peptide synthesizer (PS3, Protein Technologies Inc., Memphis, TN) employing Fmoc/HCTU based chemistry. The synthesis started by transferring Fmoc-Met-Wang resin (0.25 mmol) into a reaction vessel followed 45 min swelling in DMF. Peptide chain elongation was performed using HCTU and N-methylmorpholine. Standard amino acid coupling was carried out by incubation of 4 equiv of both HCTU and the Fmoc protected amino acid with the resin for 30 min. Coupling of Fmoc-Cys(MOM-mBhc)-OH (**17**) was performed by incubation of 1.5 equiv of both the amino acid and HCTU with the resin for 6 h. Peptide chain elongation was completed by N-terminus deprotection using 10% piperidine in DMF (v/v). Global deprotection and resin cleavage was accomplished via treatment with Reagent K. Peptides were then precipitated with Et_2O, pelleted by centrifugation and the residue rinsed twice with Et_2O. The resulting crude peptide was dissolved in CH_3OH and purified by preparative RP-HPLC. KKKSKTCC(mBhc)IM (**18**). ESI-MS: calcd for $[C_{67}H_{115}BrN_{16}O_{17}S_2 + 2H]^{2+}$ 780.3698, found 780.3777. 5-Fam-KKKSKTKC(mBhc)VIM calcd for $[C_{88}H_{125}BrN_{16}O_{23}S_2+2H]^{2+}$ 959.3937, found 959.3782.

Hc-Boc-cysteamine (7). 7-hydroxycoumarin bromide (**1a,** 1 g, 3.9 mmol), N-(tert-butoxycarbonyl)aminoethanethiol (**10**, 0.86 mL, 5.1 mmol) and 1,8-diazabicyloundec-7-ene (0.76 mL, 5.1 mmol) were dissolved in 70 mL of THF and refluxed for 4 h. The reaction was judged completed by TLC (2:3, Hexanes/EtOAc). Solvent was removed *in vacuo,* and the crude mixture was diluted in 75 mL EtOAc.

The organic layer was washed with 50 mL of 0.1 M $NH_4Cl_{(aq)}$, brine, and then dried over Na_2SO_4. The solvent was removed *in vacuo* and the crude mixture was purified via silica gel chromatography (2:1 Hexanes/EtOAc) to give 836 mg of **7** as a yellow oil (61 % yield). ^{1}H NMR (d_6-acetone) δ 7.79 (1H, d, J = 8.4 Hz), 6.95 (1H, dd, J = 8.75, 2.8 Hz), 6.32 (1H, s), 3.95 (2H, s), 3.37 (2H, q, J = 6.3 Hz), 2.74 (2H, t, J = 7 Hz), 1.54 (9H, s).

Ethyl 4-bromo-2-methyl acetoacetate (14). Compound **14** was prepared by minor modification of a published procedure.[23] To an ice cold solution of ethyl 2-methylacetoacetate (2 mL, 14 mmol) in 50 mL $CHCl_3$ was added a solution of Br_2 (0.68 mL, 14 mmol) in 10 mL $CHCl_3$ over 15 min. The mixture was then warmed to rt and stirred overnight. The organic layer was then washed with 50 mL solution of 0.1 M sodium thiosulfate, brine and then dried over Na_2SO_4. The solvent was evaporated *in vacuo* to yield 2.34 g of **14** as a pale orange oil (75 % yield). The resulting material was directly used for the next step without further purification.

6-Bromo-7-hydroxy-3-methyl coumarin-4-ylmethyl bromide (mBhc-Br, 3a). A solution of 4-bromoresrocinol (1 g, 5.3 mmol) and ethyl 4-bromo-2-methyl acetoacetate **14** (2.3 g, 10.4 mmol) in 30 mL of CH_3SO_3H was stirred at rt overnight. The mixture was then fractionated between 100 mL H_2O and 100 mL EtOAc. The organic layer was separated, washed with brine and dried over Na_2SO_4. Solvent was removed *in vacuo* and the resulting crude mixture was purified via silica gel chromatography (2:1, Hexanes/EtOAc) to give 645 mg of **3** as a pale yellow solid. ^{1}H NMR (d_6-acetone) δ 8.01 (1H, s), 6.95 (1H, s), 4.85 (2H, s), 2.21 (3H, s). ^{13}C NMR (d_6-acetone) δ 160.81, 156.32, 153.12, 143.73, 128.59,

121.46, 111.94, 106.00, 103.45, 24.14, 11.98. HR-MS (ESI) *m/z* calcd for $[C_{11}H_7Br_2O_3]^-$ 346.8720, found 346.8720.

MOM-mBhc-Br (15). To a stirred solution of **3a** (400 mg, 1.15 mmol) and chloromethyl methyl ether (MOM-Cl, 0.13 mL, 1.72 mmol) was added 1,8-diazabicyloundec-7-ene (0.19 mL, 1.3 mmol). The mixture was stirred for about 2 h until complete as judged by TLC (in CH_2Cl_2). The solvent was evaporated *in vacuo*. The resulting crude material was dissolved in a small amount of CH_2Cl_2 which was then loaded onto a silica gel column and purified to give 428 mg of **3** as pale yellow oil (95 % yield). ^{1}H NMR ($CDCl_3$) δ 7.82 (1H, s), 7.15 (1H, s), 5.31, (2H, s), 4.62 (2H, s), .352 (3H, s), .228 (3H, q, J = 6.3 Hz), ^{13}C NMR ($CDCl_3$) δ 161.40, 155.55, 152.80, 142.50, 128.03, 123.26, 113.33, 108.66, 103.96, 95.21, 56.64, 37.09, 12.91. HR-MS (ESI) *m/z* calcd for $(C_{13}H_{12}Br_2O_4 + Na)^+$ 414.8980, found 414.9001.

mBhc-cysteamine (23). mBhc-Br **(3a,** 0.8 g, 2.3 mmol), N-(tert-butoxycarbonyl)aminoethanethiol **10** (0.51 mL, 3.0 mmol) and 1,8-diazabicyloundec-7-ene (0.45 mL, 3.0 mmol) were dissolved in 50 mL of THF and refluxed for 4 h. The reaction was judged completed by TLC (2:3, Hexanes/EtOAc). The solvent was removed *in vacuo,* and the crude mixture was diluted in 50 mL EtOAc. The organic layer was washed with 50 mL of 0.1 M $NH_4Cl_{(aq)}$, brine, and then dried over Na_2SO_4. The solvent was removed *in vacuo* and the crude mixture was purified via silica chromatography (2:1 Hexanes/EtOAc) to give 664 mg of mBhc-Boc-cysteamine as a yellow oil. The purified compound was dissolved in 10 mL solution of CH_2Cl_2:TFA (1:1) and stirred for 30 min. The mixture was

evaporated and purified via silica (1:1 Hex/EtOAc) to give 514 mg (65 % yield) of the desired free amine as white solid. ^{1}H NMR (d_6-acetone) δ 7.92 (1H, s), 6.77 (1H, s), 6.32 (1H, s), 4.06 (2H, s), 3.29 (2H, q, J = 6.3 Hz), 3.02 (2H, t, J = 7 Hz), 2.19 (3H, s), ^{13}C NMR (D_2O) δ 163.53, 155.54, 151.78, 139.08, 128.88, 124.15, 113.36, 106.72, 103.38, 49.95, 48.31, 34.24, 13.52. HR-MS (ESI) *m/z* calcd for $(C_{13}H_{14}BrNO_3 + H)^+$ 343.9951, found 414.9827.

Fmoc-Cys(MOM-mBhc)-OCH$_3$ (16). Bromide **15** (400 mg, 1 mmol) and Fmoc-Cys-OCH_3 (714 mg, 2 mmol) were dissolved in 10 mL of a solution of 2:1:1 DMF/CH_3CN/H_2O/0.1% TFA (v/v/v/v). $Zn(OAc)_2$ was then added (550 mg, 2.5 mmol) and the reaction monitored by TLC (1:1 Hexanes/EtOAc). After two days, the solvent was removed and the reaction purified via column chromatography (1:1 Hexanes/EtOAc) to give 530 mg of **16** as yellow powder (81% yield). ^{1}H NMR ($CDCl_3$) 7.80 (1H, s), 7.72 (2H, t, J=8), 7.59 (2H, t, J=7), 7.32-7.40 (2H, m), 7.28 (2H, t, J=7), 7.11 (1H, s), 5.61 (1H, d, J=6.5), 5.28 (2H, s), 4.53 (1H, t, J=7), 4.45 (1H, t, J=7), 4.22 (1H, t, J=6.5), 3.70-3.80 (6H, m), 3.51 (3H, s), 3.16 (1H, q), , 2.20 (3H, s). ^{13}C NMR ($CDCl_3$) δ 170.81, 161.41, 155.74, 155.32, 152.69, 143.67, 143.59, 143.53, 141.35, 141.31 128.57, 127.79, 127.76 127.11, 127.05, 125.01, 124.96, 122.31, 120.02, 120.01, 114.16, 108.41, 103.79, 95.18, 67.07, 53.87, 52.97, 47.19, 35.62, 29.83, 13.27. HR-MS (ESI) *m/z* calcd for $[C_{32}H_{30}BrNNaO_8S + Na]^+$ 690.0773, found 690.0720.

Fmoc-Cys(MOM-mBhc)-OH (17). Ester **16** (200 mg, 0.30 mmol) and $(CH_3)_3SnOH$ (135 mg, 0.75 mmol) were dissolved in CH_2Cl_2 (5 mL) and brought to

reflux. After 7 h, the reaction was judged complete by TLC (1:1 Hexanes/EtOAc), the solvent removed *in vacuo* and the resulting oil redissolved in EtOAc (20 mL). The organic layer was washed with 5% HCl (3 x 10 mL) and brine (3 x 10 mL), dried with Na_2SO_4 and evaporated to give 173 mg of **17** as a yellow powder (90% yield). ^{1}H NMR ($CDCl_3$) δ 9.68 (1H, s), 7.73 (1H, s), 7.64 (2H, t, J=7), 7.55 (2H, t, J=7), 7.32 (2H, t, J=7.5), 7.23 (2H, m), 6.98 (1H, s), 5.93 (1H, d, J=7.5), 5.19 (2H, s), 4.72 (1H, m), 4.65 (1H, t, J=7), 4.41 (1H, t, J=7), 4.16 (1H, t, J=7), 3.70-3.80 (2H, m), 3.45 (3H, s), 3.20 (1H, m), 3.06 (1H, q), 2.14 (3H, s). ^{13}C NMR ($CDCl_3$) δ 173.41, 161.83, 156.20, 155.21, 152.43, 144.06, 143.63, 143.48, 141.26, 141.22, 128.58, 127.11, 127.06, 125.02, 119.98, 114.09, 108.52, 103.58, 95.06, 67.26, 56.63, 53.72, 47.09, 35.51, 29.79, 14.18, 13.24, 31.07, 14.07. HR-MS (ESI) *m/z* calcd for $[C_{31}H_{28}BrNNaO_8S + Na]^+$ 676.0601, found 676.0601.

General procedure for UV photolysis of caged molecules. Solutions of caged compound were prepared in photolysis buffer (50 mM phosphate buffer, pH 7.4 containing 1 mM DTT) at a final concentration of 25-250 µM. Aliquots (100 µL) of caged compound solutions were transferred into quartz cuvettes (10 x 50 mm) and irradiated for varying amounts of time with 365 nm UV light using a Rayonet reactor (2 x 14 watt RPR-3500 bulbs). After different irradiation times, the samples were analyzed by RP-HPLC or LC-MS.

General procedure for two-photon photolysis of caged molecules. Solutions of caged compounds were prepared in photolysis buffer (50 mM phosphate buffer, pH 7.4 containing 1 mM DTT) at a final concentration of 300 µM. Aliquots (15 µL) of caged compound solutions were transferred into 15 µL quartz cuvettes (Starna

Cells Corp. dimensions: 1mm × 1mm) and irradiated using two-photon laser apparatus at 800 nm for varying amount of time. After each reaction the samples were analyzed by RP-HPLC or LC-MS. The light source utilized for two-photon irradiation was a homebuilt, regeneratively amplified Ti:sapphire laser system. This laser operates at 1 kHz with 210 mw pulses centered at a wavelength of 800 nm. The laser pulses have a Gaussian full width at half maximum of 80 fs.

One-photon quantum yield (Q_u) and two-photon uncaging cross-section (δ_u) of 18. Q_u and δ_u for **18** were measured by comparing its photolysis rate with Bhc-OAc as a reference (Q_u = 0.04 at 365 nm, δ_u = 0.45 at 800 nm). As described above, aliquots containing **18** were irradiated with either a 365 nm lamp or an 800 nm laser for varying amounts of time. Each sample was analyzed by RP-HPLC to monitor the disappearance of the starting caged compound over time. Similar photolysis experiments were conducted with Bhc-OAc solutions (100 µM for UV and 300 µM for IR) in 50 mM phosphate buffer, pH 7.2. Photolyzed Bhc-OAc solutions were also analyzed by RP-HPLC. The compounds were eluted with a gradient of Solvent A and Solvent B (gradient of a 1% increase in Solvent B/min, flow rate 1 mL/min) monitored by absorbance at 220 nm. Reaction progress data was analyzed as described above and the first order decay constants for the two compounds were used in the formula Φ_u or δ_u (**18**) = Φ_u or δ_u (reference) × K_{obs} (**18**)/ K_{obs}(reference) to calculate the value of δ_u for **18** where Φ_u (reference) = 0.04 and δ_u (reference) = 0.42 GM.

UV and two-photon triggered farnesylation of 18. A 7.5 µM solution of compound **18** was prepared in prenylation buffer (15 mM DTT, 10 mM $MgCl_2$, 50

μM $ZnCl_2$, 20 mM KCl and 22 μM FPP, 50 mM PB buffer) and divided into three 100 μL aliquots. Yeast PFTase was added to the first aliquot to give a final concentration of 30 nM but the resulting sample was not subjected to photolysis; the second aliquot was irradiated in absence of yeast PFTase while the third sample was supplemented with yeast PFTase (50 nM) and then photolyzed with either UV or laser light. UV photolysis was conducted for 1 min at 365 nm while two-photon irradiation was performed for 5 min at 800 nm. Each sample was incubated for 30 min at rt and then analyzed by LC-MS as described above.

General procedure for LC-MS analysis. Aliquots (100 μL) of caged compound solutions which were diluted down to 5-20 μM were analyzed by LC-MS. The general gradient for LC-MS analysis was 0–100% H_2O/0.1% HCO_2H (v/v) to CH_3CN/0.1% HCO_2H (v/v) in 25 min.

Synthesis of mBhc- and Bhc-modified HA-furan (25 a,b). HA-furan was prepared as previously described.[28] To synthesize HA-furan (24) modified with mBhc or Bhc, HA-furan was dissolved in NMP:MES (100 mM, pH 5.5) at a ratio of 1:1 to achieve 0.50% w/v HA-furan. DMT-MM was then added (5 equiv. relative to free carboxylic acids) followed by the dropwise addition of a solution of mBhc or Bhc in DMSO (1 equiv. relative to free carboxylic acids). The reaction was stirred at rt in the dark for 24 h and then dialyzed against H_2O:NMP:DMSO (2:1:1, v/v/v) for 1 d. The organic fraction of the solution was halved every 24 h for 3 days before being replaced with only H_2O for the final 2 days and then lyophilized. The resulting HA-furan modified with either Bhc or mBhc was then dissolved in K_2CO_3 (1.0%

w/v, 10 eq relative to furans) for 24 h, dialyzed against H_2O for 3 days, and lyophilized.

Preparation of HA Hydrogels for Photopatterning. HA-furan-(mBhc or Bhc) was dissolved overnight in MES (100 mM, pH 5.5):DMSO (3:1, v/v) and mixed with an equal volume of a solution of bis-maleimide-poly(ethylene glycol) (mal_2-PEG) dissolved in MES buffer (100 mM, pH 5.5). The mixture was pipetted into 96-well glass bottom plates and allowed to react overnight at 37 °C to form hydrogels with a final concentration of 2.00% HA-furan-(mBhc or Bhc) and a 1:1 ratio of furan:maleimide. The mBhc and Bhc concentrations in the hydrogels were matched based on their UV absorbance at their maximum peak intensity at 365 nm. The unreacted furans in the hydrogel were quenched with 30 mM N-(2-hydroxyethyl)maleimide in MES buffer (100 mM, pH 5.5) for 24 h at rt. The N-(2-hydroxyethyl)maleimide was washed from the gel with borate buffer (100mM, pH 9.0) to hydrolyze any remaining maleimides, followed by extensively washing of the hydrogel with PBS (pH 6.8). A solution of Alexa Fluor 546 maleimide (100 µM in PBS pH 6.8) was then soaked into the hydrogel overnight at 4 °C and excess supernatant was removed prior to photopatterning. The resulting HA-furan-(mBhc or Bhc)/mal_2-PEG hydrogels are herein described as HA_{mBhc}/PEG and HA_{Bhc}/PEG, respectively.

Photopatterning of hydrogels. HA_{mBhc}/PEG and HA_{Bhc}/PEG hydrogels were photopatterned using a Zeiss LSM710 META confocal microscope equipped with

a Coherent Chameleon two-photon laser and a 10x objective. For patterning experiments, the two-photon laser was set to 740 nm with 38% power (1660 mW max power) and a scan dwell time of 106.83 μs/μm. Due to high non-specific binding of Alexa Fluor 546 maleimide in the HA_{Bhc}/PEG hydrogels compared to HA_{mBhc}/PEG hydrogels, unreacted Alexa Fluor 546 maleimide was not washed from the hydrogels. This maintained the same background fluorescence in the HA_{mBhc}/PEG and HA_{Bhc}/PEG hydrogels, allowing the patterns to be directly compared. The concentration of Alexa Fluor 546 maleimide immobilized in the patterns exceeded the bulk unreacted Alexa Fluor 546 maleimide solution, permitting the visualization of the patterns. Alexa Fluor 546 maleimide reacted with the uncaged thiols for 4 h prior to imaging. Patterns were imaged on an Olympus Fluoview FV1000 confocal microscope with x-y scans every 5 μm in the z direction. Imaged photopatterns were quantified using ImageJ against a standard curve of HA/PEG gels containing Alexa Fluor 546 maleimide at different concentrations. The background concentration of unreacted Alexa Fluor 546 maleimide was subtracted from the concentration immobilized in the patterns.

4 Development of caged farnesyltransferase inhibitor for photo-chemical modulation of Ras-localization

4.1 Introduction

Biological transformations occur in a highly spatio-temporally controlled manner throughout the lifetime of a cell, organism or a living animal. In order to study such complexity, reagents that can selectively switch off (or on) certain pathways at any time or any place inside living systems are needed.[1,2] Development of photo-activatable bioagents such as inhibitors provide a great tool to address these questions. In this approach, a key functionality in a bioactive molecule is masked via a photo-cleavable protecting group also called caging group. Upon irradiation, the caging group cleaves of and results in liberation of active bio-agent. Recent advances in development of two-photon sensitive protecting groups allows using longer wavelength infra-red light, which enables photo-activations inside tissues, enhances uncaging resolution, and reduces photo-toxicity.[3–5] These unique features led to development of several caged molecules which have been used for probing various enzymatic reactions and cellular properties.

Ras proteins, which belong to the family of small GTPases, involve in cellular signal transduction.[6] This signaling pathway play critical roles in various cellular properties including proliferation, differentiation and morphology.[7–9] Studies have shown misregulation in Ras activity, often caused by mutation, links to various types of disease including cancer.[10] Proper functioning of Ras requires these proteins to be post-translationally modified via protein farnesyltransferase (PFTase) enzyme. Therefore, several PFTase inhibitors that many of which are

commercially available (e. g. compound **1**), have been developed to block prenylation as a mean to target cancer cells expressing oncogenic Ras.[11] Given the critical role of Ras protein and PFTase enzyme, it would be useful to develop caged PFTase inhibitors that enables spatio-temporal control of Ras signaling. This enables probing the timing of Ras-mediated signal, as well as studying the effect of local inhibition of Ras within a group of cells, on cellular migration, differentiation and morphology.

Previous studies have shown alkylation of the sulfhydryl group present in **1** significantly reduces the binding affinity of the drug by disrupting the interaction between the sulfur and Zn (II) on the PFTase active site.[12] Hence, in order to develop a caged photo-activatable inhibitor, we elected to alkylated the sulfhydryl functionality using a photo-cleavable protecting group, so that upon irradiation the thiol functionality become unmasked and restore the activity of the inhibitor. We elected to use nitrodibenzofuran (NDBF) as the caging moiety since our previous reports demonstrate its high one- and two-photon efficiency for thiol protection.[13]

Here, we first describe the synthesis and photo-chemical properties of caged farnesyltransferase analogue, NDBF-FTI (**2**). We then demonstrate that this reagent can release the free FTI upon UV irradiation inside cells, which inhibits Ras farnesylation, localization and ultimately Ras-signaling. Finally, we showed that NDBF-FTI can be uncaged via two-photon irradiation in a highly spatially controlled manner which results in creation of defined patterns of inhibited cells among non-affected cells. This development sets the stage for probing effect of

spatio-temporal inhibition of Ras-mediated signaling not only in cell culture, but also in organisms and ultimately in animals.

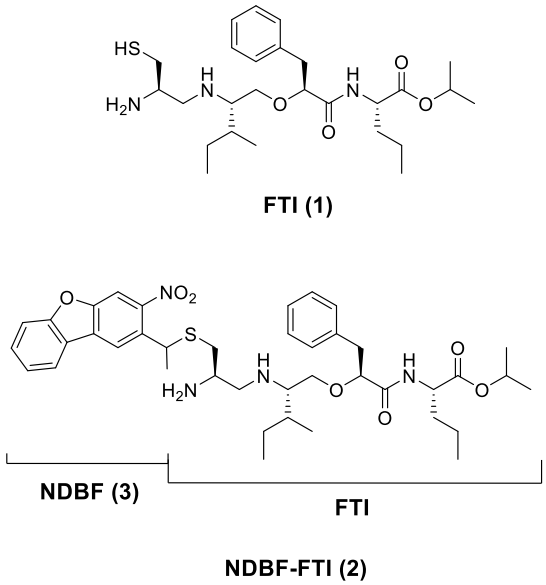

Scheme 4-1 Farnesyltransferase inhibitor (FTI, **1**) and caged FTI (NDBF-FTI, **2**).

4.2 Result and Discussion

4.2.1 Synthesis and Photo-chemical Properties of Caged FTI

To prepare caged FTI analogue, NDBF-Br was initially synthesized following a previously reported procedure,[13] and was subsequently used to alkylated the FTI under mild acidic condition in presence of $Zn(OAc)_2$ as a catalyst. Carrying out the reaction in acidic condition renders the amine functionalities protonated, thus inert toward alkylation. The crude mixture was purified via preparatory HPLC to yield desired in NDBF-FTI in ~ 70 % yield (mixture of two diastereomers).

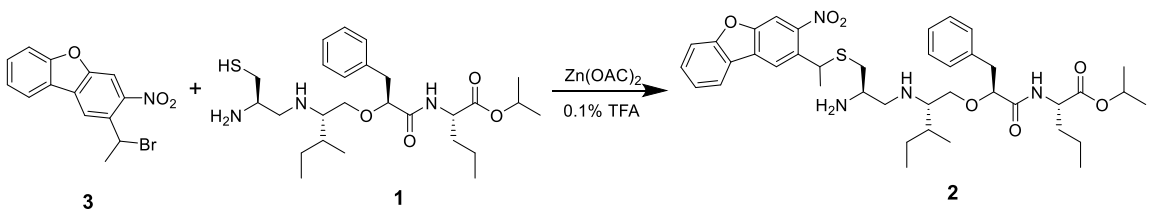

Scheme 4-2 Synthesis of NDBF-FTI.

In order to evaluate the release of the free drug upon one- and two-photon irradiation, photolysis experiments were carried out and analyzed by LC-MS. For one photon uncaging experiment, 50 µM solution of NDBF-FTI in photolysis buffer (50 mM PB, pH 7.2, 1 mM DTT) was irradiated for 60 s at 365 nm, and was subsequently analyzed by LC-MS. LC-MC traces shown in Figure 4-1 reveals the disappearance of starting caged drug **2** and generation of a new peak with the mass of 560.2826 corresponding to the free FTI (calced = 560.2823).

Similar photolysis experiment was carried out using 800 nm two-photon laser, which shows the formation of the free FTI after 5 minutes of irradiation. These data clearly demonstrate that the caged FTI analogue is capable of releasing the active drug upon both one and two-photon irradiation.

One-photon uncaging kinetics was evaluated by irradiating solutions of **2** for varying periods of time followed by analysis via RP-HPLC (Figure 4-3). These experiments yielded a half-life of 11 seconds for NDBF-FTI in a standard Rayonet photoreactor (2×16W bulbs, indicating this molecule uncage as rapidly as previously reported for caged thiols.

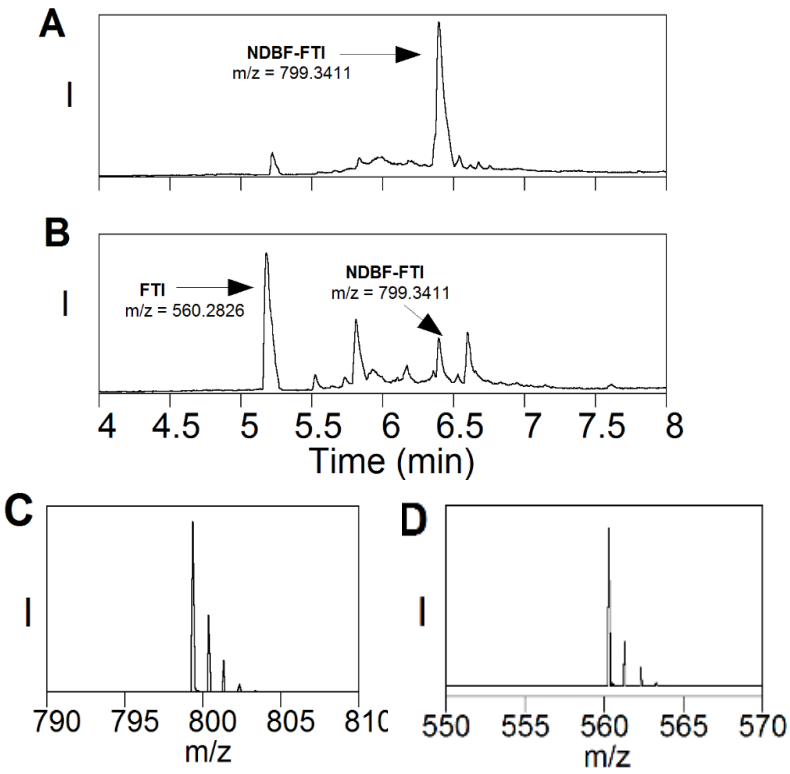

Figure 4-1 LC-MS analysis of uncaging of NDBF-FTI to form free FTI by irradiation at 365 nm. Crude LC-MS trace of a 20 µM solution of **2** in 50 mM pH 7.2, A) before irradiation and B) after 90s irradiation. These results clearly show disappearance of NDBF-FTI (m/z calcd for $([M + H]^+$ 799.3405, found 735.3411) and appearance of free FTI ($[M + H]^+$ 560.2823, found 560.2826). C) MS/MS of pure **2**, D) MS/MS of **1** produced from UV photolysis

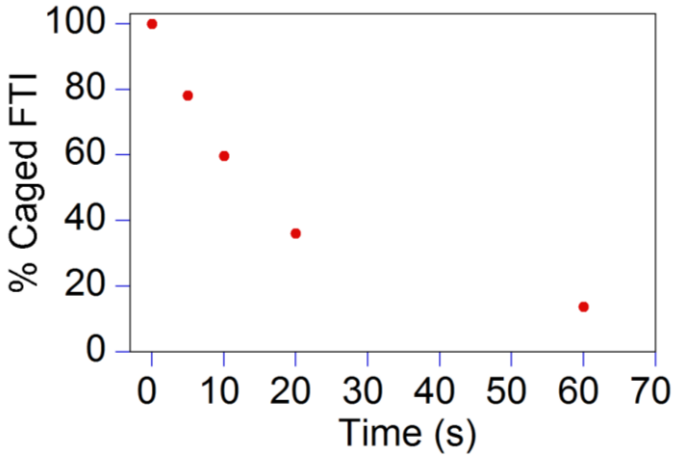

Figure 4-2 HPLC quantification of disappearance of **2** and formation of the uncaged peptide (**1**) as a function of irradiation time at 365 nm.

4.2.2 Photo-triggered Release of FTI Inside Cells and Modulation of Ras Localization

The caged drug was designed for selective on-demand modulation of cellular properties. In order to evaluate the utility of NDBF-FTI for photo-controlled inhibition of farnesylation, we examined its ability for altering Ras localization inside live cells. To achieve this, experiments were carried out using Madin-Darby Canine Kidney Epithelial (MDCK) cell line which expresses H-Ras as an N-terminal GFP fusion (GFP-Ras). This would allow monitoring the Ras localization via fluorescence microscopy. Under normal condition, GFP-Ras gets farnesylated and localizes to plasma membrane. However, presence of FTI blocks farnesylation results in cytosolic accumulation of GFP-Ras. Figure 4-3 represents confocal microscopy images for such experiments. As expected, similar to the untreated cells, treatment of MDCK cells with NDBF-FTI without irradiation results in membrane localization of GFP-Ras proteins. However, irradiation of cells that are treated with NDBF-FTI for 2 min at 330 nm, results in drastic cytosolic accumulation of GFP-Ras, similar to the cells that are treated with free FTI. It has to be noted that images were obtained 12 hours after irradiation, so that enough GFP-Ras get expressed and be accumulated in the cytosol and the left-over membrane localized GFP-Ras proteins be proteolyzed and removed from membrane. Control experiments in which untreated cells were irradiated for 3 min showed no alteration in GFP-Ras localization. These date clearly demonstrates the utility of NDBF-FTI for photo-controlled modulation of farnesylation inside live cells.

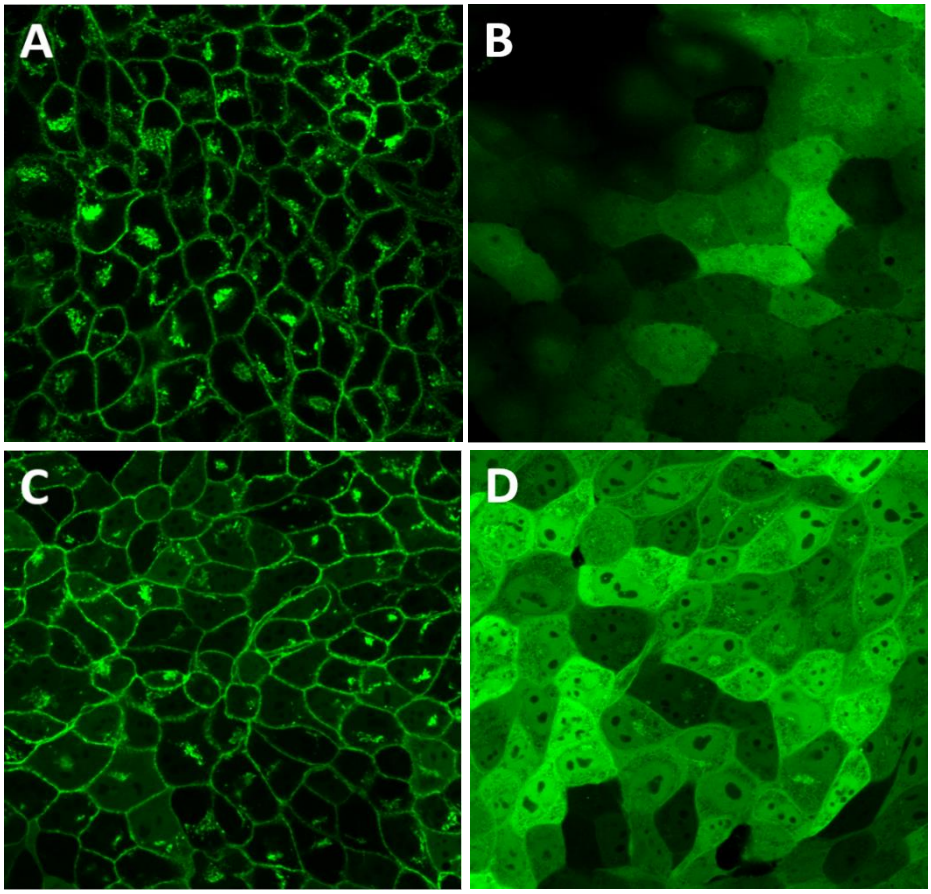

Figure 4-3 GFP-H-ras localization in MDCK cells treated with NDBF-FTI (**2**) after 330 nm irradiation. Treatments were as follows: A) Vehicle (0.2% DMSO (v/v)). B) 10 µM FTI (1). C) 5 µM NDBF-FTI (**2**), no irradiation. D) 5 µM NDBF-FTI (**2**) plus 2 min irradiation.

Successful one-photon uncaging of NDBF-FTI inside live cells, led us to test its ability to be activated upon longer wavelength irradiation using two-photon laser. This would broaden the applicability of this probe for studies inside tissues or organisms where UV light could not penetrate deep enough, or for experiments where photo-toxicity is a concern. Therefore, NDBF-FTI treated cells where irradiated using Nikon multi-photon microscope tuned to 700 nm. According to

confocal images shown in Fig, 1 min irradiation of cells using two-photon laser, resulted in inhibition of farnesylation and cytosolic accumulation of GFP-Ras.

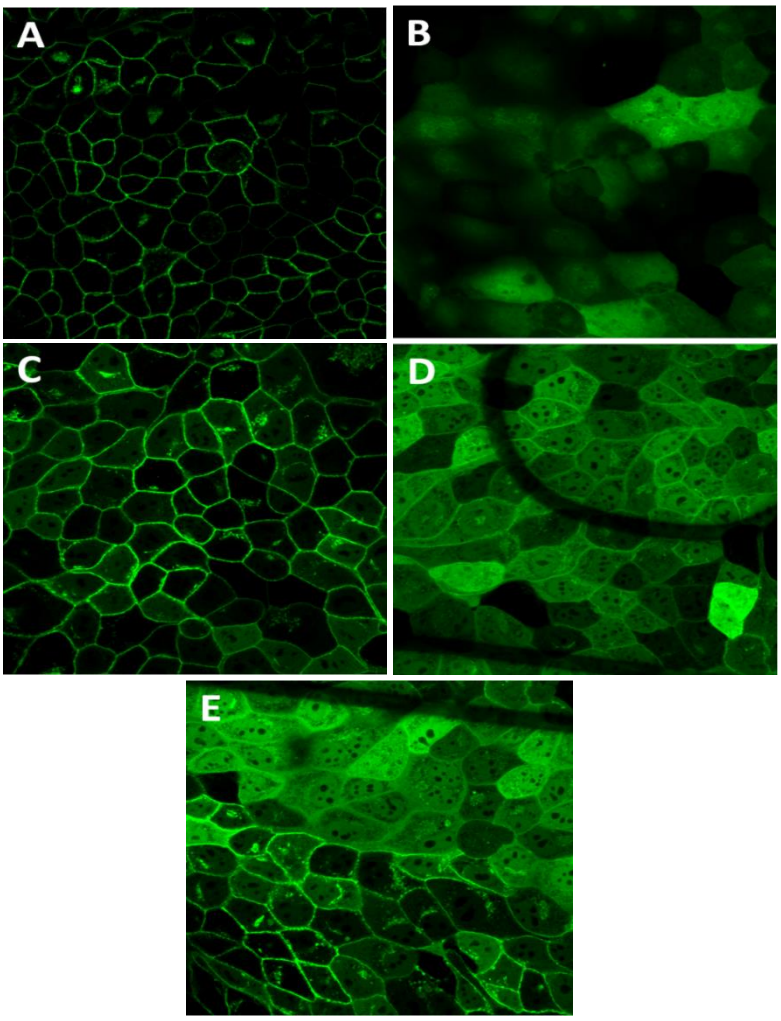

Figure 4-3 GFP-H-ras localization in MDCK cells treated with NDBF-FTI (**2**) after 700 nm two-photon irradiation. Treatments were as follows: A) Vehicle (0.2% DMSO (v/v)). B) 10 µM FTI (1). C) 5 µM NDBF-FTI (**2**), no irradiation. D) 5 µM NDBF-FTI (**2**) plus two-photon irradiation (300 µs/pixel). E) 5 µM NDBF-FTI (**2**) plus two-photon irradiation (300 µs/pixel), this image demonstrates the boundary between irradiated area and non-irradiated area. As expected two-photon laser NDBF-FTI can be locally uncaged in a group of cells, which results in creation of patterns of inhibited versus inhibited cells.

The great advantage of using laser for uncaging is that it allows spatio-temporal release of the drug inside cells. Figure 4-4E demonstrates a local release of FTI on MDCK cells showing a pattern of inhibited versus non-inhibited cells. These experiments demonstrate the designed NDBF-FTI is capable of spatio-temporal modulation of Ras mediated signal, as well as any other pathways involves farnesylation inside cells.

4.3 Conclusion

In summary, we have prepared a caged farnesyltransferase inhibitor capable of releasing the active inhibitor upon one- and two-photon irradiation. Unlike previously reported Bhc-FTI, analysis of the uncaging reactions clearly shows efficient release of the FTI without the formation of any unwanted byproduct. Cellular experiments demonstrate that the designed caged drug efficiently penetrates inside mammalian cells and liberates the drug upon one- and two-photon irradiation. The released FTI inhibits farnesylation, membrane localization of Ras and its upstream signaling. Irradiation of the cells treated with the caged drug via longer wavelength two-photon laser not only allowed temporal control over Ras signaling, but more importantly enables highly localized inhibition in a group of irradiated cells. This reagent sets the stage for highly spatio-temporal modulation and probing of various prenylation-related pathways inside tissues or even whole organisms such as C. elegans, zebrafish and mice.

4.4 Experimental Section

All solvents and reagents used for synthesis and other experiments were purchased from Sigma-Aldrich (St. Louis, MO). High-performance liquid chromatography (HPLC) analysis (analytical and preparative) was performed using a Beckman model 125/166 instrument, equipped with a UV detector and C18 columns (Varian Microsorb-MV, 5 µm, 4.6 × 250 mm and Phenomenex Luna, 10 µm, 10 × 250 mm, respectively). LC/MS analysis was performed employing a Thermo LCQ Deca ion trap mass spectrometer (Thermo Scientific, San Jose, CA) interfaced with an Agilent 1100 Capillary HPLC equipped with an Agilent Zorbax 300SB-C18, 5 µm, 0.5 x 150 mm column. ^{1}H NMR data of synthetic compounds were recorded at 500 MHz on a Varian Instrument at 25 °C. MDCK cells stably expressing GFP-H-ras were the generous gift of Dr. Mark Philips (NYU School of Medicine).

Synthesis of NDBF-FTI. NDBF-Br was synthesized following a previously reported procedure. NDBF-Br (9.7 mg, 0.03 mmol) and FTI (10 mg, 0.01 mmol) were dissolved in a solution of 2:1:1 DMF/CH3CN/H2O containing 0.1% TFA (1 mL) under a N_2 atmosphere. $Zn(OAc)_2.6H_2O$ was then added (30.8 mg, 0.3 mmol) and the reaction monitored by TLC. After overnight incubation, the solvents were removed and the reaction purified via HPLC using a preparative method (flow rate: 8 mL/min, gradient: 0% solvent B, 15 min; 0-100% B in 100 min; solvent A: H_2O and 0.1% TFA, solvent B: CH3CN and 0.1% TFA). The product eluted at 65% B and was then lyophilized to give 2.9 mg of a fluffy white solid in 40% yield. LC-MS calcd for $[C_{40}H_{54}N_4O_7S + H]^+$ 799.3405, found 735.3411.

General Procedure for UV Photolysis of NDBF-FTI. The caged compound was dissolved in photolysis buffer (50 mM phosphate buffer (PB), pH 7.2 containing 1 mM DTT) at a final concentration of 50 μM. The solutions were transferred into a quartz cuvette (10 × 50 mm) and irradiated with 365 nm UV light using a Rayonet reactor (2 × 14 W RPR-3500 bulbs). After each reaction the samples were analyzed by RP-HPLC or liquid chromatography−mass spectrometry (LC-MS).

Laser Apparatus for Two-Photon Irradiations of NDBF-FTI. The light source that was utilized for two-photon irradiation is a home-built, regeneratively amplified Ti:sapphire laser system. This laser operates at 1 kHz with 210 mW pulses centered at a wavelength of 800 nm. The laser pulses have a Gaussian full width at half-maximum of 80 fs. Samples were irradiated in a 15 μL quartz cuvettes (Starna Cells Corp.).

General Procedure for LC-MS Analysis. Aliquots (100 μL) containing 15 μM caged compound in photolysis buffer were irradiated in a Rayonet UV photoreactor or using an 800 nm laser (see below for description). Each irradiated sample was then analyzed by LC-MS. The general gradient for LC-MS analysis was 0−100% H_2O (0.1% HCO2H) to CH_3CN (0.1% HCO_2H) in 25 min.

Cell Culture and Microscopy. MDCK cells were grown in DMEM supplemented with 10% FBS at 37 °C under CO2 (5.0%). They were seeded in 35 mm glass-bottomed dishes at the density of 2.2 x 10^4 cells/cm^2. To carry out photo-triggered Ras inhibition, cells were treated with a 15 μM solution of **2** in DMEM supplemented with 10% FBS. After 3 h of incubation, the medium was removed, and cells were washed three times with warm phosphate-buffered saline (PBS),

followed by addition of dye-free DMEM medium (10% FBS, no phenol red). For UV uncaging experiment, the plates were irradiated at 330 nm for 2-5 min using a transilluminator (Fotodyne Inc.). Two-photon uncaging experiments were carried out using Nikon A1RMP microscope equipped with a Spectra Physics 15W Mai Tai eHP tunable IR laser, and a 20X objective. For photo-patterned inhibition, two-photon laser was set to 700 nm with 10 % power and scan time of 200-300 µs/pixel. After irradiation the dye-free medium was removed and replaced with normal DMEM medium containing phenol red, then incubated for 12 h. Right before imaging, medium was again replaced with dye-free medium. Cells were directly imaged using an Olympus FluowView IX2 inverted confocal microscope with a 60X objective.

5 Synthesis of a nitrodibenzofuran-based caging group with red-shifted absorption

Many of the available caging groups, particularly the ones that have used for thiol protection, require ultra-violet (UV) irradiation to be uncaged via one-photon excitation.[1] This is a major constraint since UV irradiation results in major photo-toxicity in living systems and cells. Additionally, UV light is significantly absorbed by endogenous biomolecules and is also scattered in tissues, which results in very low penetration.

In order to overcome this problem, new caging groups with red-shifted absorption maxima has to be prepared. Since, nitrodibenzofuran (NDBF) has been successfully applied for caging variety of functionalities including thiols, we used that as a starting point for development of a novel caging group. Similar approach was previously implemented by Specht and coworkers who demonstrated that the addition of an electron donating substituents to biphenyl 2-(o-nitrophenyl)propen derivatives which are structurally similar to NDBF, not only shifts the absorption maxima to the longer wavelengths, but also significantly enhances the two-photon sensitivity to unprecedented value of 11 GM.[2] Additionally, a computational study carried out by Knippenberg and coworkers showed derivatizing the NDBF with an amino group at the endocyclic C-7 position, similarly red-shifts the absorption absorption maxima and improves two-photon cross-section up to 15 times higher relative to NDBF.[3]

Here we describe the synthesis of methyl 7-dimethylamino nitrodibenzofuran acetate (Scheme 5-1) as a new caging group with the red-shifted lambda max. The

compound was synthesized in 9-steps. Initial spectral studies showed λ_{max} of 440 nm which is 90 nm longer than that of NDBF which is 330 nm.

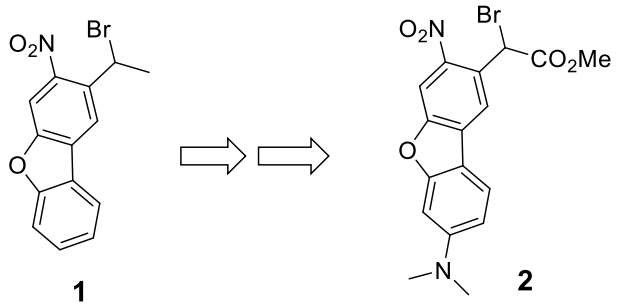

Scheme 5-1 Nitrodibenzofuran and 7-amino nitrodibenzofuran.

5.1 Results and discussion

5.1.1 Synthesis of 7-amino nitrodibenzofuran (AminoNDBF)

Compound **2** was prepared in a 9-step synthesis route starting from commercially available dibenzofuran (Scheme 5-2). Dibenzofuran (**3**) was acetylated using acetyl chloride and aluminum trichloride as a catalyst to yield **4** (73 %). The acetyl group was then converted to methyl acetate using diacetoxy iodobenzene ($PhI(OAc)_2$) and sulfuric acid in methanol to generate methyl dibenzofuran acetate (**5**) in 95 % yield. Compound **5** was nitrated at the C-7 position via treatment with sodium nitrate and trifluoroacetic acid to give **6** in 80 % yield. The nitro group was then reduced to amine using iron powder in presence of acid under reflux to yield **7** in 50 %. The free amine was then boc protected (**8**) using boc anhydride and base in 60 % yield. Compound **8** was brominated at the benzylic position using NBS and benzoyl peroxide as the radical initiator to generate **9** (90 %). The boc

group on compound **9** was then de-protected using TFA. The generated free amine was then methylated through reductive amination to generate molecule **11** in 75 %. Compound **11** was then nitrated using nitric acid in ice cold sulfuric acid to generate the target molecule **2** in 75 % yield. Protonation in strong acidic condition renders the amine functionality an electron withdrawing group pushing the nitration to selectively occur at the C-3 position.

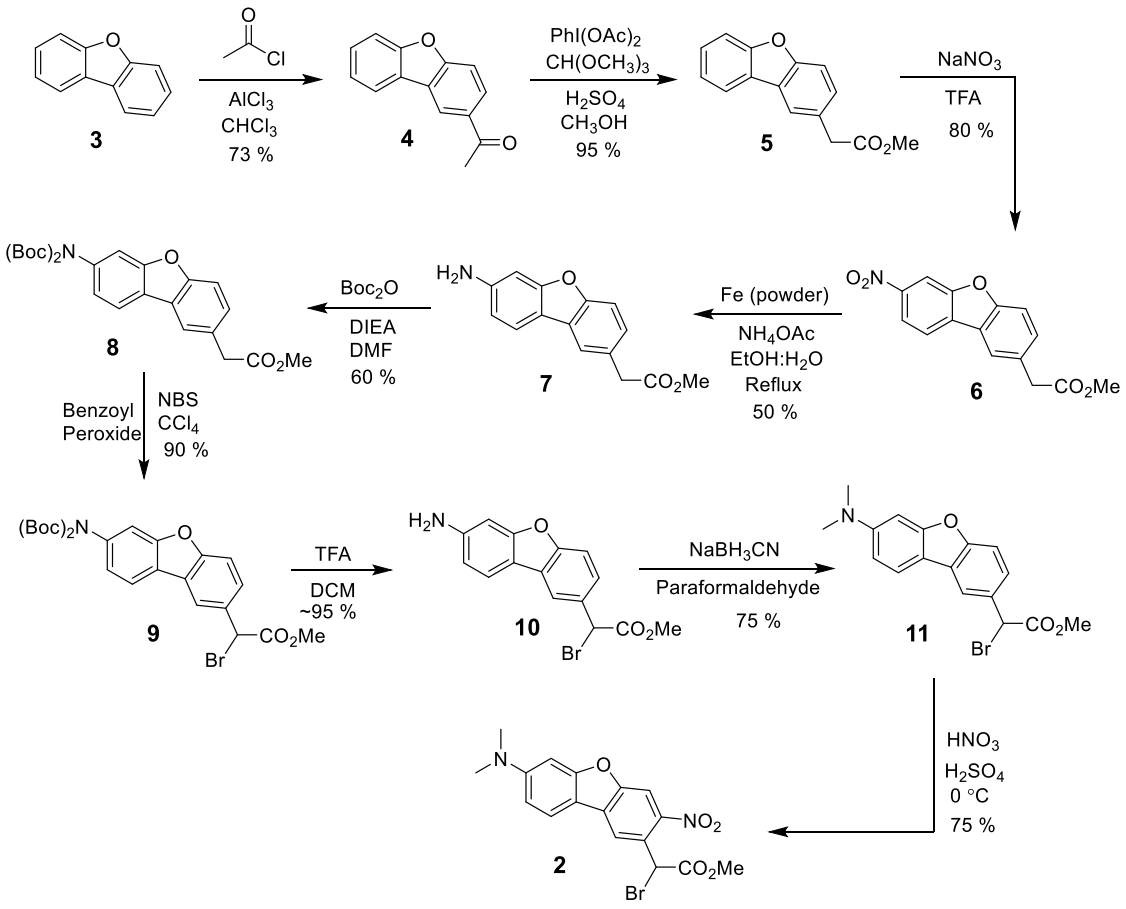

Scheme 5-2 Synthesis of 7-amino nitrodibenzofuran.

Spectral properties of compound **2** was measured in 50 mM PB (pH 7.2) demonstrating the absorption maxima to be 440 nm. This shows addition of the

dimethyl amino group led to a 90 nm bathochromic shift in the λmax of NDBF which is in correlation with our initial hypothesis and previous computational calculations by Knippenberg and coworkers.[3]

5.2 Conclusion and future directions

The synthesis of methyl 7-dimethylamino nitrodibenzofuran acetate (**2**) was accomplished in 9 steps. The absorption maxima of compound **2** was measured to be 440 nm. This clearly shows addition of the diamethyl amino group led to a 110 nm bathochromic shift in the λmax of NDBF. It remains to be seen whether this molecule can be efficiently uncaged via one- and two-photon excitation. To test this, a caged thiol such as Fmoc-Cys-OMe has to be prepared and photolyzed under one- and two-photon conditions. The photolysis mixtures have to be analyzed via HPLC to monitor the disappearance of caged compound and formation of the free thiol overtime. These data will be used to evaluate the uncaging efficiency of 7-dimethylamino nitrodibenzofuran acetate.

5.3 Experimental secion

2-acetyldibenzofuran (4). This compound was synthesized following a previously reported procedure.[4]

Methyl dibenzofuran acetate (5). Compound **5** (11.8 g, 56.2 mmol) was dissolved in 5 mL of CH_2Cl_2 and then added to 160 mL of CH_3OH. While stirring, 49 mL (449.0 mmol) of trimethyl orthoformate ($CH(OCH_3)_3$) was added to the solution, followed by dropwise addition of 24 mL of H_2SO_4(conc.) (caution: generates heat!). Diacetoxy iodobenzene, $PhI(OAc)_2$ (21.2 g, 67.4 mmol), was gradually added to

the reaction mixture for over 10 minutes. The mixture was stirred for 1 h and then the reaction judged completed by TLC (4:1 EtOAc/Hexanes). 100 mL of water was added to the mixture and CH_3OH was removed *in vacuo*. Product was extracted using 200 mL of CH_2Cl_2 (highly acidic aqueous waste was neutralized by baking soda). The solution was washed with brine, dried over Na_2SO_4, and the solvent was removed in vacuo. The crude mixture was run through silica plug to yield 12.8 g of **5** in 95 %. The purity of the sample was sufficient to be used for the next step. ^{1}H NMR ($CDCl_3$): δ 7.94 (1H, dd) 7.56 (1H, d), 7.52 (1H, d), 7.43 (1H, m), 7.31 – 7.38 (2H, m), 3.79 (2H, s), 3.72 (3H, s). ^{13}C NMR: 172.23, 156.56, 155.41, 128.28, 128.35, 127.28, 127.10, 124.57, 124.04, 122.75, 121.36, 120.74, 120.60, 52.14, 41.06.

Methyl 2-(7-nitrodibenzofuran-2-yl)acetate (6). Compound **5** (12.0 g, 49.9 mmol) was dissolved in 150 mL of TFA. While stirring, sodium nitrate (4.6 g, 55.3 mmol) was gradually added to the solution which generated dark color. The mixture was stirred for 1 h and the reaction was judged completed by TLC (2:3 EtOAc/Hexanes). The reaction was quenched by adding 100 mL of water and the product was extracted with 150 mL of EtOAc. The organic layer was neutralized by 10 % NaHCO3(aq), washed with brine and dried over Na_2SO_4. The solution was evaporated. The obtained crude sample was pure enough to be used for the following step. In order to obtain high quality NMR, the final product was purified via column chromatography (1:2 EtOAc/Hexanes) to give 11.38 g of **6** as yellow powder in 80 % yield. ^{1}H NMR ($CDCl_3$): δ 8.45 (1H, d) 8.28 (1H, dd), 8.05 (1H, d), 7.96 (1H, d), 7.61 (1H, dd), 7.51 (1H, dd), 3.82 (2H, s), 3.74 (3H, s).

Methyl 2-(7-aminodibenzofuran-2-yl)acetate (7). Compound **6** (10.0 g, 35.0 mmol), Iron powder (9.8 g, 175 mmol) and ammonium acetate (18.7 g, 350 mmol) was suspended in 250 mL of 3:1 H_2O: EtOH and refluxed for 6 h. The reaction was completed judged by TLC (3:1 Hexanes: EtOAc). The iron powder removed by filtration, EtOH removed under vacuum and the product was extracted using 100 mL of EtOAc. The organic layer was washed with 10 % $NaHCO_3$(aq) and Brine, and then dried over Na_2SO_4. Solvent was removed under vacuum and the final product was purified via column chromatography (3:1 Hexanes: EtOAc) to yield 4.47 g of **7** as a yellow oil in 50 % yield. ^{1}H NMR ($CDCl_3$): δ 7.73 (1H, d) 7.68 (1H, d), 7.28 (1H, s), 7.24 (1H, dd), 6.85 (1H, d), 6.69 (1H, dd), 3.77 (2H, s), 3.73 (3H, s). ^{13}C NMR: 172.42, 158.32, 155.14, 146.87, 128.26, 126.24, 125.20, 121.31, 120.03, 115.40, 111.31, 111.10, 97.45, 52.10, 41.13.

Methyl 2-(7-((boc)amino)dibenzofuran-2-yl)acetate (8). Compound **7** (2.2 g, 8.8 mmol) was dissolved in dried DMF and cooled down to 0 °C. N,N-Diisopropylethylamine, DIEA (3.1 mL , 17.6 mmol) was added to the solution and stirred for 5 min. Boc_2O (8.1 mL ,35.2 mmol) was then added to the reaction mixture. The mixture was warmed up to room temperature and stirred for 5 h. The reaction completed judged by TLC (3:1 Hexanes: EtOAc). DMF was evaporated under vacuum and the crude mixture was taken up into 50 mL of EtOAc. The organic layer was then washed with brine, and dried over Na_2SO_4. Solvent was removed under vacuum. The mixture was purified via column chromatography (3:1 Hexanes: EtOAc) to yield 2.4 g of **8** as a yellow oil in 60 % yield. ^{1}H NMR (CDCl3):

δ 7.86 (2H, m) 7.50 (1H, dd), 7.35 – 7.37 (2H, m), 7.10 – 7.12 (1H, dd), 5.46 (1H, s), 3.77 (2H, s), 3.70 (3H, s), 1.39 (18H, s).

Methyl 2-bromo-2-(7-((boc)amino)dibenzofuran-2-yl)acetate (9). Compound **8** (2.4 g, 5.3 mmol) and 50 mg of benzoyl peroxide was dissolved in 50 mL of CCl_4. The mixture was refluxed for 6 h. The reaction completed judged by TLC (2.5:1 Hexanes: EtOAc). Reaction mixture was diluted by adding 50 mL of CH_2Cl_2, washed with 10 % $NaHCO_3$(aq) and Brine, and dried over Na_2SO_4. Solvent was evaporated under vacuum and the resulting crude was purified via column chromatography (2.5:1 Hexanes: EtOAc) to give 2.56 g of **9** as a yellow solid (90 %). ^{1}H NMR (CDCl3): δ 7.91 (2H, m) 7.80 (1H, dd), 7.54 (1H, d), 7.39 – 7.41 (2H, m), 7.15 (1H, dd), 5.50 (1H, s), 3.75 (3H, s), 1.41 (18H, s).

Methyl 2-bromo-2-(7-(dimethylamino)dibenzofuran-2-yl)acetate (11). Compound **9** (2.6 g, 4.7 mmol) was dissolved in 30 mL of CH_2Cl_2, followed by addition of 0.5 mL of water. 15 mL of TFA was added to the mixture and stirred for 30 min to afford complete deprotection of the boc groups. Solvents were evaporated under vacuum, and the resulting crude was taken up in 30 mL of EtOAc. The organic layer was washed with 10 % $NaHCO_{3(aq)}$ and Brine, and dried over Na_2SO_4. EtOAc was removed under vacuum to give **10** in quantitative yield (1.5 g), which was pure enough to be used for the next step. Compound **10** (4.5 mmol) was suspended in 80 mL of 3:1 AcOH: H_2O, followed by portion-wise addition of sodium cyanoborohydride, $NaBH_3CN$, (22.5 mmol, 1.4 g). The mixture stirred for 5 h and the reaction completed judged by TLC (2:1 Hexanes: EtOAc). The mixture was diluted with 100 mL EtOAc. The organic layer was washed three

times with saturated $NaHCO_{3(aq)}$ and then washed with brine. The resulting solution was dried over Na_2SO_4 and evaporated under vacuum. The crude mixture was purified using column chromatography (2.5:1 Hexanes: EtOAc) to yield 1.7 g of **11** as a pale yellow oil (75 %). δ 8.16 (1H, m) 7.91 (1H, d), 7.64 (1H, dd), 7.54 (1H, d), 7.36 (1H, d), 7.15 (1H, dd), 5.54, (1H, s), 3.81 (3H, s), 1.4 (6H, s).

Methyl 2-bromo-2-(7-(dimethylamino)-3-nitrodibenzofuran-2-yl)acetate (2). Compound **11** (1.7g, 4.7 mmol) was dissolved in least amount of THF, and was subsequently added to a 30 mL stirring solution of ice cold H_2SO_4(conc.). The mixture was stirred for 5 min, followed by dropwise addition of 68% v/v HNO_3 (the solution turns dark). The mixture was stirred for 1 h. The reaction was judged complete by TLC (2:1 Hexanes: EtOAc). Water (60 mL) was added to quench the reaction, followed by addition of 60 mL of EtOAc. All the acid was neutralized by slow addition of $NaHCO_3$ to the biphasic mixture (caution: generation heat and vigorous release of gas). The organic layer was separated, washed with brine and dried over Na_2SO_4. Solvent was evaporated under vacuum, and the obtained crude was purified using column chromatography (2:1 Hexanes: EtOAc) to give 1.4 g of **2** as yellow oil (75 %). δ 8.30 (1H, s) 8.19 (1H, s), 7.83 (1H, d), 6.84 (2H, m), 6.30 (1H, s), 3.83 (3H, s), 3.12 (6H, s).

6 References

6.1 Chapter 1

1 V. N. Rajasekharan Pillai, *Synthesis*, 1980, 1980, 1–26.

2 G. Mayer and A. Heckel, *Angew. Chem. Int. Ed.*, 2006, 45, 4900–4921.

3 H.-M. Lee, D. R. Larson and D. S. Lawrence, *ACS Chem. Biol.*, 2009, 4, 409–427.

4 P. Klán, T. Šolomek, C. G. Bochet, A. Blanc, R. Givens, M. Rubina, V. Popik, A. Kostikov and J. Wirz, *Chem. Rev.*, 2013, 113, 119–191.

5 Q. Shao and B. Xing, *Chem. Soc. Rev.*, 2010, 39, 2835.

6 Y. Luo and M. S. Shoichet, *Nat. Mater.*, 2004, 3, 249–253.

7 C. Yang, F. W. DelRio, H. Ma, A. R. Killaars, L. P. Basta, K. A. Kyburz and K. S. Anseth, *Proc. Natl. Acad. Sci.*, 2016, 113, E4439–E4445.

8 G. C. R. Ellis-Davies, *Nat. Methods*, 2007, 4, 619–628.

9 G. Bort, T. Gallavardin, D. Ogden and P. I. Dalko, *Angew. Chem. Int. Ed.*, 2013, 52, 4526–4537.

10 X. Chen, S. Tang, J.-S. Zheng, R. Zhao, Z.-P. Wang, W. Shao, H.-N. Chang, J.-Y. Cheng, H. Zhao, L. Liu and H. Qi, *Nat. Commun.*, 2015, 6, 7220.

11 X. Ouyang, I. A. Shestopalov, S. Sinha, G. Zheng, C. L. W. Pitt, W.-H. Li, A. J. Olson and J. K. Chen, *J. Am. Chem. Soc.*, 2009, 131, 13255–13269.

12 N. Haugaard, *Ann. N. Y. Acad. Sci.*, 2000, 899, 148–158.

13 H. A. Chapman, R. J. Riese and G.-P. Shi, *Annu. Rev. Physiol.*, 1997, 59, 63–88.

14 F. V. Chorkina and A. I. Karataev, *Cysteine: biosynthesis, chemical structure and toxicity*, Nova Science ; Gazelle [distributor, Hauppauge, N.Y.; Lancaster, 2012.

15 K. D. Philipson, J. P. Gallivan, G. S. Brandt, D. A. Dougherty and H. A. Lester, *Am. J. Physiol. Cell Physiol.*, 2001, 281, C195-206.

16 M. M. Mahmoodi, D. Abate-Pella, T. J. Pundsack, C. C. Palsuledesai, P. C. Goff, D. A. Blank and M. D. Distefano, *J. Am. Chem. Soc.*, 2016.

17 H. Li, J.-M. Hah and D. S. Lawrence, *J. Am. Chem. Soc.*, 2008, 130, 10474–10475.

18 R. G. Wylie, S. Ahsan, Y. Aizawa, K. L. Maxwell, C. M. Morshead and M. S. Shoichet, *Nat. Mater.*, 2011, 10, 799–806.

19 A. Otaka, K. Sato, H. Ding and A. Shigenaga, *Chem. Rec.*, 2012, 12, 479–490.

20 K. Aihara, K. Yamaoka, N. Naruse, T. Inokuma, A. Shigenaga and A. Otaka, *Org. Lett.*, 2016, 18, 596–599.

21 J. H. Kaplan, B. Forbush and J. F. Hoffman, *Biochemistry (Mosc.)*, 1978, 17, 1929–1935.

22 A. P. Pelliccioli and J. Wirz, *Photochem. Photobiol. Sci.*, 2002, 1, 441–458.

23 N. Kotzur, B. Briand, M. Beyermann and V. Hagen, *Chem. Commun.*, 2009, 3255.

24 R. K. McGinty, J. Kim, C. Chatterjee, R. G. Roeder and T. W. Muir, *Nature*, 2008, 453, 812–816.

25 J. A. Karas, D. B. Scanlon, B. E. Forbes, I. Vetter, R. J. Lewis, J. Gardiner, F. Separovic, J. D. Wade and M. A. Hossain, *Chem. - Eur. J.*, 2014, 20, 9549–9552.

26 A. J. DeGraw, M. A. Hast, J. Xu, D. Mullen, L. S. Beese, G. Barany and M. D. Distefano, *Chem. Biol. Drug Des.*, 2008, 72, 171–181.

27 M. Ghosh, I. Ichetovkin, X. Song, J. S. Condeelis and D. S. Lawrence, *J. Am. Chem. Soc.*, 2002, 124, 2440–2441.

28 M. Ghosh, *Science*, 2004, 304, 743–746.

29 P. Pan and H. Bayley, *FEBS Lett.*, 1997, 405, 81–85.

30 N. Wu, A. Deiters, T. A. Cropp, D. King and P. G. Schultz, *J. Am. Chem. Soc.*, 2004, 126, 14306–14307.

31 R. Uprety, J. Luo, J. Liu, Y. Naro, S. Samanta and A. Deiters, *ChemBioChem*, 2014, 15, 1793–1799.

32 N. Kotzur, B. Briand, M. Beyermann and V. Hagen, *J. Am. Chem. Soc.*, 2009, 131, 16927–16931.

33 M. M. Mahmoodi, S. A. Fisher, R. Y. Tam, P. C. Goff, R. B. Anderson, J. E. Wissinger, D. A. Blank, M. S. Shoichet and M. D. Distefano, *Org Biomol Chem*, 2016, 14, 8289–8300.

34 D. Abate-Pella, N. A. Zeliadt, J. D. Ochocki, J. K. Warmka, T. M. Dore, D. A. Blank, E. V. Wattenberg and M. D. Distefano, *ChemBioChem*, 2012, 13, 1009–1016.

35 R. G. Wylie, S. Ahsan, Y. Aizawa, K. L. Maxwell, C. M. Morshead and M. S. Shoichet, *Nat. Mater.*, 2011, 10, 799–806.

36 J. H. Wosnick and M. S. Shoichet, *Chem. Mater.*, 2008, 20, 55–60.

37 R. G. Wylie and M. S. Shoichet, *Biomacromolecules*, 2011, 12, 3789–3796.

38 G. Arabaci, X.-C. Guo, K. D. Beebe, K. M. Coggeshall and D. Pei, *J. Am. Chem. Soc.*, 1999, 121, 5085–5086.

39 A. Specht, S. Loudwig, L. Peng and M. Goeldner, *Tetrahedron Lett.*, 2002, 43, 8947–8950.

40 M. C. Pirrung and J.-C. Bradley, *J. Org. Chem.*, 1995, 60, 6270–6276.

41 P. B. Jones, M. P. Pollastri and N. A. Porter, *J. Org. Chem.*, 1996, 61, 9455–9461.

42 H. K. Agarwal, R. Janicek, S.-H. Chi, J. W. Perry, E. Niggli and G. C. R. Ellis-Davies, *J. Am. Chem. Soc.*, 2016, 138, 3687–3693.

43 L. Fournier, I. Aujard, T. Le Saux, S. Maurin, S. Beaupierre, J.-B. Baudin and L. Jullien, *Chem. - Eur. J.*, 2013, 19, 17494–17507.

44 L. Donato, A. Mourot, C. M. Davenport, C. Herbivo, D. Warther, J. Léonard, F. Bolze, J.-F. Nicoud, R. H. Kramer, M. Goeldner and A. Specht, *Angew. Chem.*, 2012, 124, 1876–1879.

45 N. Komori, S. Jakkampudi, R. Motoishi, M. Abe, K. Kamada, K. Furukawa, C. Katan, W. Sawada, N. Takahashi, H. Kasai, B. Xue and T. Kobayashi, *Chem Commun*, 2016, 52, 331–334.

6.2 Chapter 2

(1) Brieke, C.; Rohrbach, F.; Gottschalk, A.; Mayer, G.; Heckel, A. Angew. Chem., Int. Ed. 2012, 51, 8446.

(2) Adamantidis, A. R.; Zhang, F.; Aravanis, A. M.; Deisseroth, K.; de Lecea, L. Nature 2007, 450, 420.

(3) Baker, A. S.; Deiters, A. ACS Chem. Biol. 2014, 9, 1398.

(4) Gautier, A.; Gauron, C.; Volovitch, M.; Bensimon, D.; Jullien, L.; Vriz, S. Nat. Chem. Biol. 2014, 10, 533.

(5) Ellis-Davies, G. C. R. Nat. Methods 2007, 4, 619.

(6) Lee, H.-M.; Larson, D. R.; Lawrence, D. S. ACS Chem. Biol. 2009, 4, 409.

(7) Rea, A. C.; Vandenberg, L. N.; Ball, R. E.; Snouffer, A. A.; Hudson, A. G.; Zhu, Y.; McLain, D. E.; Johnston, L. L.; Lauderdale, J. D.; Levin, M.; Dore, T. M. Chem. Biol. 2013, 20, 1536.

(8) Schäfer, F.; Wagner, J.; Knau, A.; Dimmeler, S.; Heckel, A. Angew. Chem., Int. Ed. 2013, 52, 13558.

(9) Walsh, S.; Gardner, L.; Deiters, A.; Williams, G. J. ChemBioChem 2014, 15, 1346.

(10) Bort, G.; Gallavardin, T.; Ogden, D.; Dalko, P. I. Angew. Chem., Int. Ed. 2013, 52, 4526.

(11) Donato, L.; Mourot, A.; Davenport, C. M.; Herbivo, C.; Warther, D.; Léonard, J.; Bolze, F.; Nicoud, J.-F.; Kramer, R. H.; Goeldner, M.; Specht, A. Angew. Chem. 2012, 124, 1876.

(12) Ouyang, X.; Shestopalov, I. A.; Sinha, S.; Zheng, G.; Pitt, C. L. W.; Li, W.-H.; Olson, A. J.; Chen, J. K. J. Am. Chem. Soc. 2009, 131, 13255.

(13) Olson, J. P.; Kwon, H.-B.; Takasaki, K. T.; Chiu, C. Q.; Higley, M. J.; Sabatini, B. L.; Ellis-Davies, G. C. R. J. Am. Chem. Soc. 2013, 135, 5954.

(14) Amatrudo, J. M.; Olson, J. P.; Lur, G.; Chiu, C. Q.; Higley, M. J.; Ellis-Davies, G. C. R. ACS Chem. Neurosci. 2014, 5, 64.

(15) Klán, P.; Šolomek, T.; Bochet, C. G.; Blanc, A.; Givens, R.; Rubina, M.; Popik, V.; Kostikov, A.; Wirz, J. Chem. Rev. 2013, 113, 119.

(16) Pelliccioli, A. P.; Wirz, J. Photochem. Photobiol. Sci. 2002, 1, 441.

(17) Schafer, F. Q.; Buettner, G. R. Free Radical Biol. Med. 2001, 30, 1191.

(18) Dawson, P.; Muir, T.; Clark-Lewis, I.; Kent, S. Science 1994, 266, 776.

(19) Barron, E. S. G. In Advances in Enzymology and Related Areas of Molecular Biology; Nord, F. F., Ed.; John Wiley & Sons, Inc.: Hoboken, NJ, 2006; pp 201−266.

(20) Philipson, K. D.; Gallivan, J. P.; Brandt, G. S.; Dougherty, D. A.; Lester, H. A. Am. J. Physiol. Cell Physiol. 2001, 281, C195.

(21) Li, H.; Hah, J.-M.; Lawrence, D. S. J. Am. Chem. Soc. 2008, 130, 10474.

(22) Uprety, R.; Luo, J.; Liu, J.; Naro, Y.; Samanta, S.; Deiters, A. ChemBioChem 2014, 15, 1793.

(23) Shao, Q.; Xing, B. Chem. Soc. Rev. 2010, 39, 2835.

(24) Cysteine: biosynthesis, chemical structure and toxicity; Nova Science Publishers, Inc.: Hauppauge, NY, 2012.

(25) Pan, P.; Bayley, H. FEBS Lett. 1997, 405, 81.

(26) Arabaci, G.; Guo, X.-C.; Beebe, K. D.; Coggeshall, K. M.; Pei, D. J. Am. Chem. Soc. 1999, 121, 5085.

(27) Jones, P. B.; Pollastri, M. P.; Porter, N. A. J. Org. Chem. 1996, 61, 9455.

(28) Wosnick, J. H.; Shoichet, M. S. Chem. Mater. 2008, 20, 55.

(29) DeGraw, A. J.; Hast, M. A.; Xu, J.; Mullen, D.; Beese, L. S.; Barany, G.; Distefano, M. D. Chem. Biol. Drug Des. 2008, 72, 171.

(30) Wieboldt, R.; Gee, K. R.; Niu, L.; Ramesh, D.; Carpenter, B. K.; Hess, G. P. Proc. Natl. Acad. Sci. U. S. A. 1994, 91, 8752.

(31) Furuta, T.; Wang, S. S.-H.; Dantzker, J. L.; Dore, T. M.; Bybee, W. J.; Callaway, E. M.; Denk, W.; Tsien, R. Y. Proc. Natl. Acad. Sci. U. S. A. 1999, 96, 1193.

(32) Kotzur, N.; Briand, B.; Beyermann, M.; Hagen, V. J. Am. Chem. Soc. 2009, 131, 16927.

(33) Wylie, R. G.; Shoichet, M. S. Biomacromolecules 2011, 12, 3789.

(34) Wylie, R. G.; Ahsan, S.; Aizawa, Y.; Maxwell, K. L.; Morshead, C. M.; Shoichet, M. S. Nat. Mater. 2011, 10, 799.

(35) Abate-Pella, D.; Zeliadt, N. A.; Ochocki, J. D.; Warmka, J. K.; Dore, T. M.; Blank, D. A.; Wattenberg, E. V.; Distefano, M. D. ChemBioChem 2012, 13, 1009.

(36) Momotake, A.; Lindegger, N.; Niggli, E.; Barsotti, R. J.; Ellis- Davies, G. C. R. Nat. Methods 2006, 3, 35.

(37) Hatchard, C. G.; Parker, C. A. Proc. R. Soc. London, Ser. A 1956, 235, 518.

6.3 Chapter 3

1 P. Klán, T. Šolomek, C. G. Bochet, A. Blanc, R. Givens, M. Rubina, V. Popik, A. Kostikov and J. Wirz, *Chem. Rev.*, 2013, **113**, 119–191.

2 A. P. Pelliccioli and J. Wirz, *Photochem. Photobiol. Sci.*, 2002, **1**, 441–458.

3 G. C. R. Ellis-Davies, *Nat. Methods*, 2007, **4**, 619–628.

4 H.-M. Lee, D. R. Larson and D. S. Lawrence, *ACS Chem. Biol.*, 2009, **4**, 409–427.

5 G. Bort, T. Gallavardin, D. Ogden and P. I. Dalko, *Angew. Chem. Int. Ed.*, 2013, **52**, 4526–4537.

6 X. Chen, S. Tang, J.-S. Zheng, R. Zhao, Z.-P. Wang, W. Shao, H.-N. Chang, J.-Y. Cheng, H. Zhao, L. Liu and H. Qi, *Nat. Commun.*, 2015, **6**, 7220.

7 X. Ouyang, I. A. Shestopalov, S. Sinha, G. Zheng, C. L. W. Pitt, W.-H. Li, A. J. Olson and J. K. Chen, *J. Am. Chem. Soc.*, 2009, **131**, 13255–13269.

8 V. Gatterdam, R. Ramadass, T. Stoess, M. A. H. Fichte, J. Wachtveitl, A. Heckel and R. Tampé, *Angew. Chem. Int. Ed.*, 2014, **53**, 5680–5684.

9 R. G. Wylie and M. S. Shoichet, *Biomacromolecules*, 2011, **12**, 3789–3796.

10 A. M. Kloxin, A. M. Kasko, C. N. Salinas and K. S. Anseth, *Science*, 2009, **324**, 59–63.

11 Y. Luo and M. S. Shoichet, *Nat. Mater.*, 2004, **3**, 249–253.

12 H. A. Chapman, R. J. Riese and G.-P. Shi, *Annu. Rev. Physiol.*, 1997, **59**, 63–88.

13 N. Haugaard, *Ann. N. Y. Acad. Sci.*, 2000, **899**, 148–158.

14 R. Uprety, J. Luo, J. Liu, Y. Naro, S. Samanta and A. Deiters, *ChemBioChem*, 2014, **15**, 1793–1799.

15 K. D. Philipson, J. P. Gallivan, G. S. Brandt, D. A. Dougherty and H. A. Lester, *Am. J. Physiol. Cell Physiol.*, 2001, **281**, C195-206.

16 G. Capozzi and G. Modena, in *The Thiol Group: Vol. 2 (1974)*, ed. S. Patai, John Wiley & Sons, Ltd., Chichester, UK, 1974, pp. 785–839.

17 A. J. DeGraw, M. A. Hast, J. Xu, D. Mullen, L. S. Beese, G. Barany and M. D. Distefano, *Chem. Biol. Drug Des.*, 2008, **72**, 171–181.

18 J. Luo, R. Uprety, Y. Naro, C. Chou, D. P. Nguyen, J. W. Chin and A. Deiters, *J. Am. Chem. Soc.*, 2014, **136**, 15551–15558.

19 N. Kotzur, B. Briand, M. Beyermann and V. Hagen, *J. Am. Chem. Soc.*, 2009, **131**, 16927–16931.

20 D. Abate-Pella, N. A. Zeliadt, J. D. Ochocki, J. K. Warmka, T. M. Dore, D. A. Blank, E. V. Wattenberg and M. D. Distefano, *ChemBioChem*, 2012, **13**, 1009–1016.

21 M. M. Mahmoodi, D. Abate-Pella, T. J. Pundsack, C. C. Palsuledesai, P. C. Goff, D. A. Blank and M. D. Distefano, *J. Am. Chem. Soc.*, 2016, **18**, 5848-5859.

22 T. Furuta, S. S.-H. Wang, J. L. Dantzker, T. M. Dore, W. J. Bybee, E. M. Callaway, W. Denk and R. Y. Tsien, *Proc. Natl. Acad. Sci.*, 1999, **96**, 1193–1200.

23 A. Svendsen and P. M. Boll, *Tetrahedron*, 1973, **29**, 4251–4258.

24 K. C. Nicolaou, A. A. Estrada, M. Zak, S. H. Lee and B. S. Safina, *Angew. Chem. Int. Ed.*, 2005, **44**, 1378–1382.

25 C. C. Palsuledesai and M. D. Distefano, *ACS Chem. Biol.*, 2015, **10**, 51–62.

26 J. D. Ochocki and M. D. Distefano, *Med Chem Commun*, 2013, **4**, 476–492.

27 R. G. Wylie, S. Ahsan, Y. Aizawa, K. L. Maxwell, C. M. Morshead and M. S. Shoichet, *Nat. Mater.*, 2011, **10**, 799–806.

28 C. M. Nimmo, S. C. Owen and M. S. Shoichet, *Biomacromolecules*, 2011, **12**, 824–830.

6.4 Chapter 4

1 P. Klán, T. Šolomek, C. G. Bochet, A. Blanc, R. Givens, M. Rubina, V. Popik, A. Kostikov and J. Wirz, *Chem. Rev.*, 2013, **113**, 119–191.

2 G. C. R. Ellis-Davies, *Nat. Methods*, 2007, **4**, 619–628.

3 G. Bort, T. Gallavardin, D. Ogden and P. I. Dalko, *Angew. Chem. Int. Ed.*, 2013, **52**, 4526–4537.

4 X. Chen, S. Tang, J.-S. Zheng, R. Zhao, Z.-P. Wang, W. Shao, H.-N. Chang, J.-Y. Cheng, H. Zhao, L. Liu and H. Qi, *Nat. Commun.*, 2015, **6**, 7220.

5 X. Ouyang, I. A. Shestopalov, S. Sinha, G. Zheng, C. L. W. Pitt, W.-H. Li, A. J. Olson and J. K. Chen, *J. Am. Chem. Soc.*, 2009, **131**, 13255–13269.

6 S. Lukman, B. J. Grant, A. A. Gorfe, G. H. Grant and J. A. McCammon, *PLoS Comput. Biol.*, 2010, **6**, e1000922.

7 P. Crespo and J. León, *Cell. Mol. Life Sci. CMLS*, 2000, **57**, 1613–1636.

8 N. Mitin, K. L. Rossman and C. J. Der, *Curr. Biol.*, 2005, **15**, R563–R574.

9 D. W. Stacey, M. H. Tsai, C. L. Yu and J. K. Smith, *Cold Spring Harb. Symp. Quant. Biol.*, 1988, **53 Pt 2**, 871–881.

10 A. Fernandez-Medarde and E. Santos, *Genes Cancer*, 2011, **2**, 344–358.

11 J. Ohkanda, D. B. Knowles, M. A. Blaskovich, S. M. Sebti and A. D. Hamilton, *Curr. Top. Med. Chem.*, 2002, **2**, 303–323.

12 D. B. Rozema, S. T. Phillips and C. D. Poulter, *Org. Lett.*, 1999, **1**, 815–817.

13 M. M. Mahmoodi, D. Abate-Pella, T. J. Pundsack, C. C. Palsuledesai, P. C. Goff, D. A. Blank and M. D. Distefano, *J. Am. Chem. Soc.*, 2016.

6.5 Chapter 5

1 Klán, T. Šolomek, C. G. Bochet, A. Blanc, R. Givens, M. Rubina, V. Popik, A. Kostikov and J. Wirz, *Chem. Rev.*, 2013, **113**, 119–191.

2 Donato, A. Mourot, C. M. Davenport, C. Herbivo, D. Warther, J. Léonard, F. Bolze, J.-F. Nicoud, R. H. Kramer, M. Goeldner and A. Specht, *Angew. Chem.*, 2012, **124**, 1876–1879.

3 Dreuw, M. A. Polkehn, R. Binder, A. Heckel and S. Knippenberg, *J. Comput. Chem.*, 2012, **33**, 1797–1805.

4 M. Mahmoodi, D. Abate-Pella, T. J. Pundsack, C. C. Palsuledesai, P. C. Goff, D. A. Blank and M. D. Distefano, *J. Am. Chem. Soc.*, 2016, **138**, 5848–5859.